

Using NMR to study Macromolecular Interactions

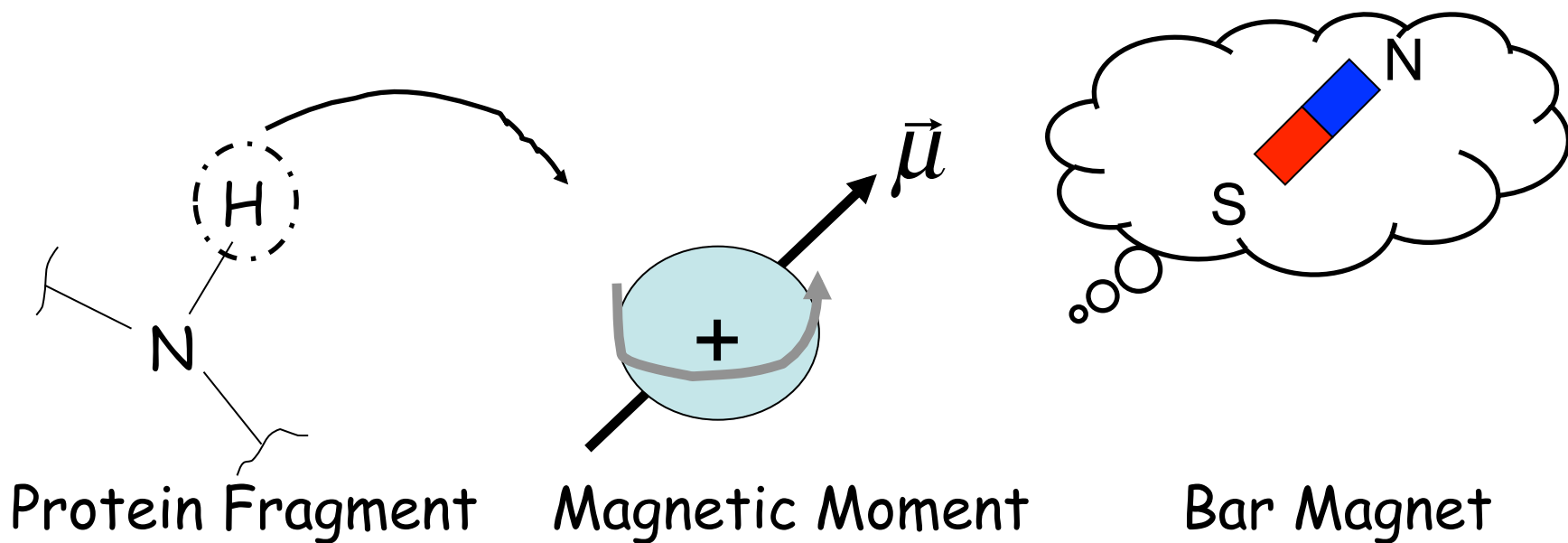
John Gross, BP204A
UCSF

Nov 27, 2017

Outline

- Review of basic NMR experiment
- Multidimensional NMR
- Monitoring ligand binding
- Structure Determination

Review: Nuclear Spins are Microscopic Bar Magnets



Magnetic moment $\vec{\mu} = \gamma \vec{S}$ Angular Momentum

The proportionality constant γ : strength of bar magnet

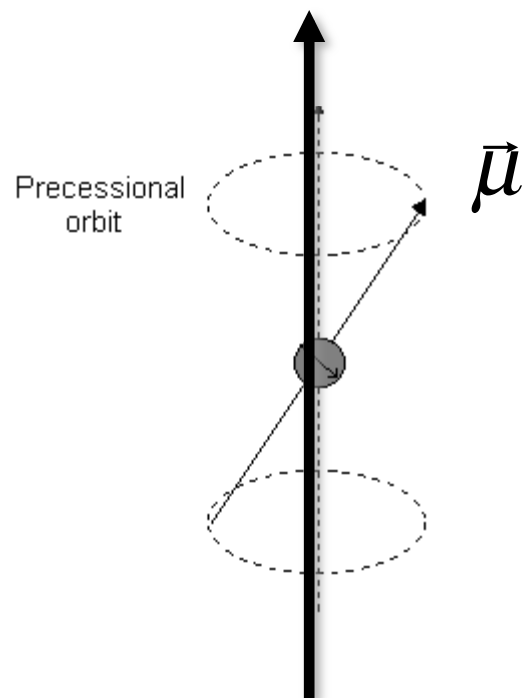
Equation of Motion

$$\frac{d\vec{\mu}}{dt} = \gamma \vec{B} \times \vec{\mu}$$

Based on magnetic torque:

$$\frac{d\vec{L}}{dt} = \vec{B} \times \vec{L}$$

Spin Precession



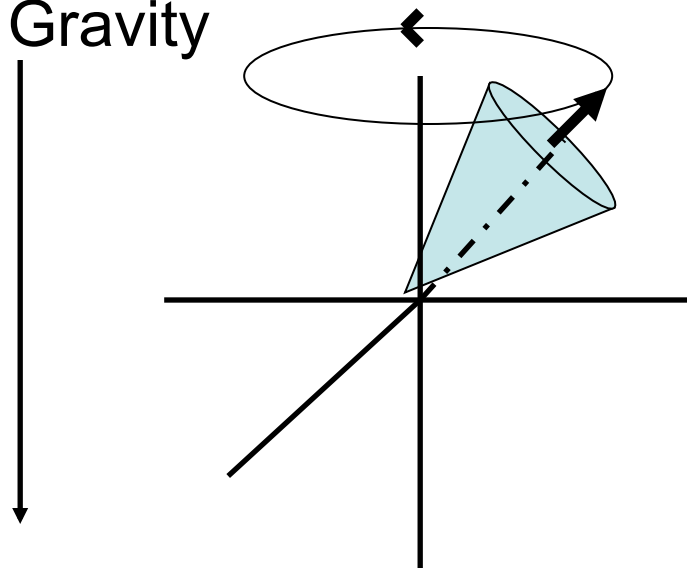
Magnetic Field, B_0

Precession frequency: $\gamma B_0 = \omega_0$

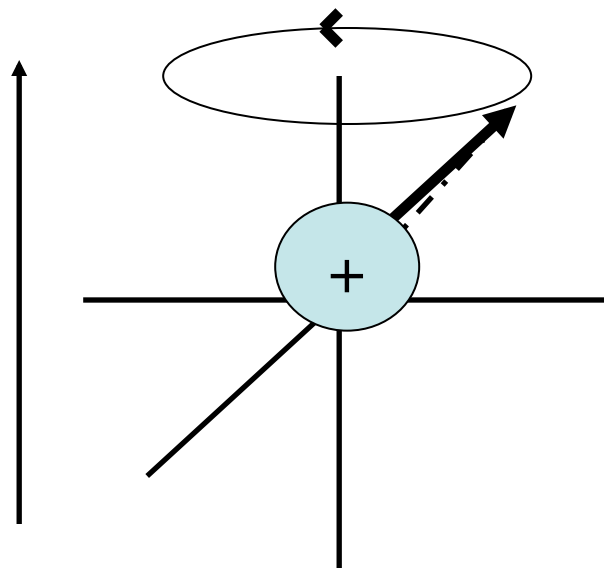
Driving Forces for Precession

Precessional Orbits

Gravity

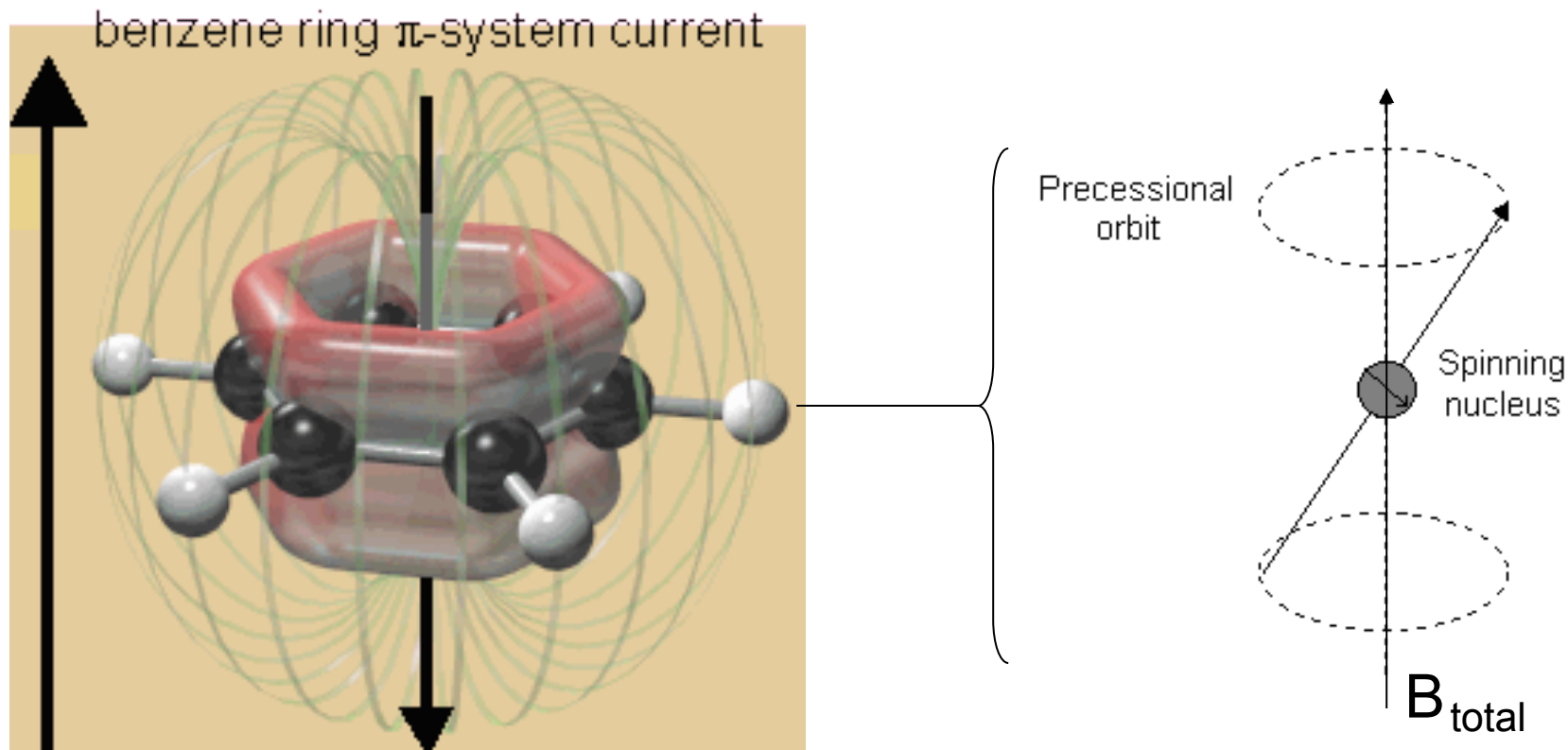


Spinning Top



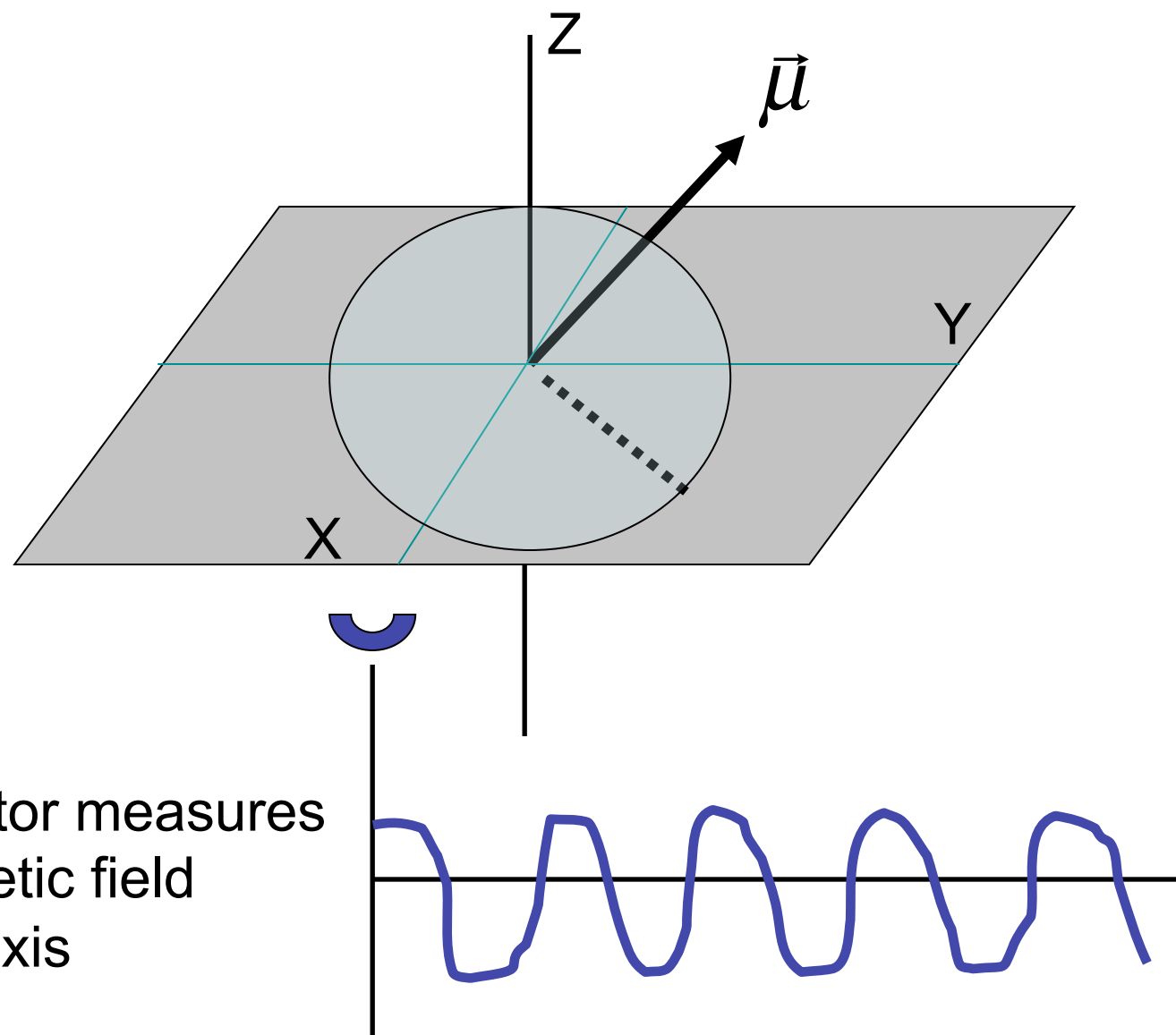
Spinning Nucleus

Nuclear Spins Report Local Environment

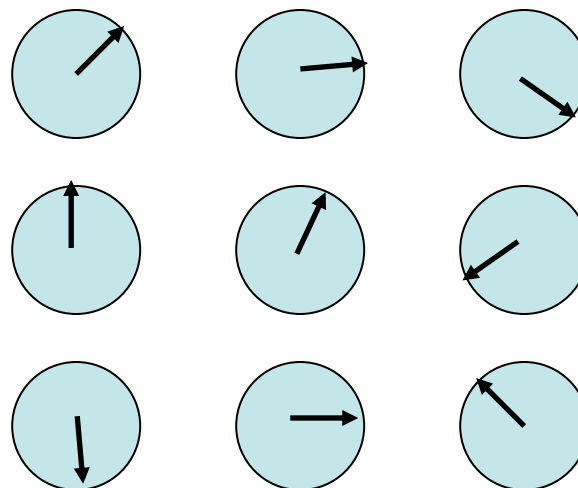


$B_{\text{applied}} + B_{\text{local}} = B_{\text{total}}$ **determines precession**

Detection of Spin Precession



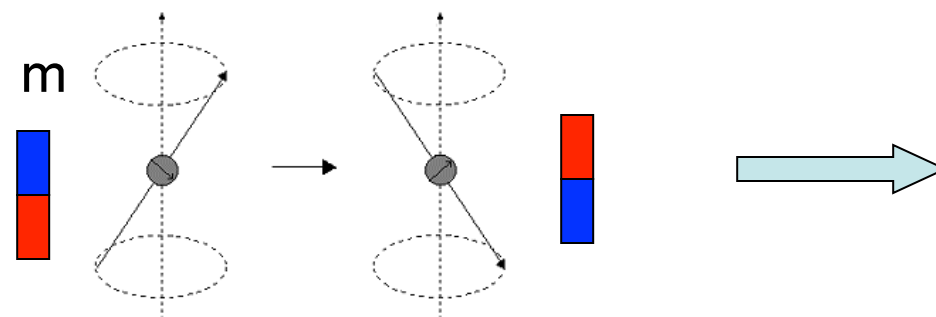
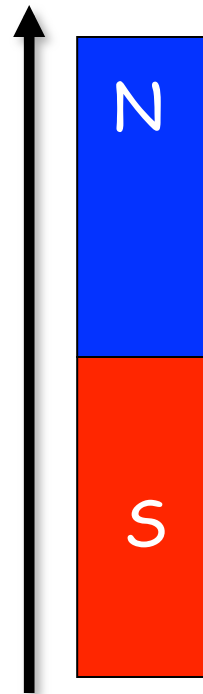
Net Magnetization



$$\left. \begin{aligned} M_x &= \sum_j \mu_x^j = 0 \\ M_y &= \sum_j \mu_y^j = 0 \end{aligned} \right\} \text{No Transverse Magnetization at equilibrium}$$

Magnetic Energy

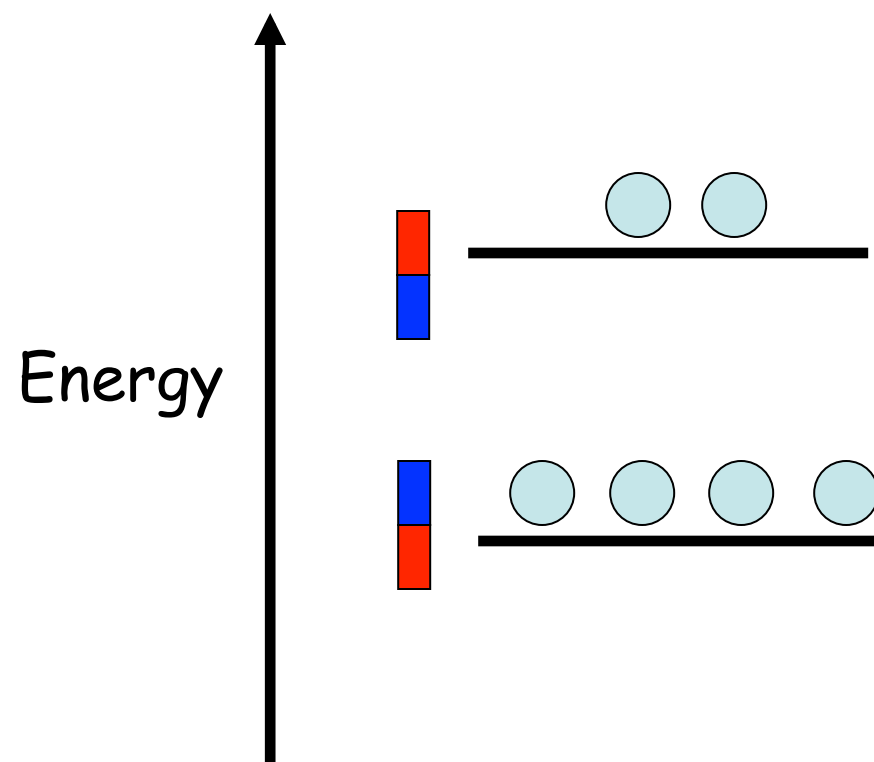
$$E = -\vec{\mu} \bullet \vec{B}$$



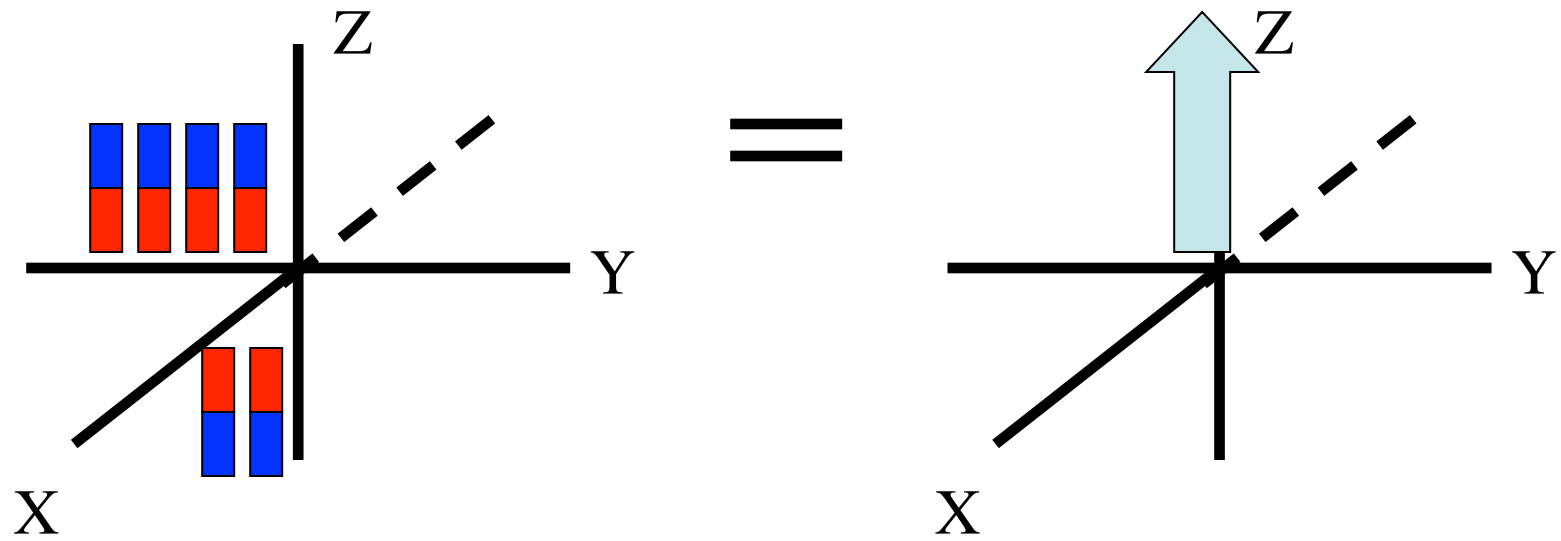
$$E = -\mu_z B_z$$

Static Magnetic Field
Oriented Along Z-Axis

Energy States (spin-1/2 nucleus)

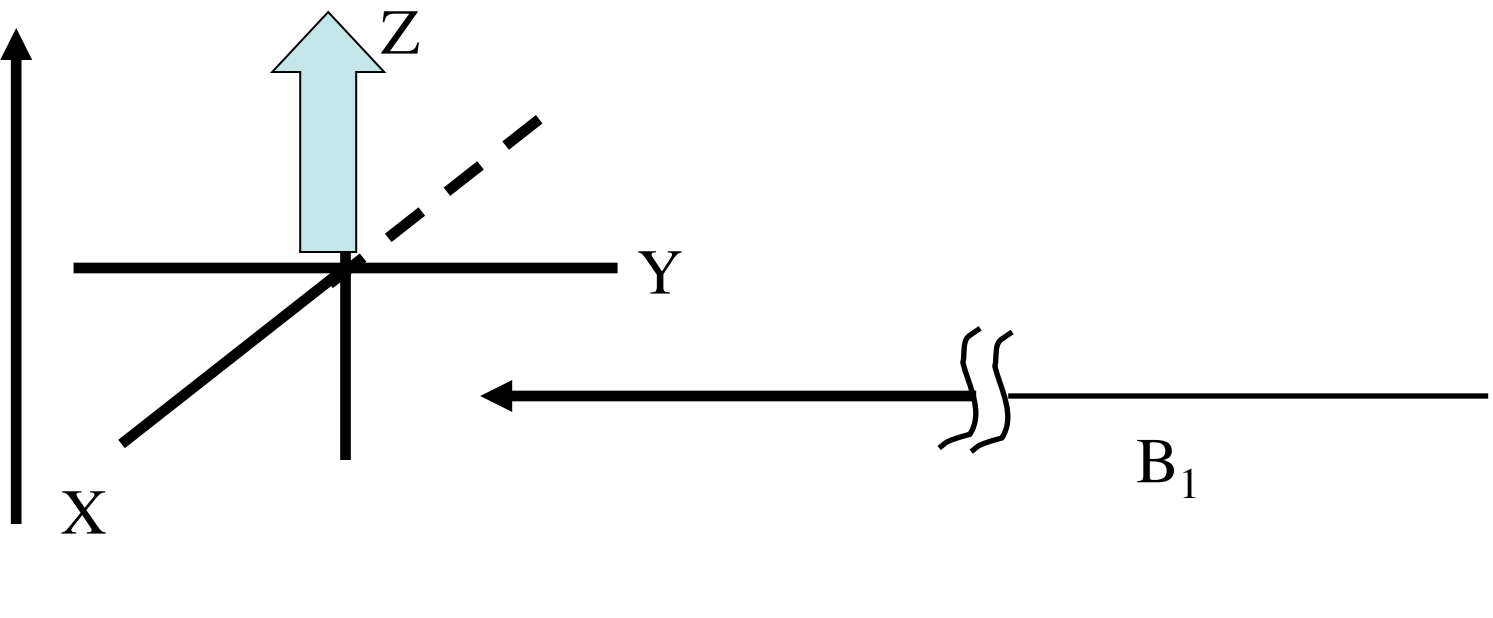


Net Magnetization along Z Axis



$$\sum_j \mu_z^j = M_z$$

Thought experiment: apply 2nd field along Y Axis



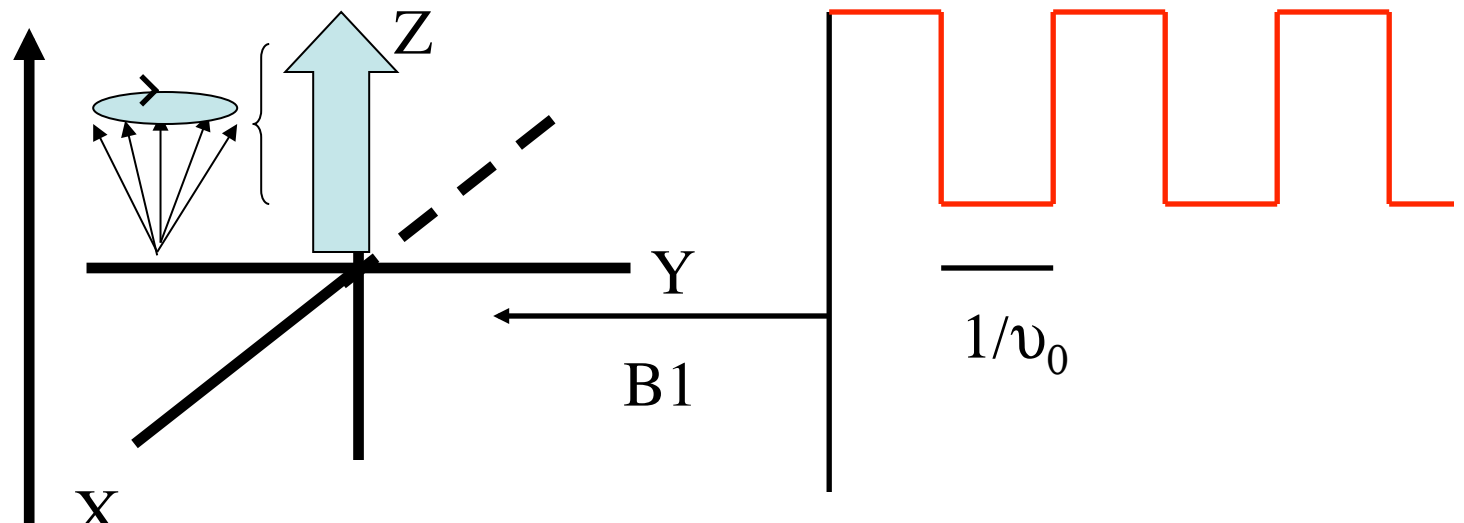
If $B_1 \gg B_0$, M_Z would rotate about B_1 .

Leave B_1 on until X axis reached ----> transverse magnetization
Approach is not practical.

Same effect achieved with weak, resonant oscillating field



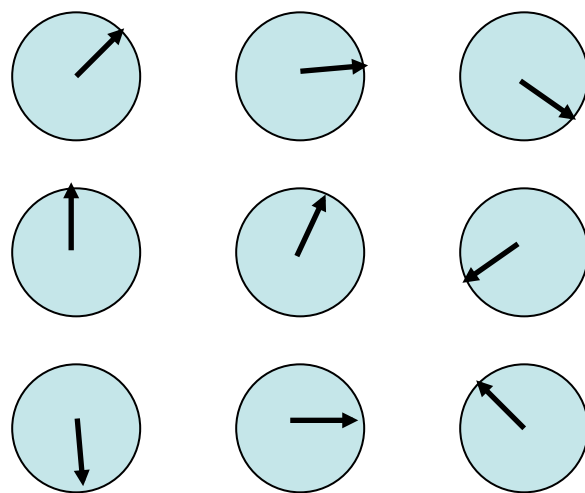
B_0



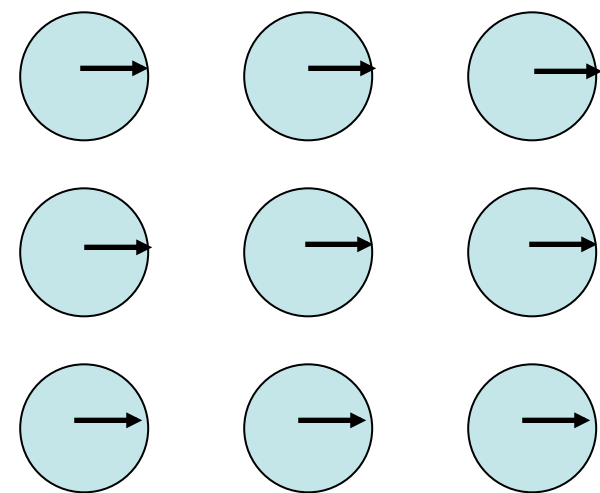
Turn B_1 on and off with a frequency matching the precessional frequency

Resonance

Ensemble of Nuclear Spins



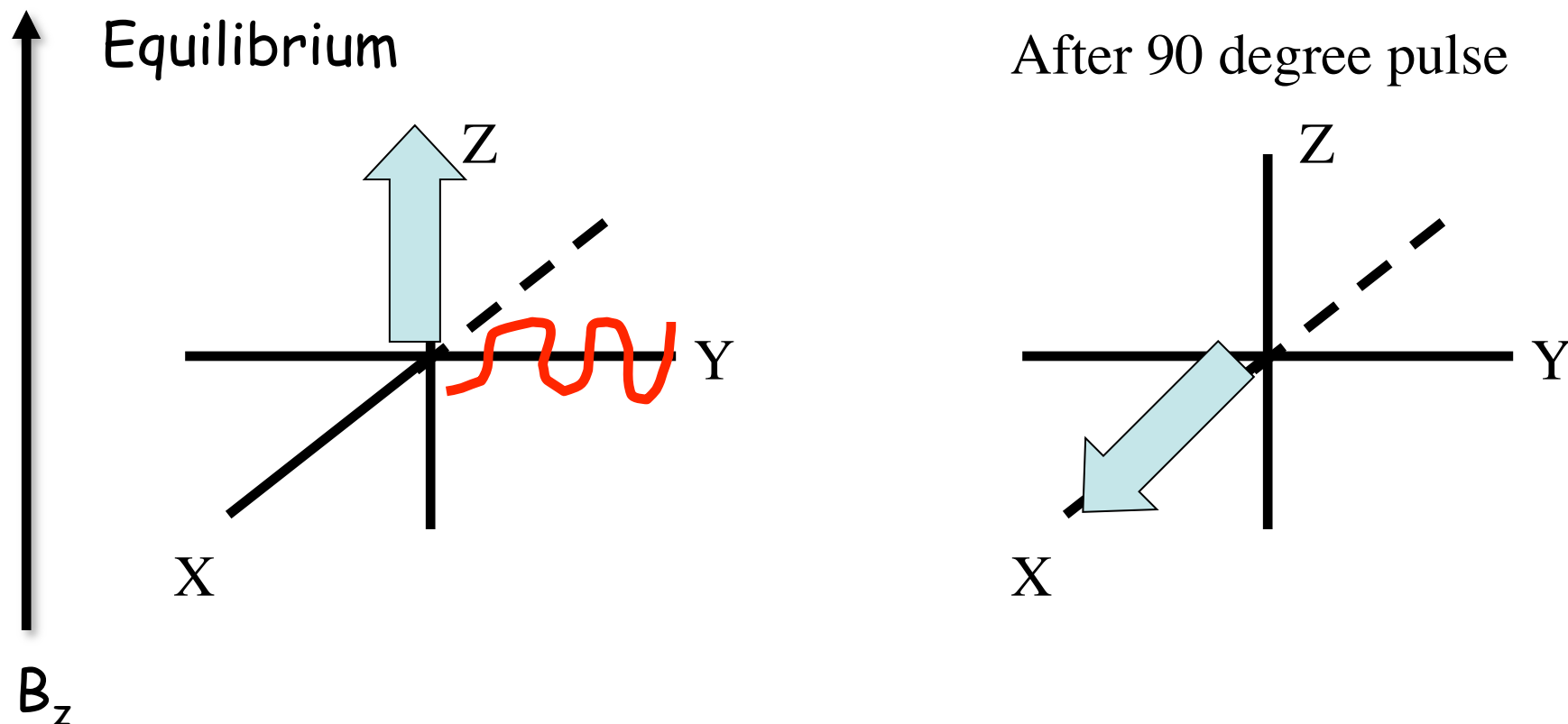
Resonant RF Field
→



Random Phase
No NMR Signal

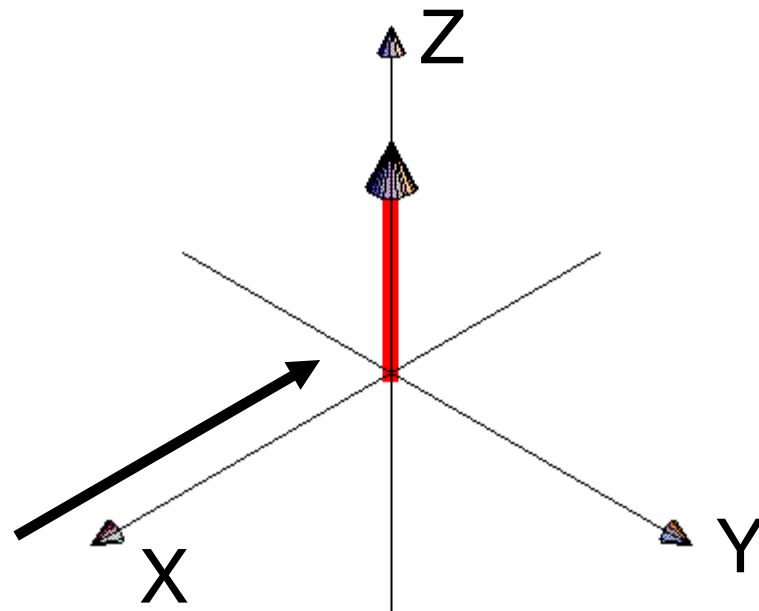
Phase Synchronization
NMR Signal!

Magnetization Vector Model



90y: Resonant 90 Degree Pulse

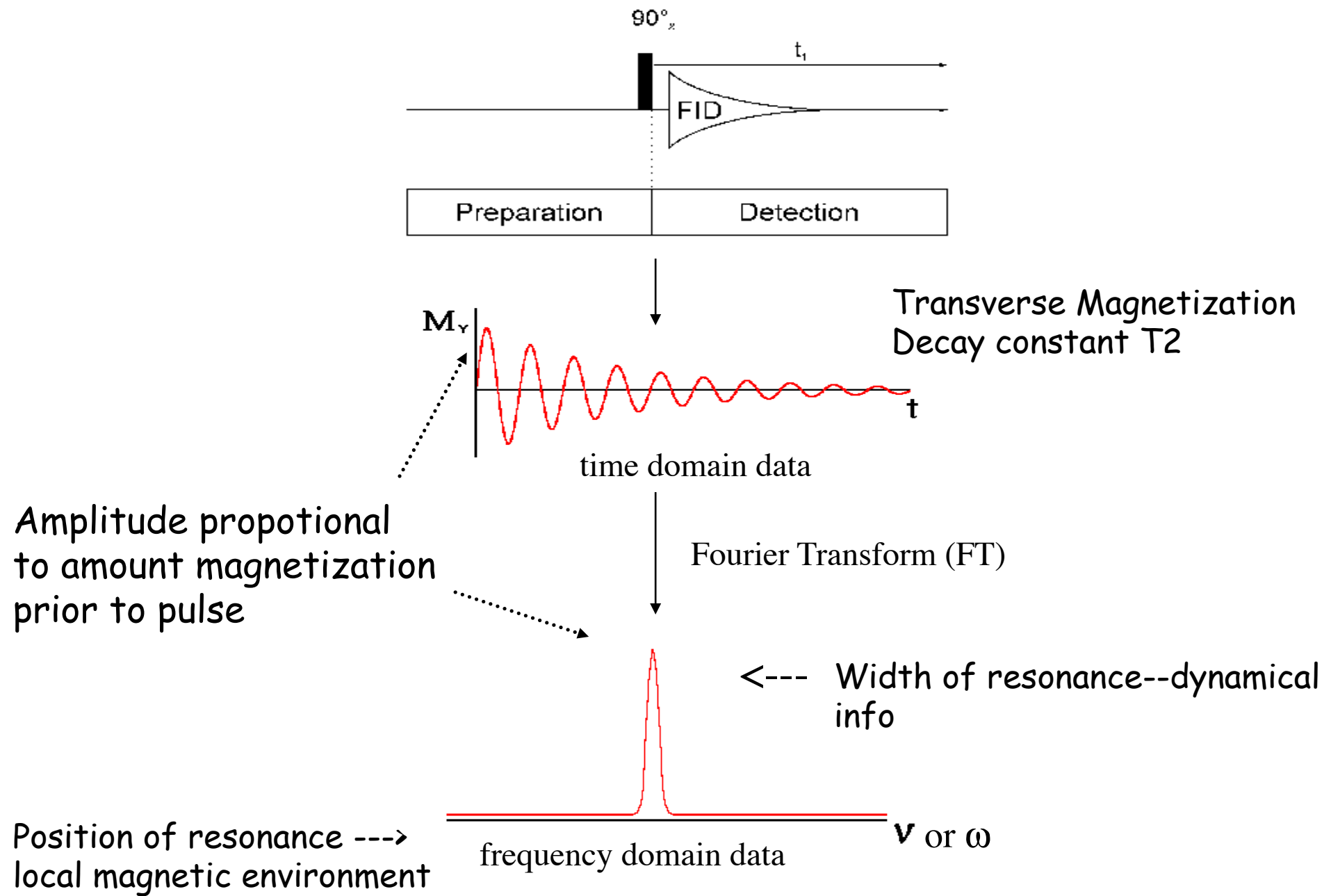
Resonant Pulse in Real Time



R.F. Field (applied at precession frequency)

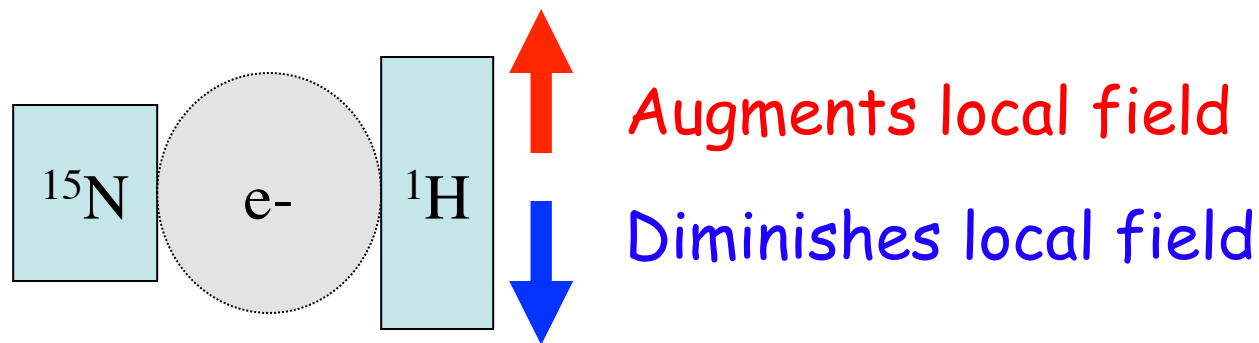
Net magnetization rotated into transverse plane
Rotates due to static and local fields

Summary of 1D Experiment



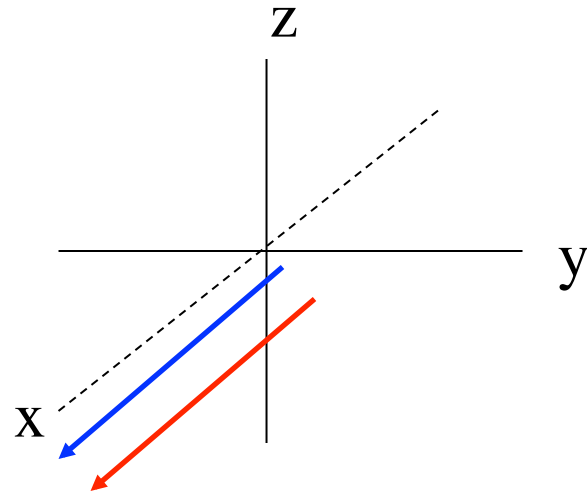
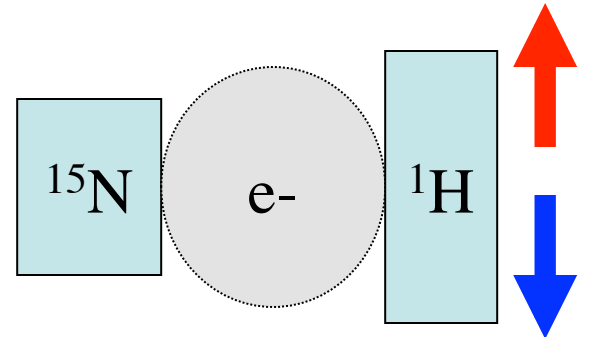
The J Coupling

Consider two spin-1/2 nuclei (ie, ^1H and ^{15}N):

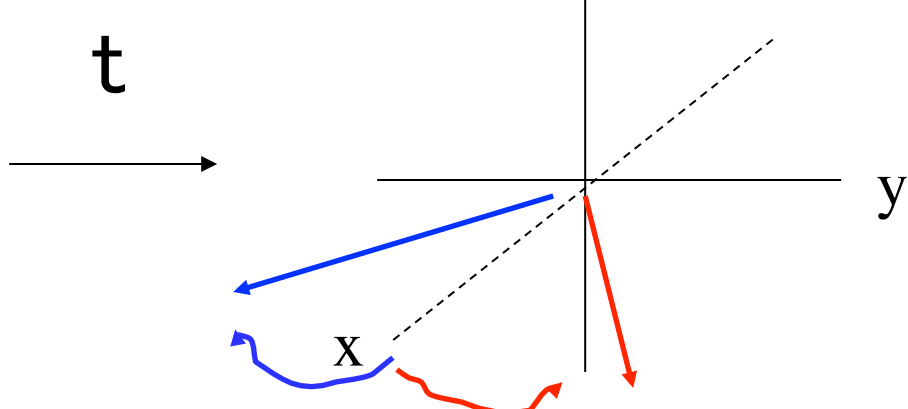


Effect transmitted through electrons in intervening bonds

Vector View

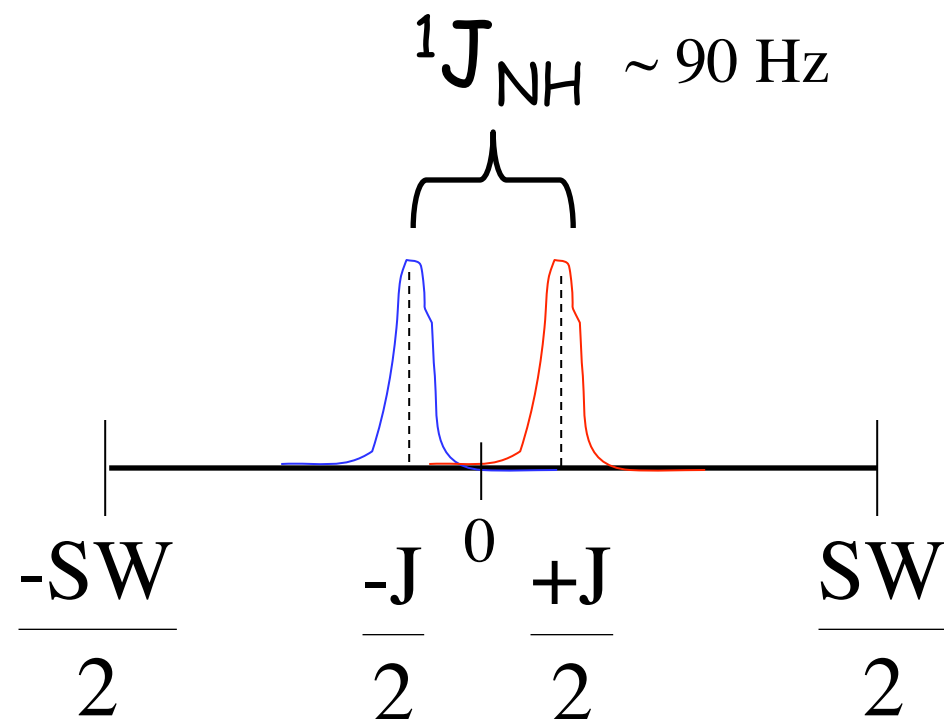


(After 90y pulse)



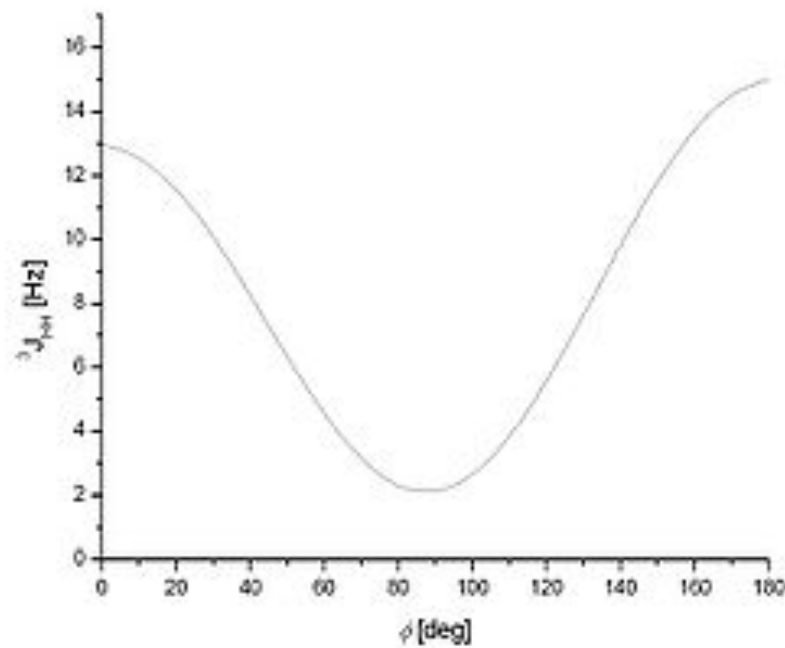
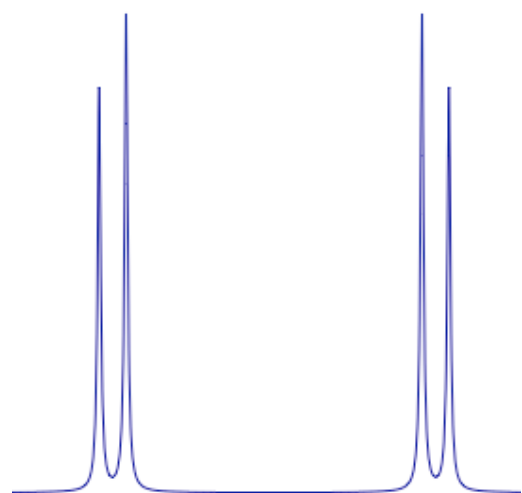
Components rotate **faster** or **slower** than rotating frame by $\pm J/2$

Spectrum with J coupling



^{15}N Detected Spectrum

J couplings contain information on structure



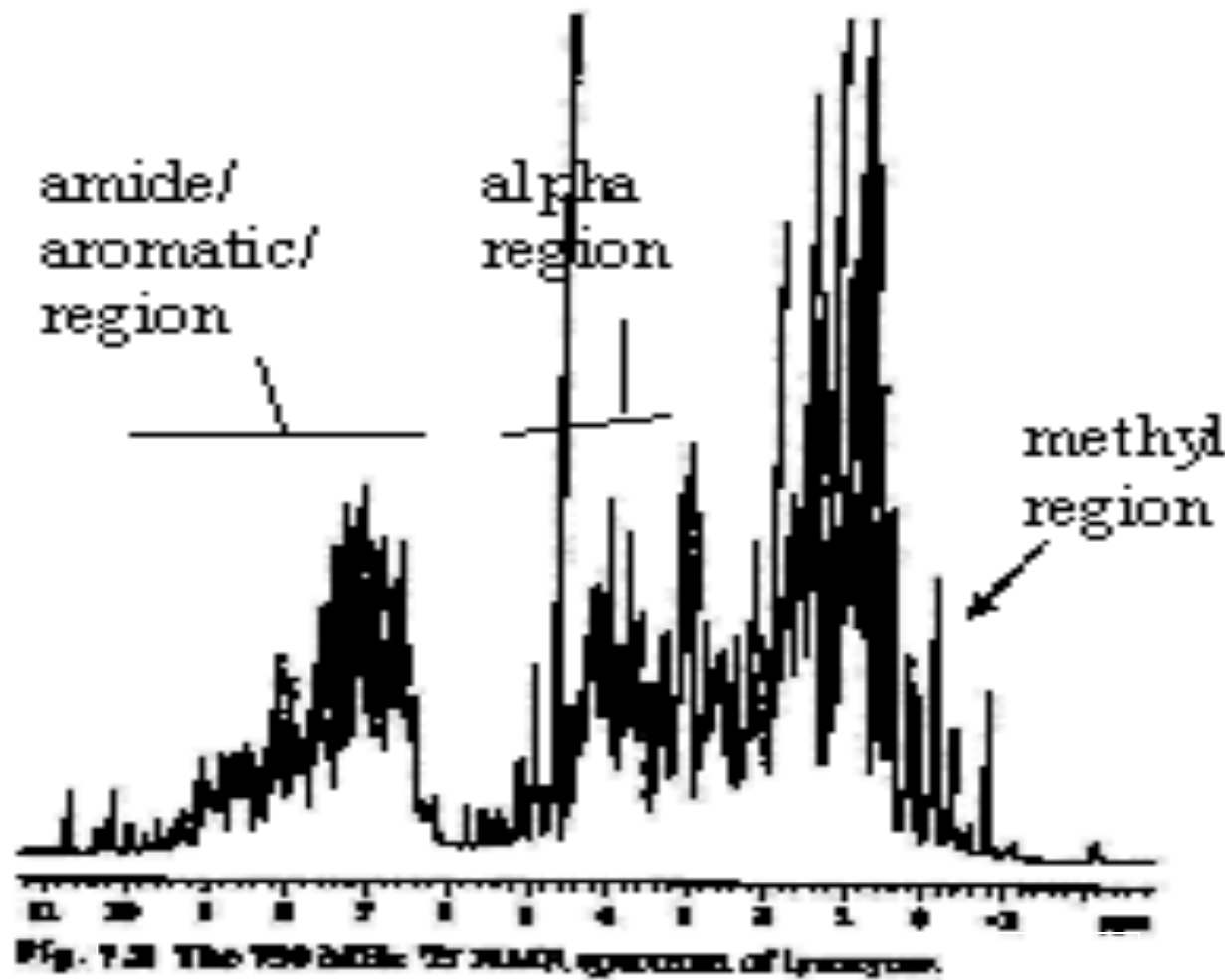
$$J(\phi) = A \cos^2 \phi + B \cos \phi + C$$

Important Observables

Chemical shift is a reporter of magnetic environment

The J coupling can inform torsion angles

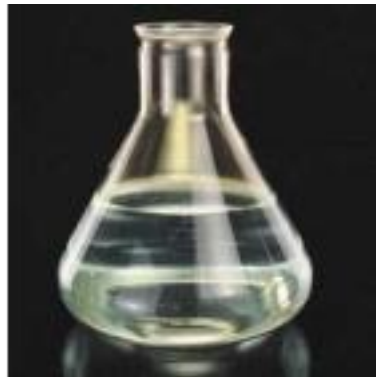
Protein NMR Spectroscopy



Periodic Table of NMR active Nuclei

IA										VIIA			
H	IIA									He			
Li	Be												
		Spin = $\frac{1}{2}$											
		Spin > $\frac{1}{2}$											
Na	Mg	IIIB	IVB	VB	VIIB	VIIIB	IB	IIIB	IIIB	IIIB			
K	Ca	Sc	Ti	V	Cr	Mn	Fe	Co	Ni	Cu	Zn		
Rb	Sr	Y	Zr	Nb	Mo	Tc	Ru	Rh	Pd	Ag	Cd		
Cs	Ba	La	Hf	Ta	W	Re	Os	Ir	Pt	Au	Hg		
Fr	Rd	Ac											
Ce	Pr	Nd	Pm	Sm	Eu	Gd	Tb	Dy	Ho	Er	Tm	Yb	Lu
Th	Pa	U	Np	Pu	Am	Cm	Bk	Cf	Es	Fm	Md	No	Lr

Isotopic Labeling Proteins for NMR



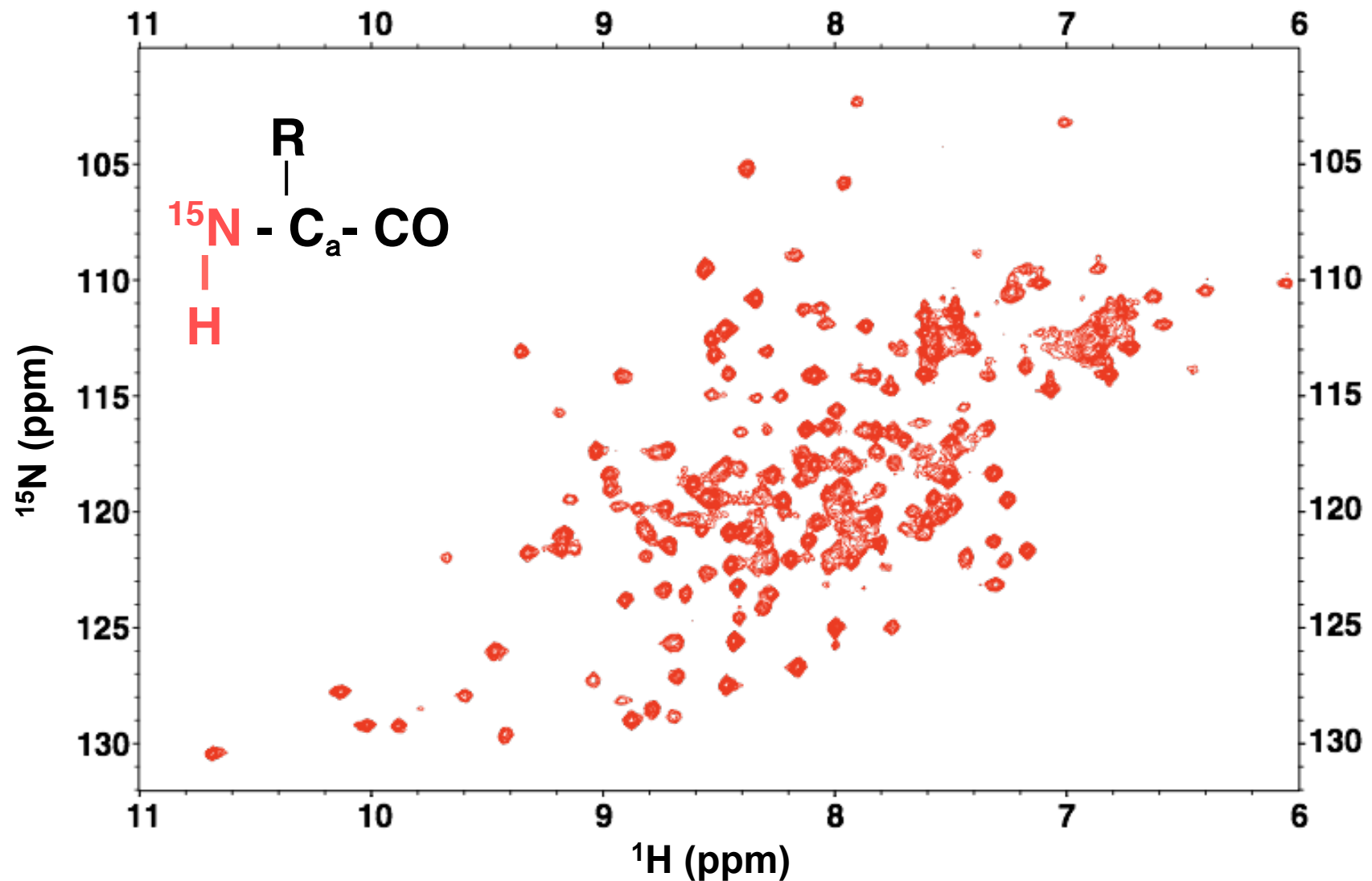
Bacterial expression:
Minimal media, ^{15}N NH_4Cl or
 ^{13}C glucose as sole nitrogen and
carbon source

Amino acid-type labeling
Auxotrophic or standard strains
(ei, BL21(DE3) depending on scheme

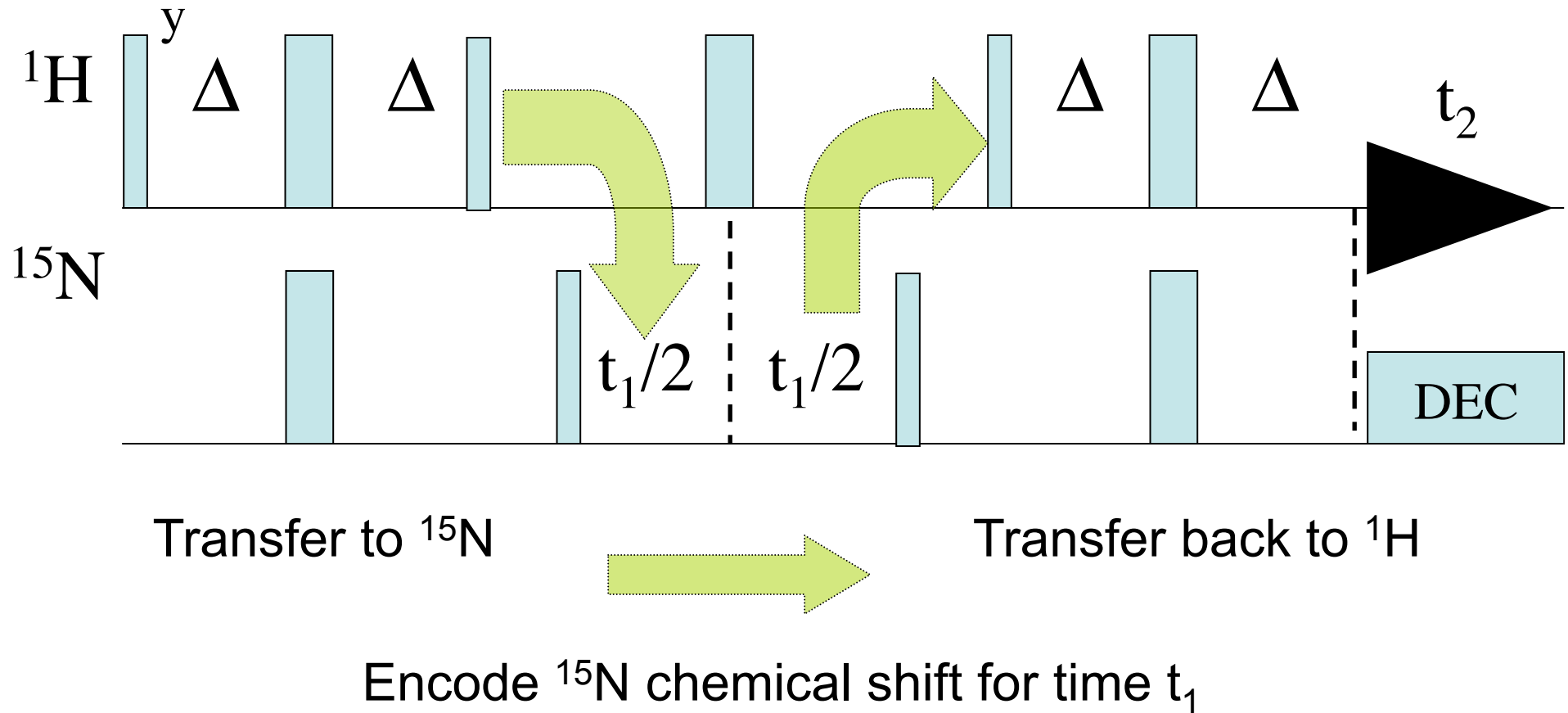
Labeling post purification ; reductive
methylation of lysines

Results in additional spin-1/2 nuclei which can be used as probes

The HSQC is an NH chemical shift correlation map

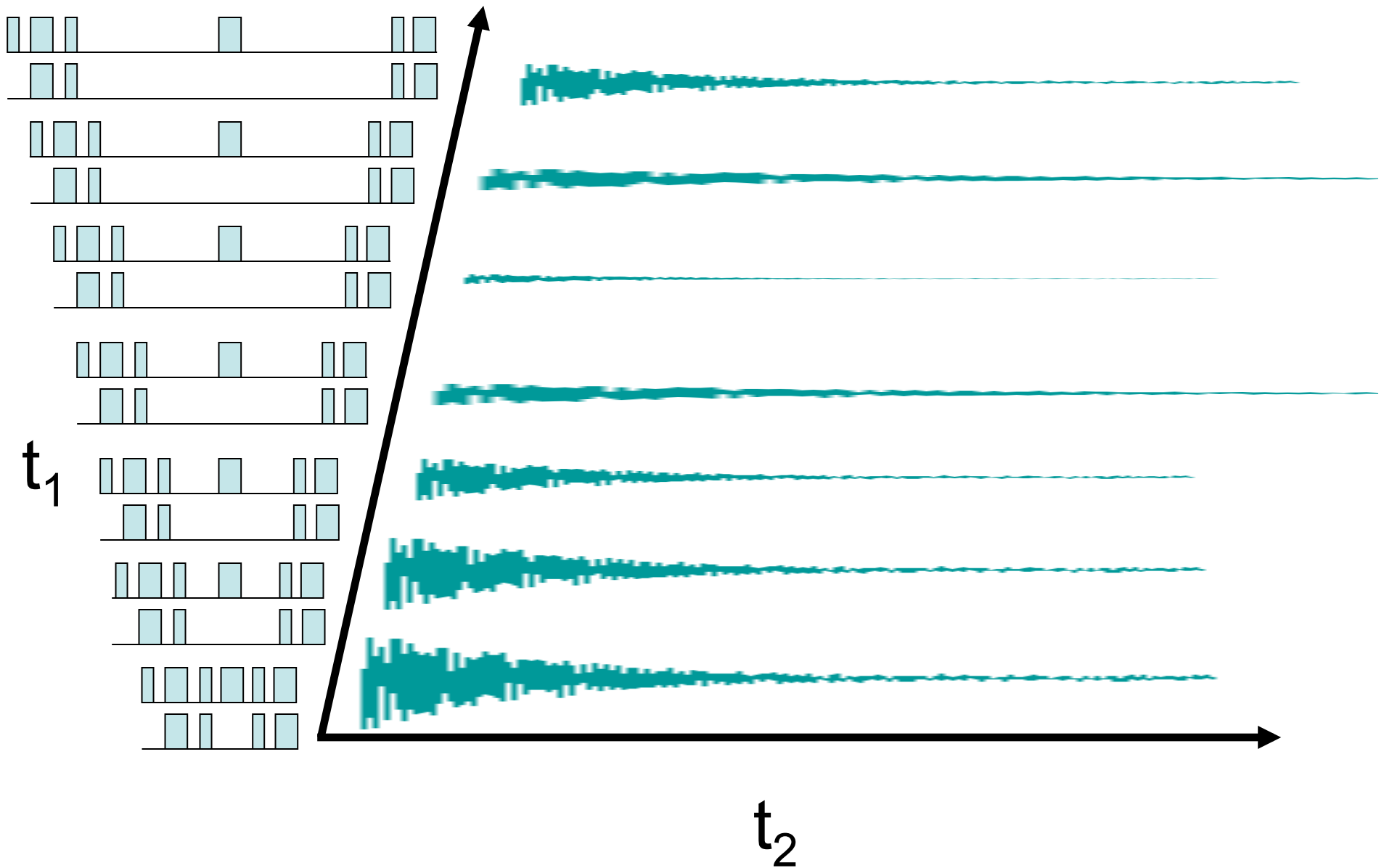


An overview of the HSQC



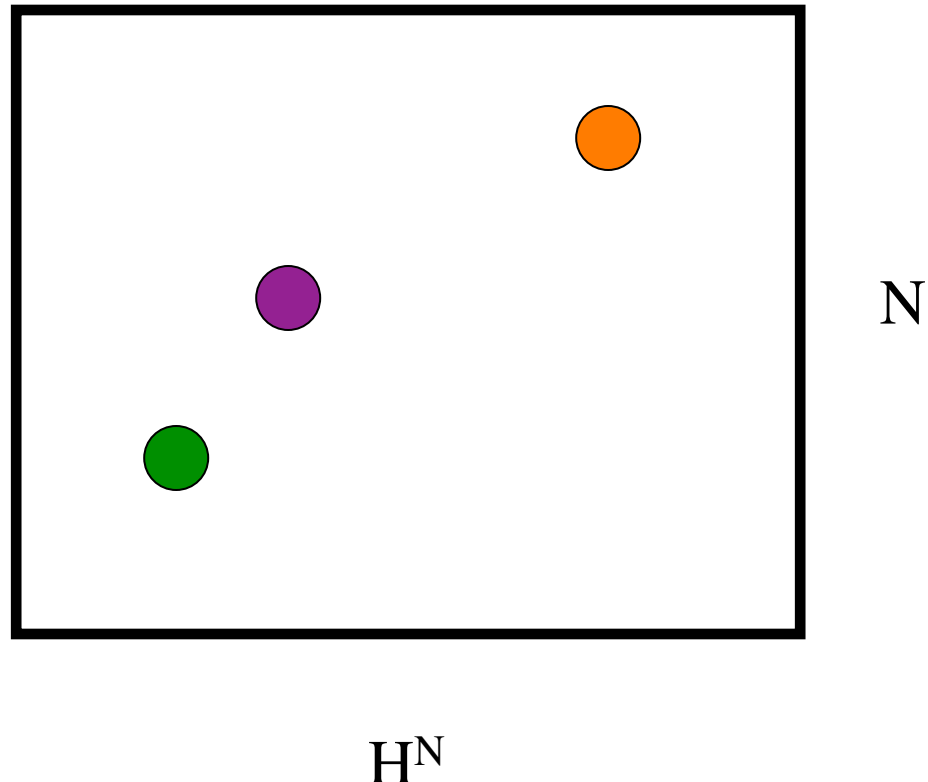
Bodenhausen & Ruben

2D Time-Domain Data

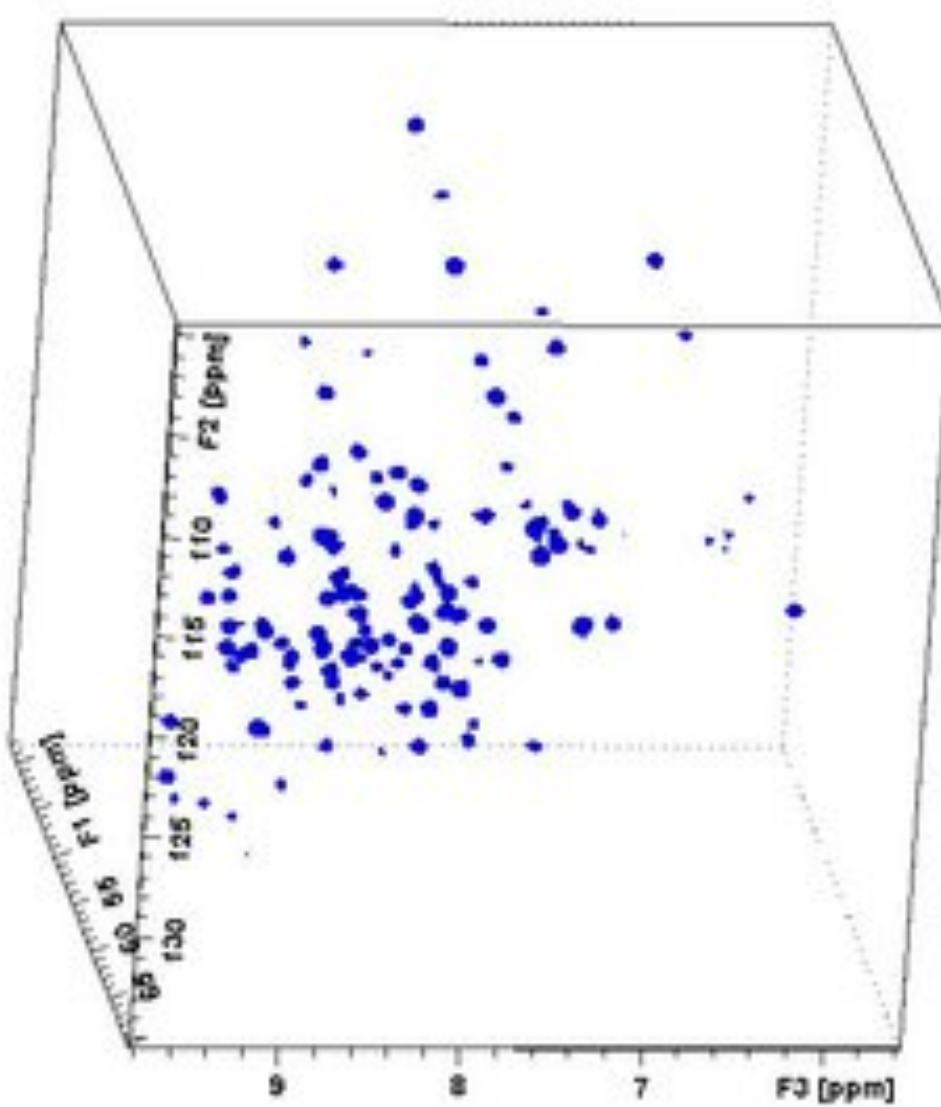


Some data shuffling then 2D FT =the HSQC Spectrum

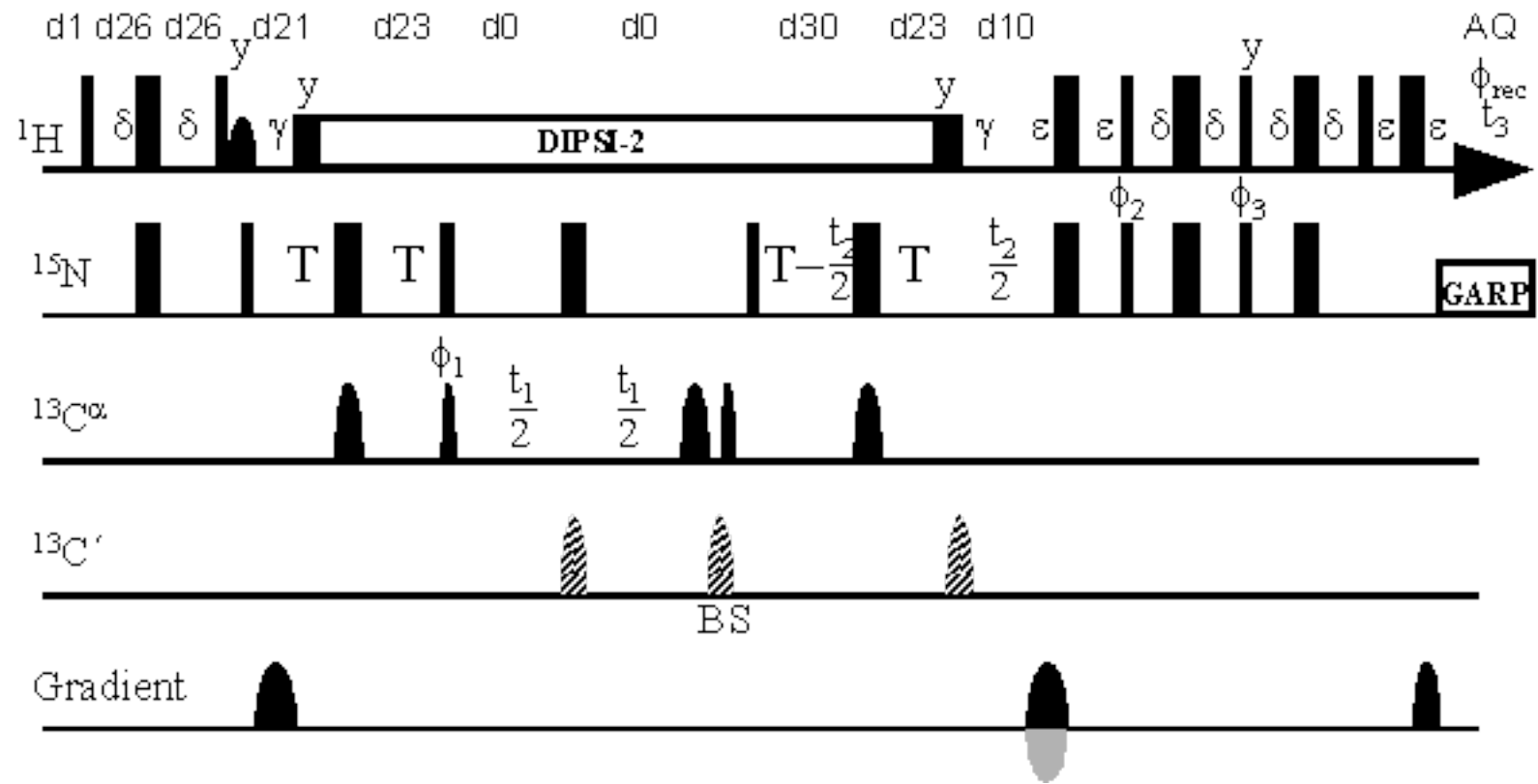
$$\text{Re} [S'(\nu_1, \nu_2)] = A_1^N A_2^H$$



3D Dimensional NMR

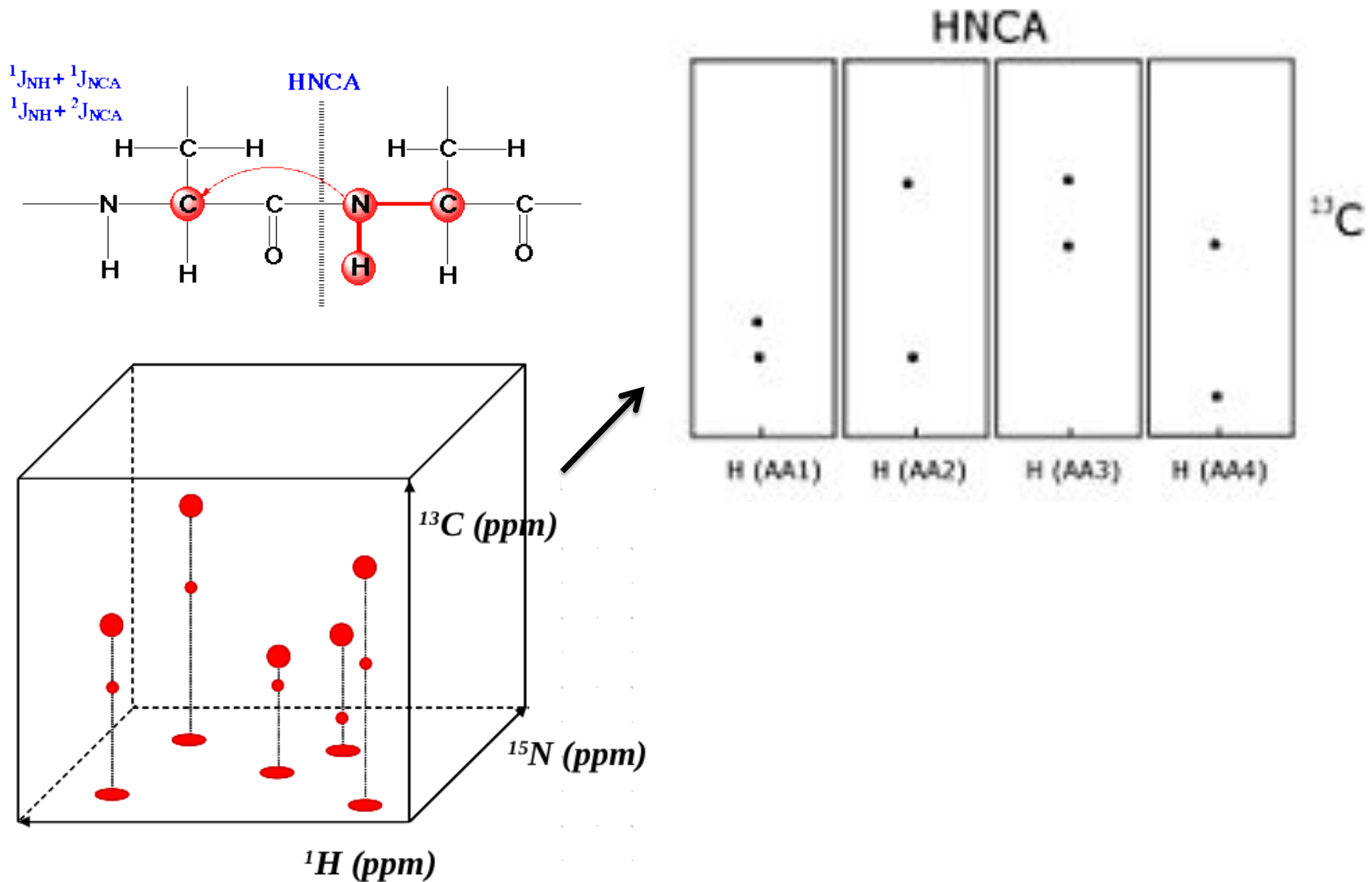


Resonance Assignments from Triple Resonance Experiments



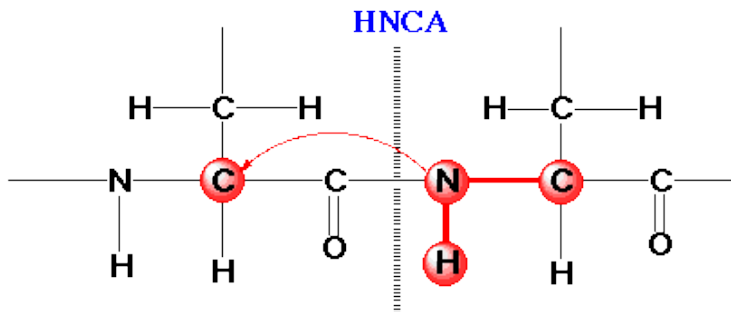
The 3D HNCA Experiment

Backbone Resonance Assignments from HNCA

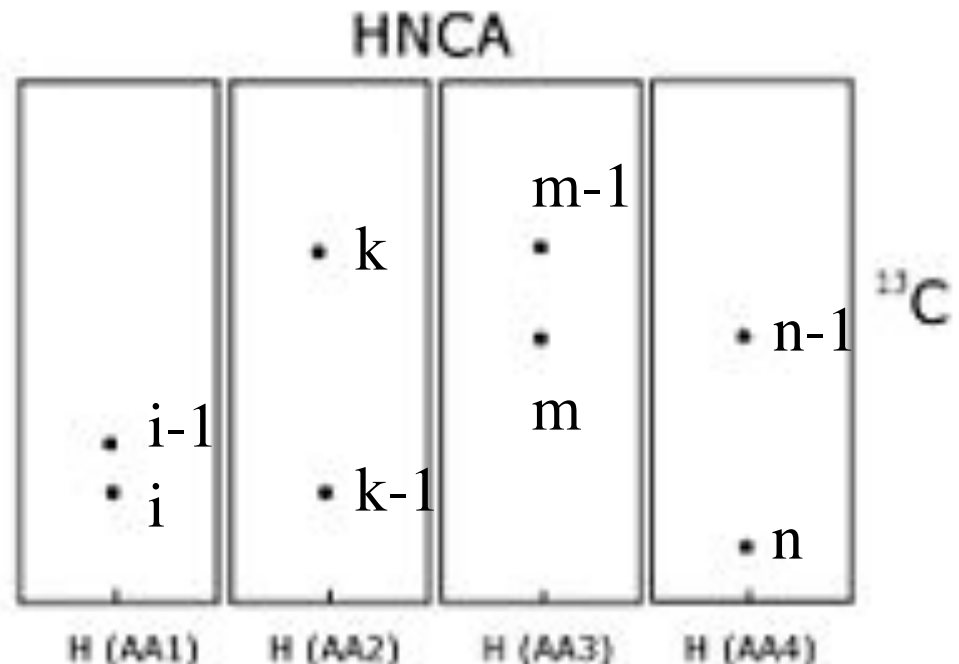


Triple Resonance Pairs

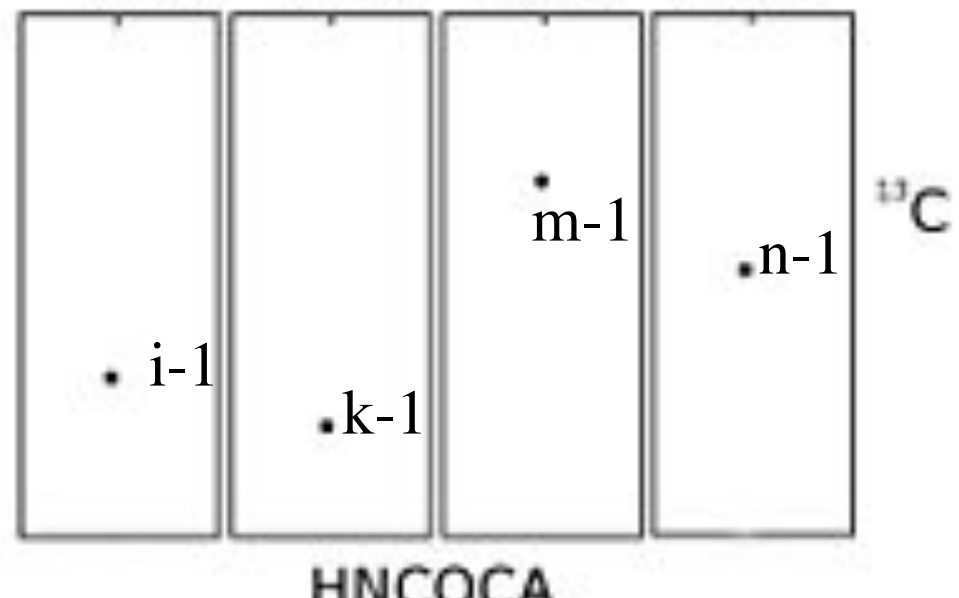
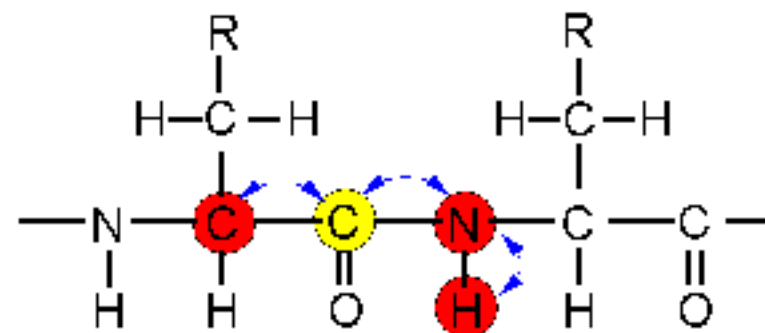
Residue i-1



Residue i



HN(CO)CA



sequential correlation only

THE RANGE OF ^{13}C CHEMICAL SHIFTS OBSERVED FOR EIGHT DIFFERENT PROTEINS

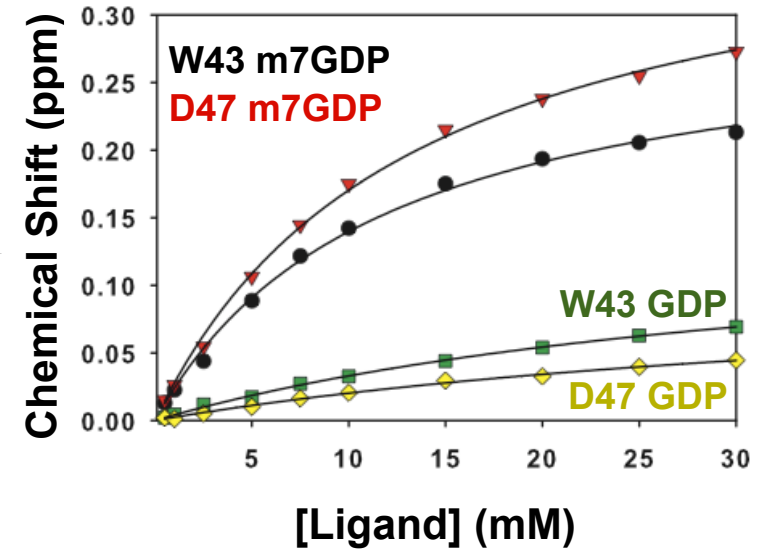
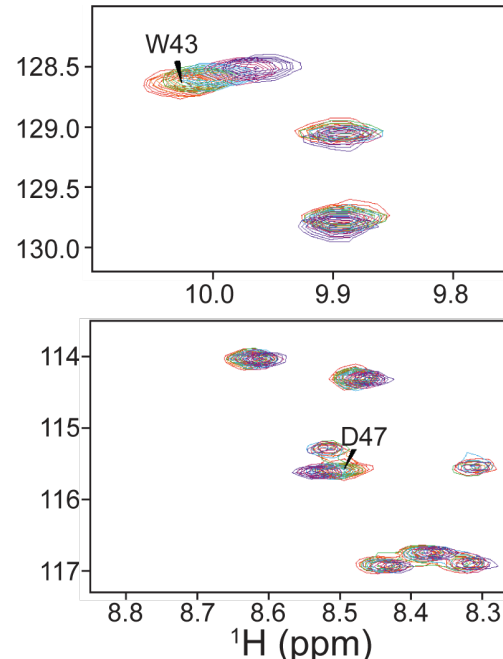
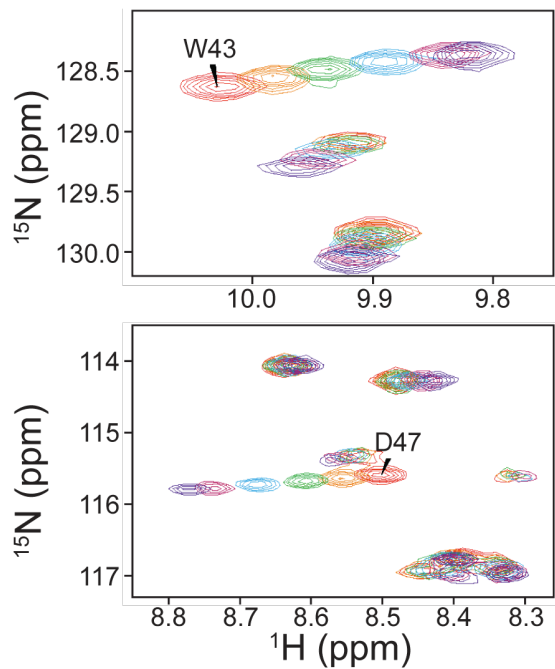
Res.	α	β	γ	δ	ϵ
Gly	42-48				
Ala	49-56	18-24			
Ser	55-62	61-67			
Thr	58-68	66-73	19-26		
Val	57-67	30-37	16-25		
Leu	51-60	39-48	22-29	21-28	
Ile	55-66	34-47	25-31	14-22	9-16
Lys	52-61	29-37	21-26	27-34	40-43
Arg	50-60	28-35	25-30	41-45	
Pro	60-67	27-35	24-29	49-53	
Glu	52-62	27-34	32-38		
.
.
.

WAGNER AND BRUHWILER, 1986...et al.

Or http://www.bmrb.wisc.edu/ref_info/statsel.htm

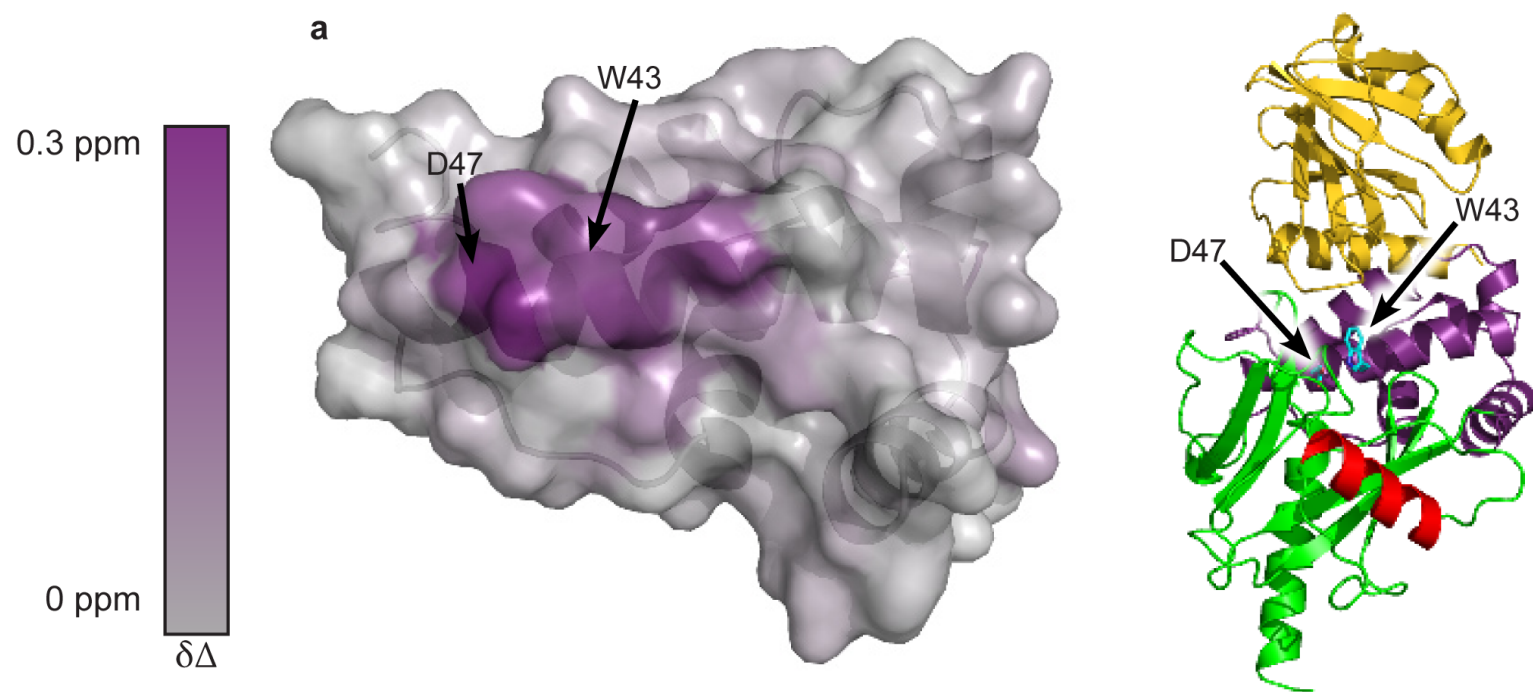
Part II:
Macromolecular Interactions
Detected by NMR

Binding of nucleotide to protein



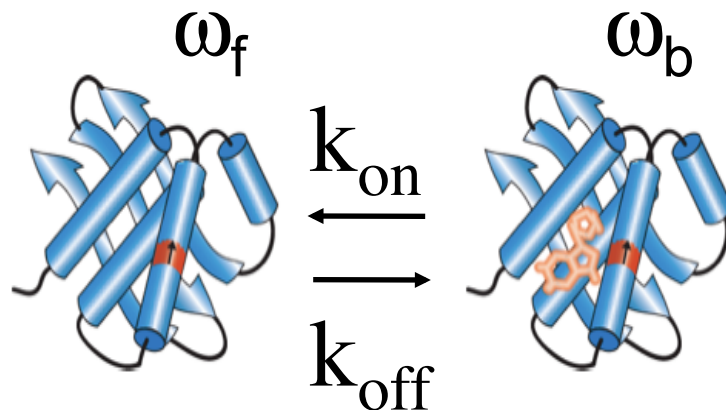
Dose dependent resonance shifts
can be fit to obtain K_d

Shifts may be color coded onto surface to identify ligand binding site



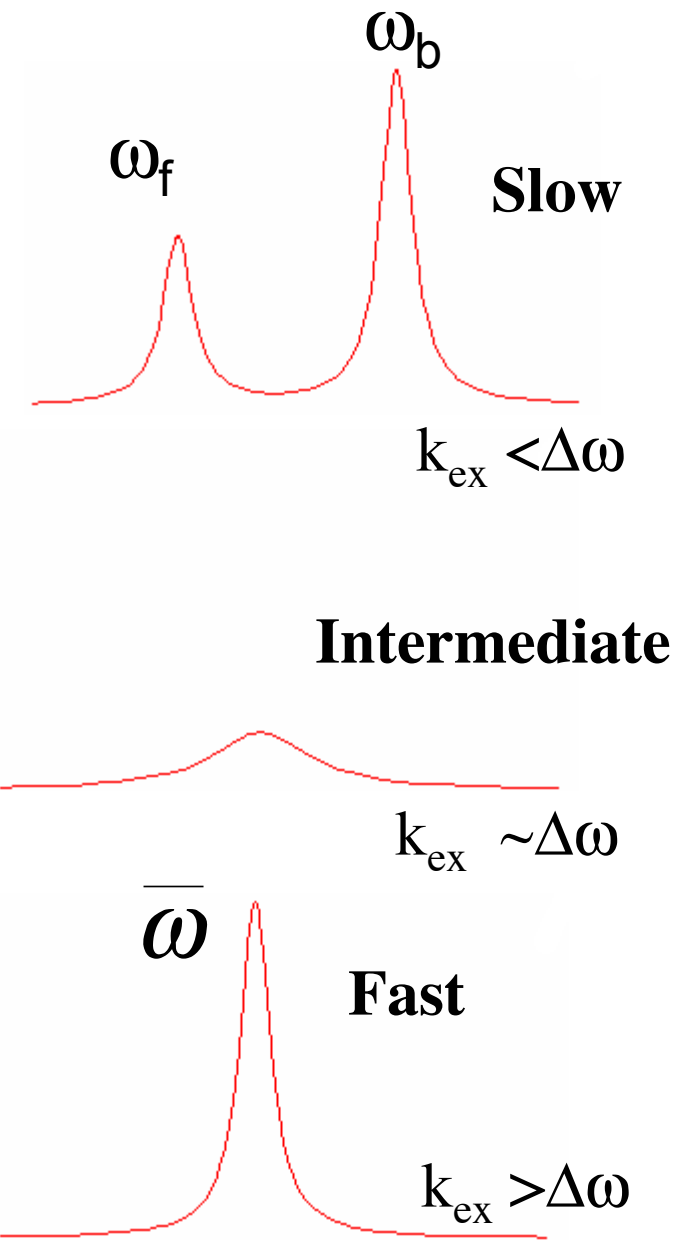
Caveats?

NMR to monitor ligand binding



$$k_{\text{ex}} = k_{\text{on}}[L] + k_{\text{off}}$$

$$\Delta\omega = \omega_f - \omega_b$$

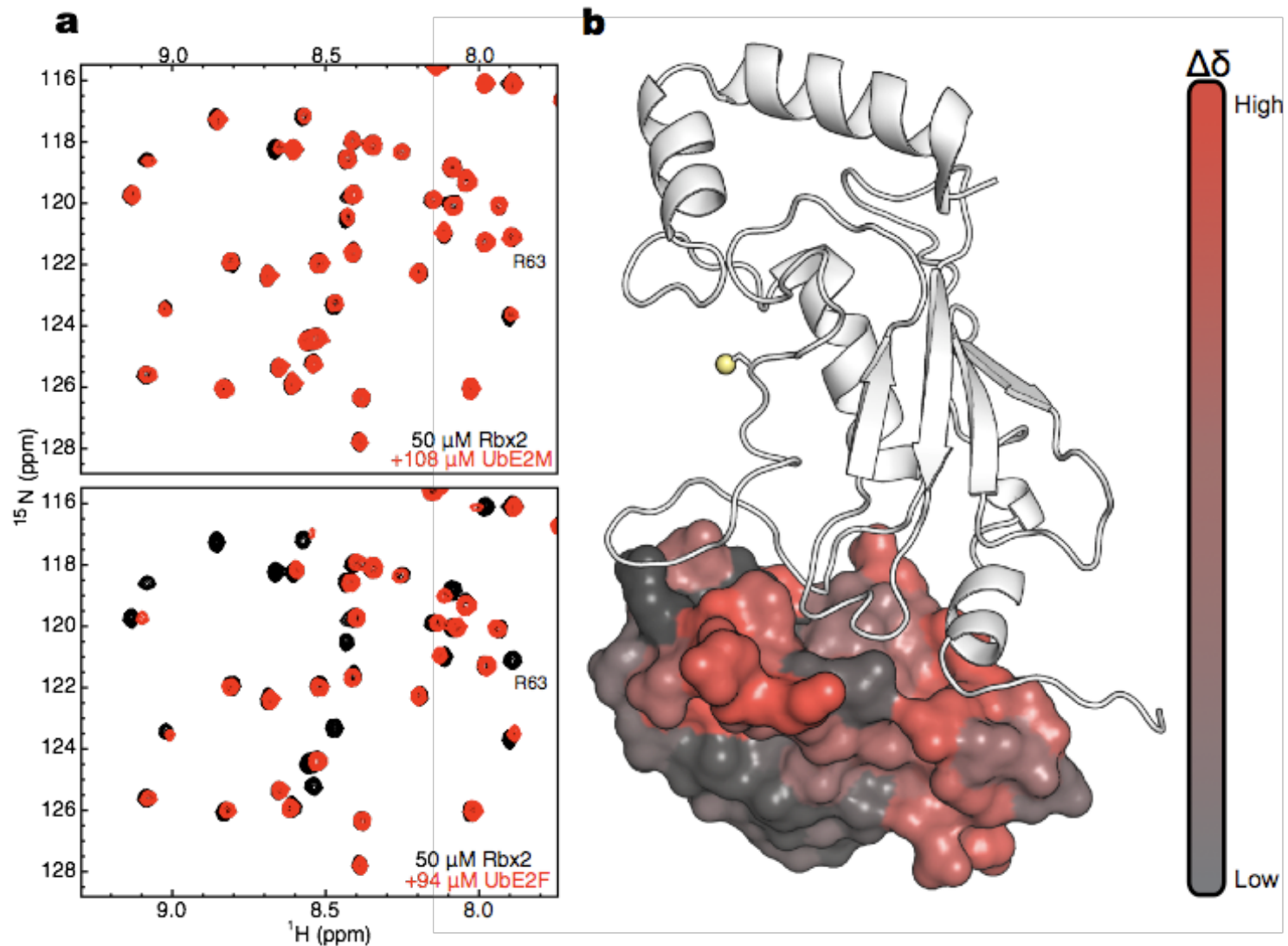


Fraction bound of labeled protein

$$P_b = \frac{\bar{\omega} - \omega_f}{\omega_b - \omega_f} = \frac{[L]}{[L] + K_d}$$

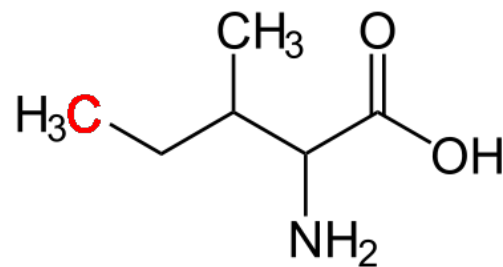
$\bar{\omega}$: observed chemical shift

Monitoring Protein/Protein Interactions by HSQC

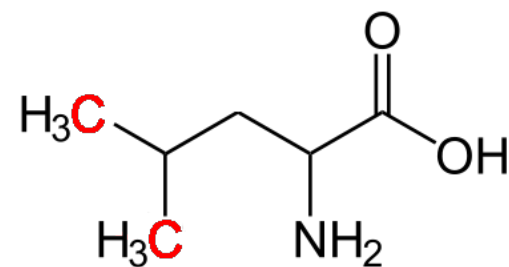


Sparse Labeling to Simplify Spectra

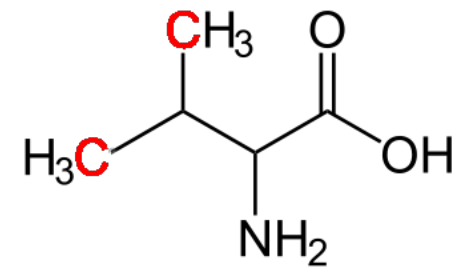
Selectively label R group methyls with C-13 (NMR visible)



Isoleucine



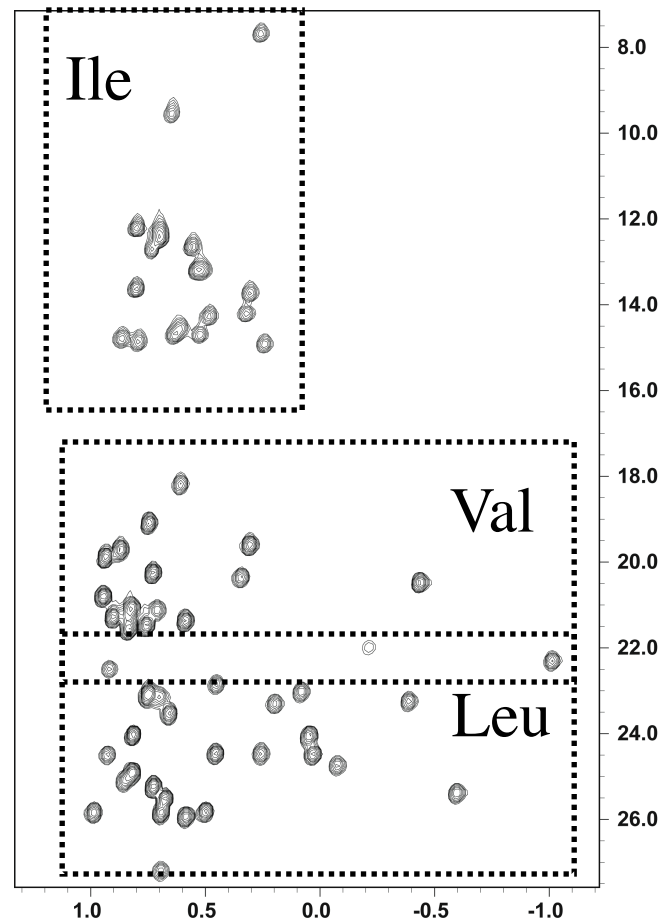
Leucine



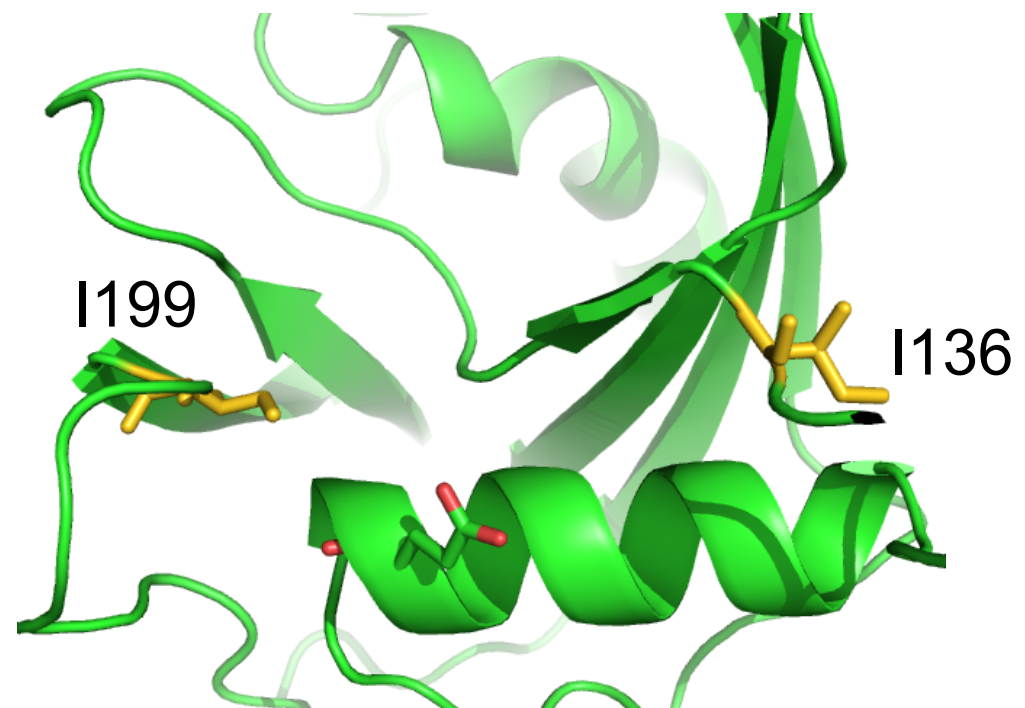
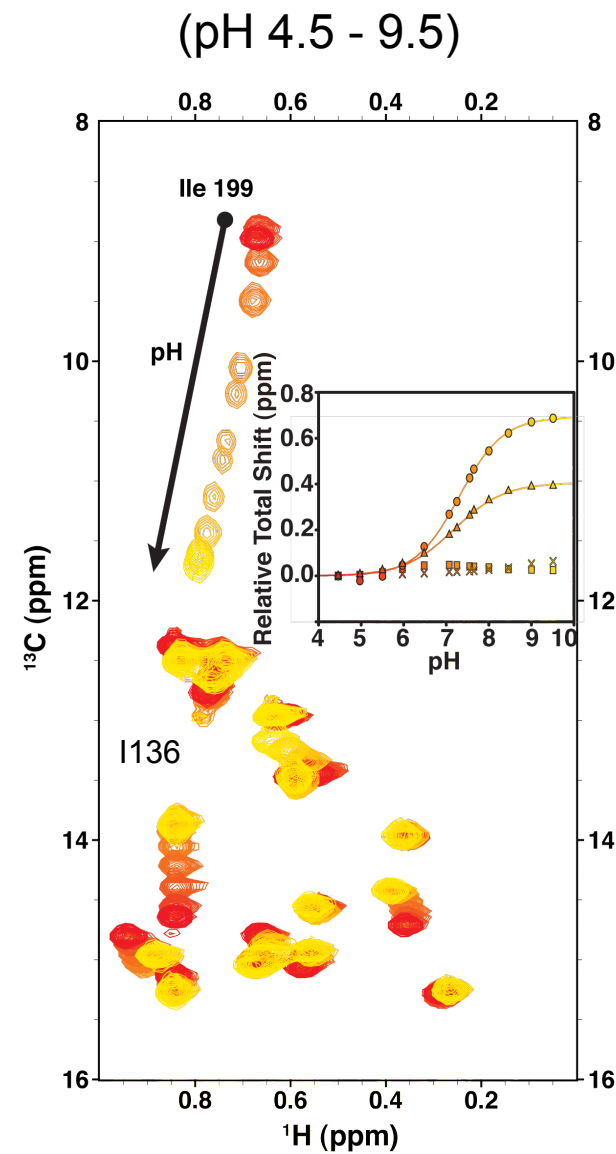
Valine

(add alpha-ketoacid precursors to ILV 30 minutes prior to induction)

^{13}C HSQC of ILV labeled protein



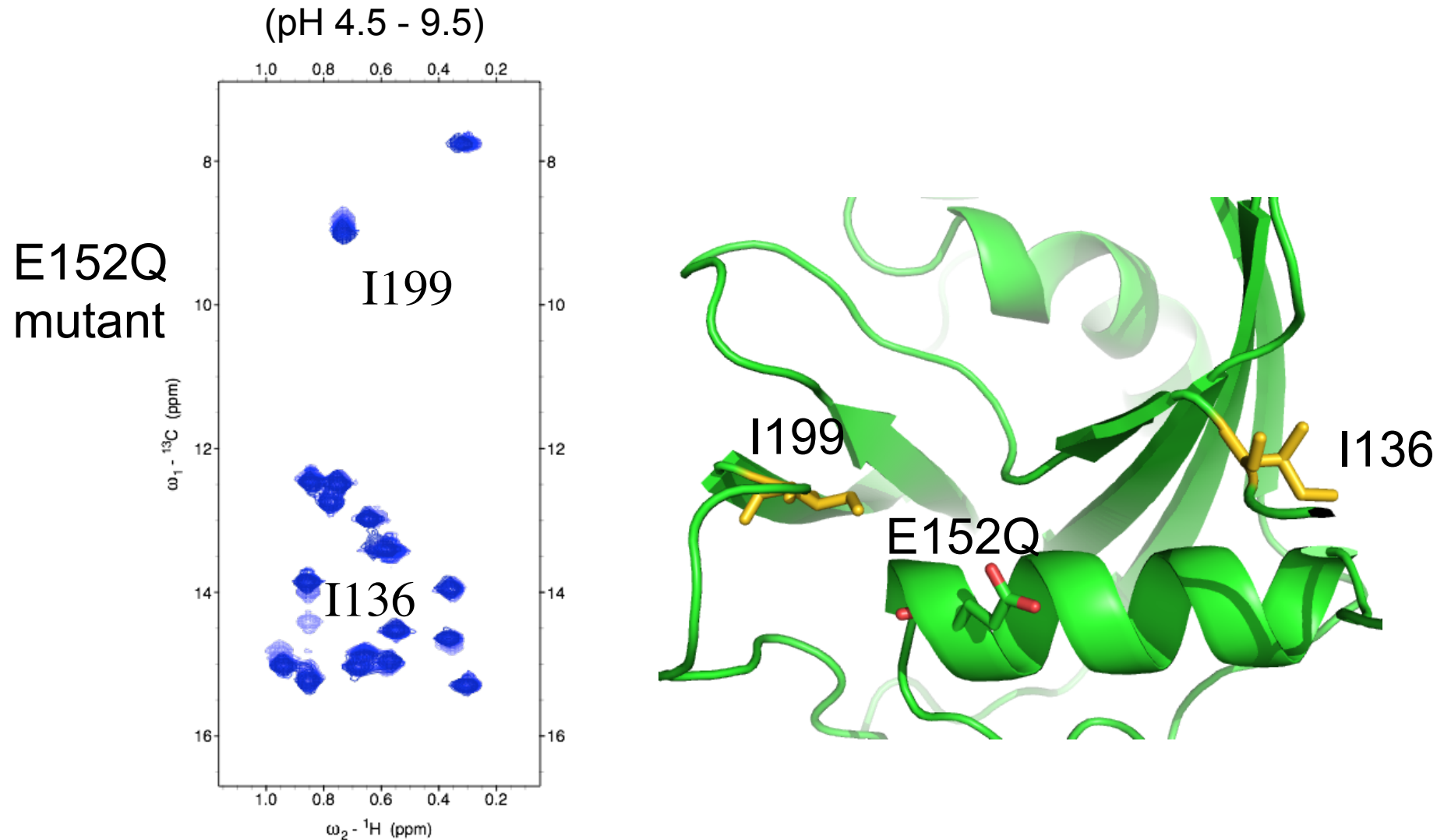
Measuring pKa by NMR



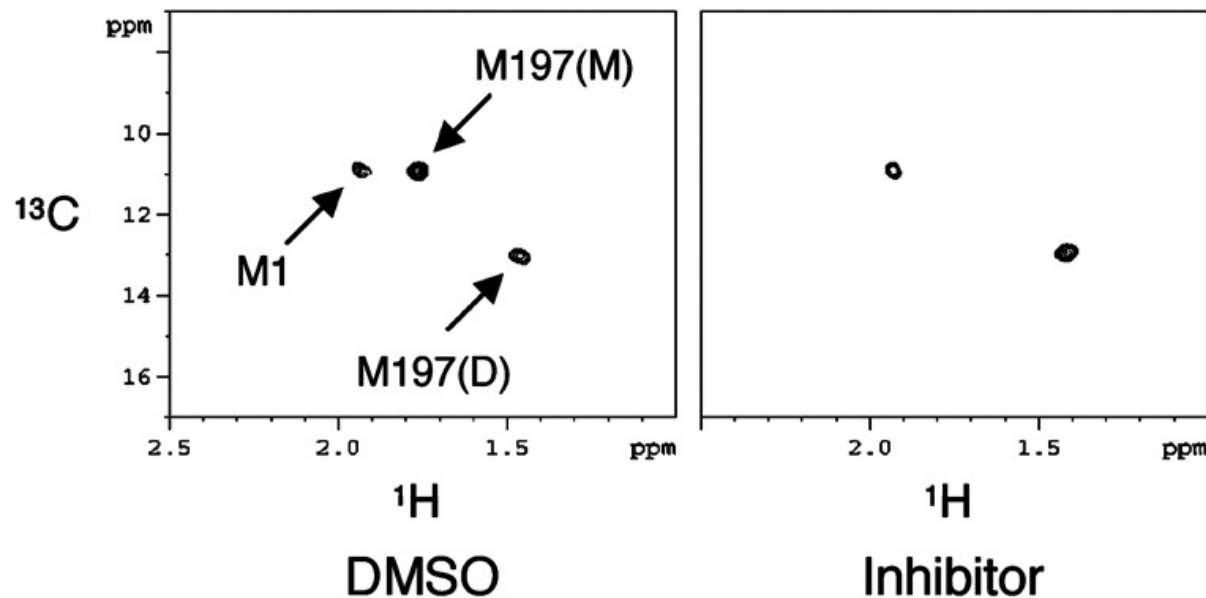
pKa of 7.2, elevated for Glu

Aglietti et al, Structure 2013

Identification of titratable residue by site-directed mutagenesis and NMR



Example of slow exchange: monomer-dimer equilibrium



Inhibition of KSHV Pr
stabilizes
the dimeric conformation

Methionine specific labeling simplifies analysis

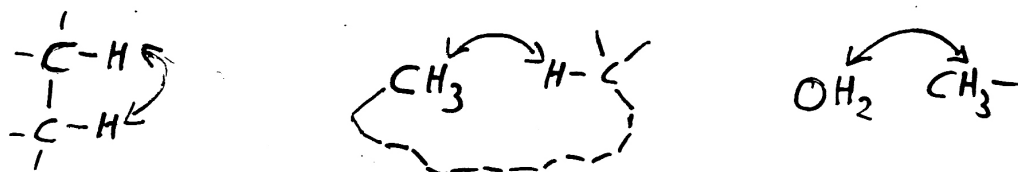
Marnett A. B. et.al. PNAS
2004;101:6870-6875

Part III: Structure by NMR

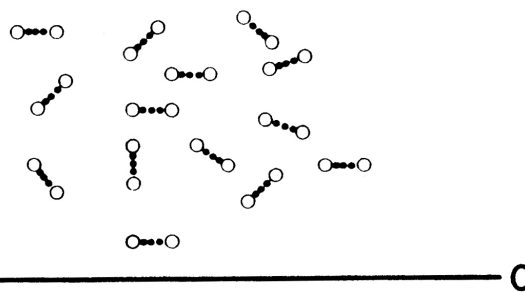
Calculating 3D structures: we need distance measurements & assignments

$$NOE = f(\varepsilon_c) \cdot \frac{1}{r^6}$$

We can see distances that are
 $\leq 5 \text{ \AA}$

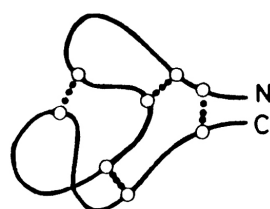


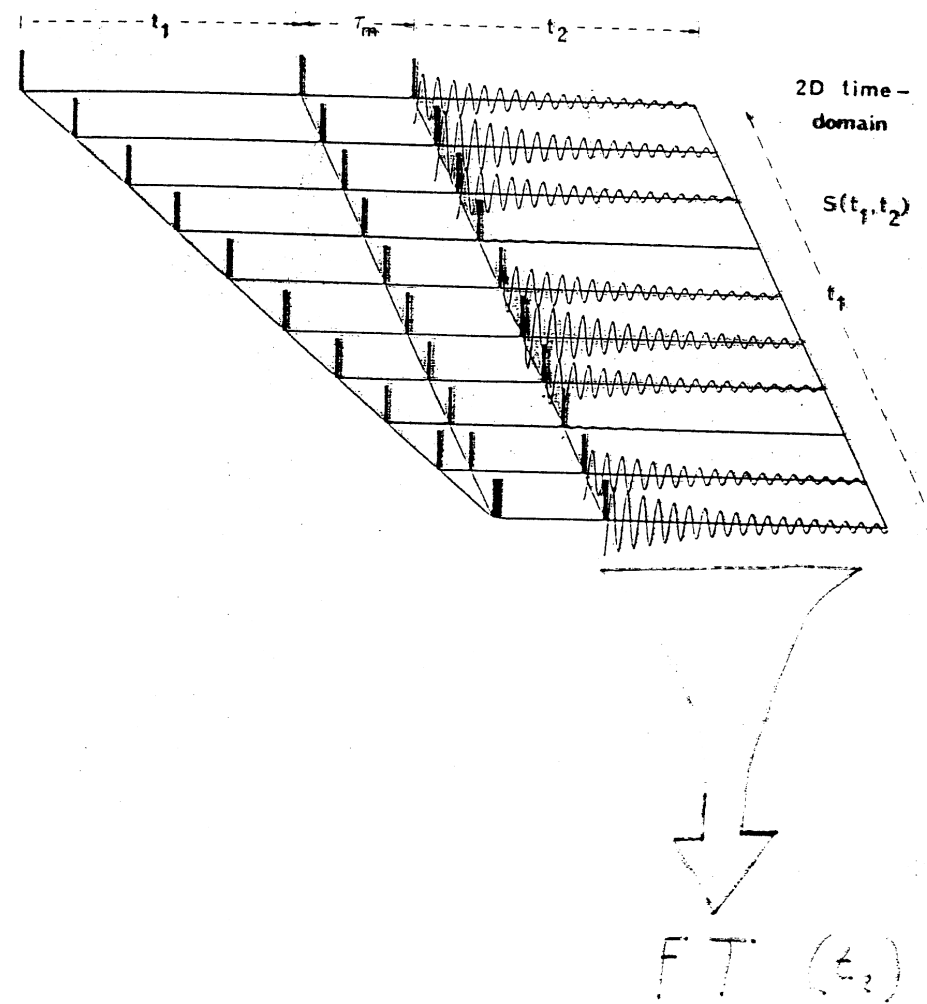
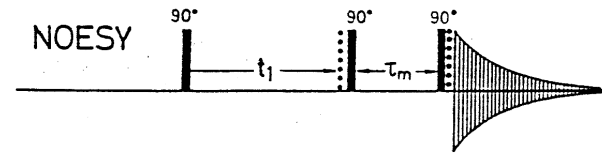
NO ASSIGNMENTS



N ————— C

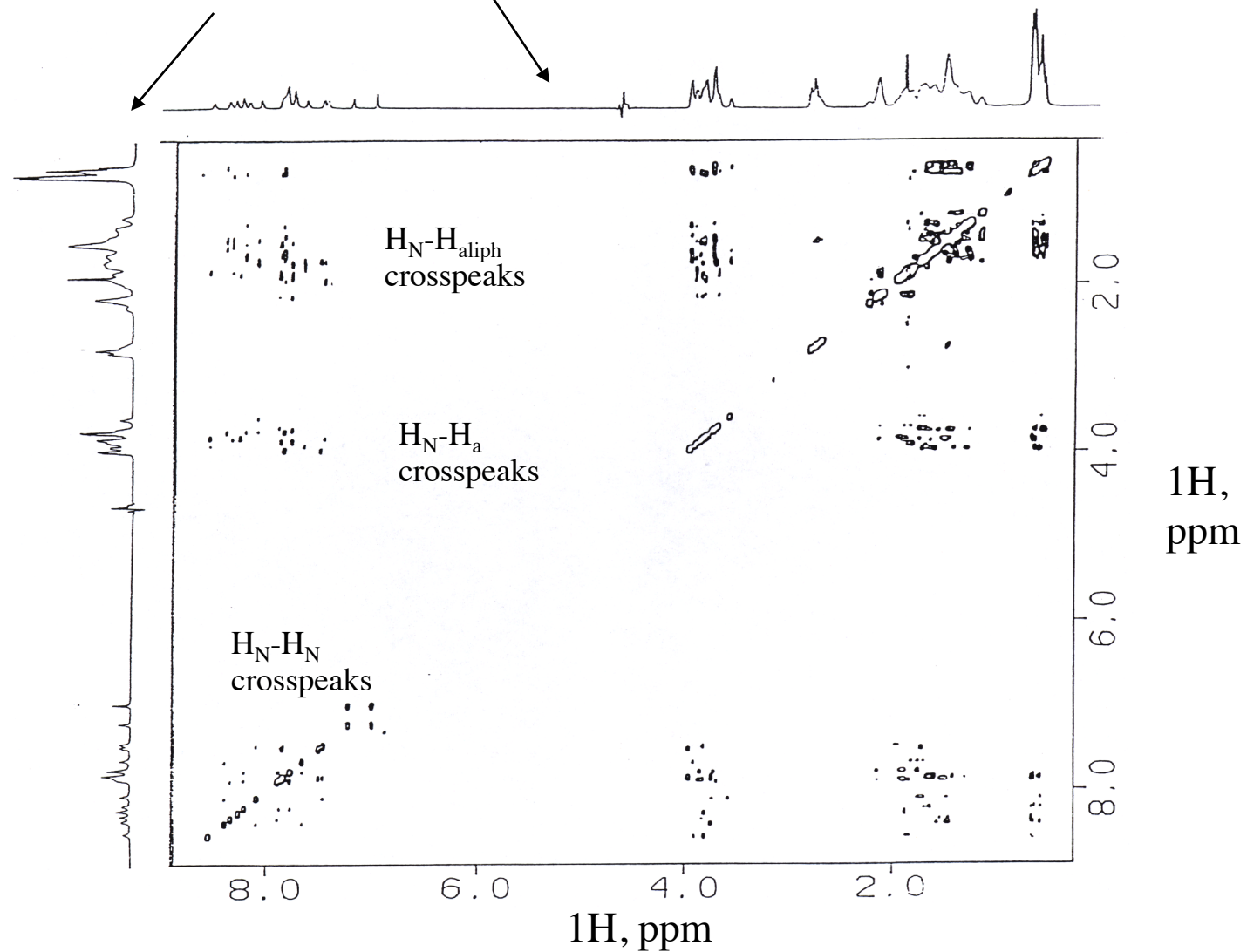
WITH ASSIGNMENTS





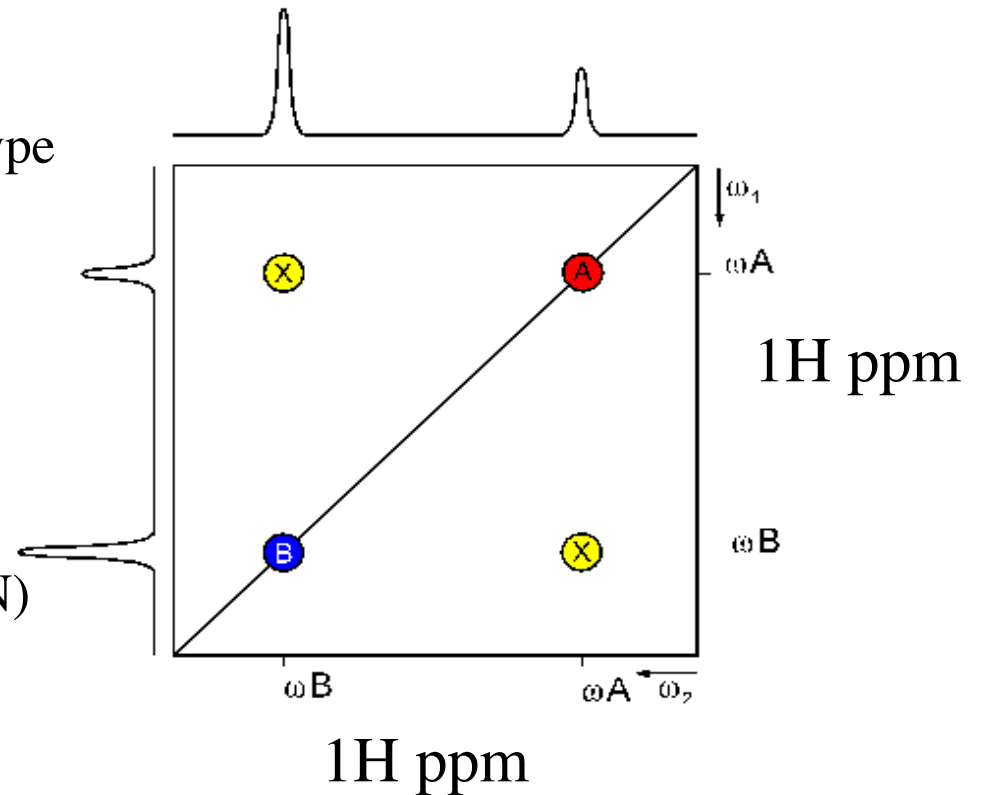
A Real 2D NOE Experiment of a Small Peptide

A projection through both dimensions gives a 1D spectrum



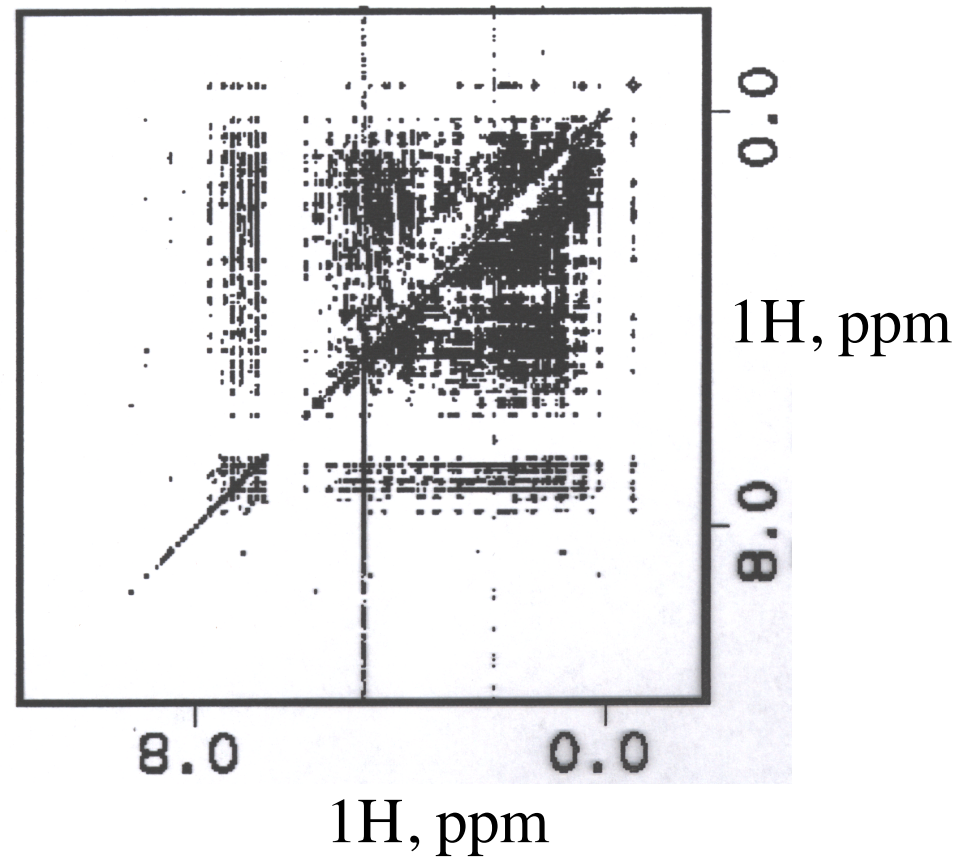
Interpretation of 2D NMR Spectra

- Crosspeaks are a measure of some type of interaction between 2 spins (NOE, J-coupling....)
- The intensity of the crosspeak often quantifies the interaction.
- A heteronuclear experiment (^1H - ^{15}N) would not have diagonal crosspeaks.



Higher Dimensionality 3 and 4D Heteronuclear Experiments on Isotopically Labeled (¹⁵N-¹³C) Proteins

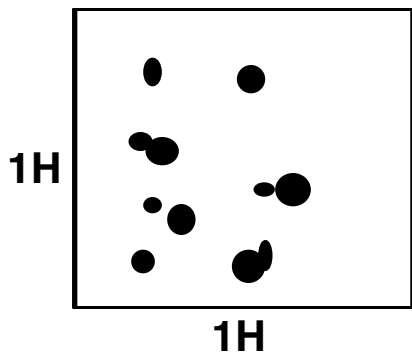
2D NOESY of a 76 residue protein homodimer (effectively 18kD) in D₂O



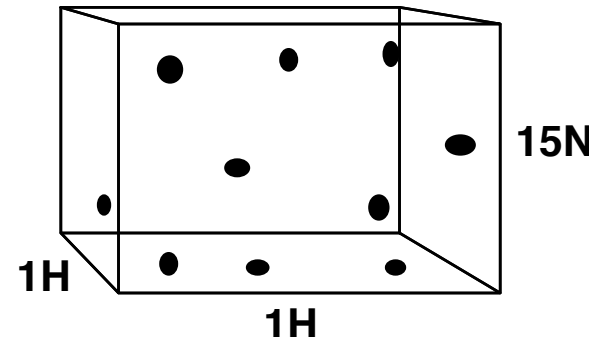
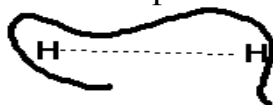
In practice, even small proteins have very crowded 2D spectra making assignment very difficult. In this case the fact that it is in D₂O simplifies the spectra because the amide protons exchange for deuterium and are not visible.

Benefit of C13 and N15 labeling of Proteins for NMR

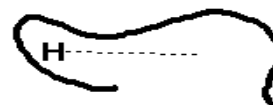
Higher Dimensionality (3 and 4D) Experiments Reduce Overlap Compared to 2D Experiments



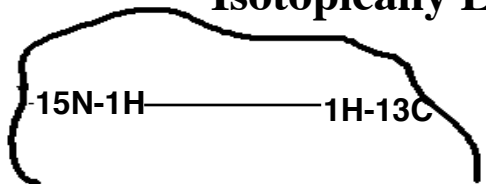
2D nOe Expt. on unlabeled protein



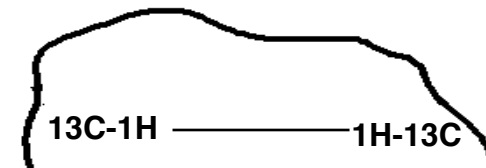
3D nOe Expt. on N15-labeled protein



Many More Types of Experiments Can be Done on Isotopically Labeled Protein



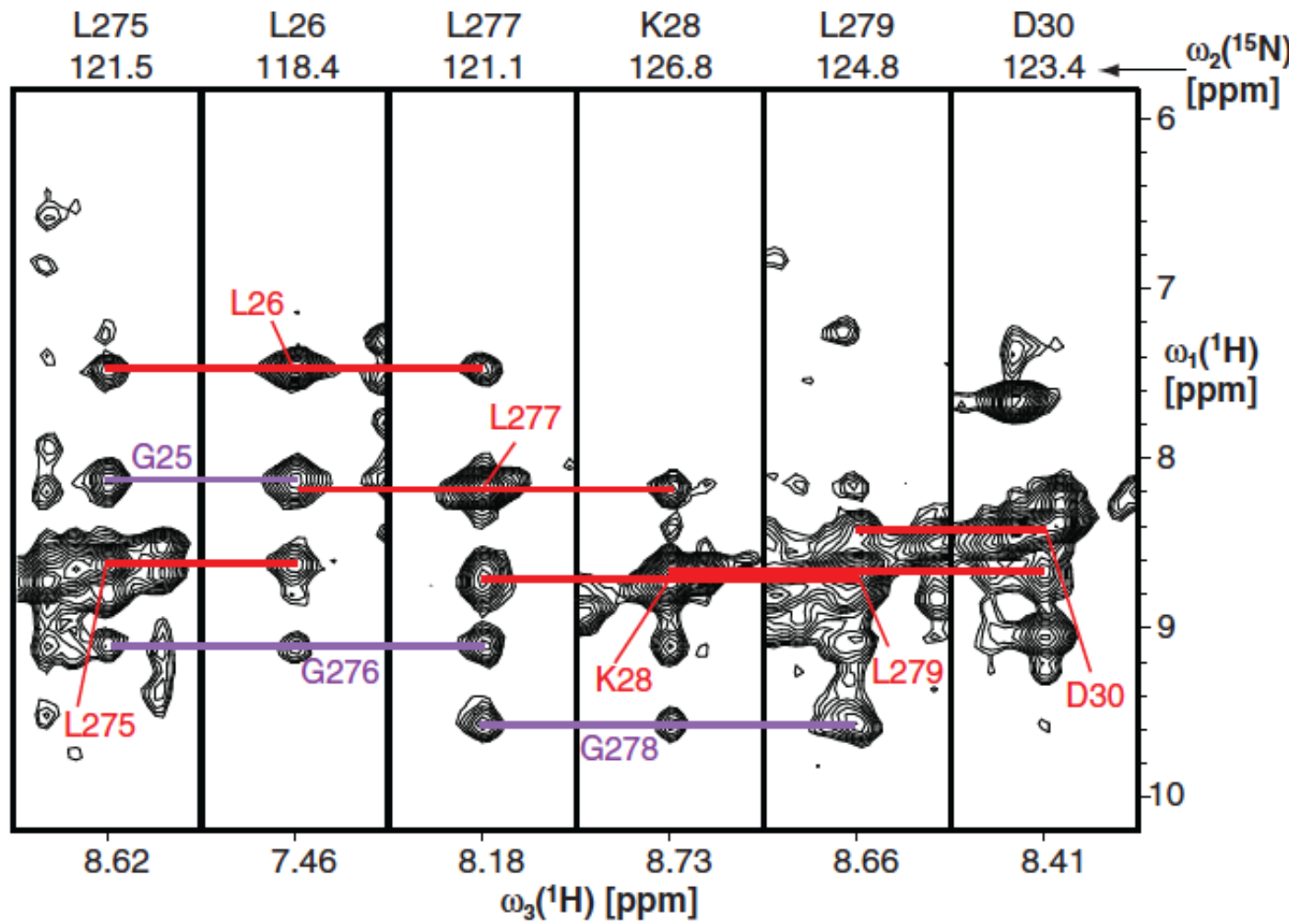
nOes between Protons Attached to N15 and Protons Attached to 13C



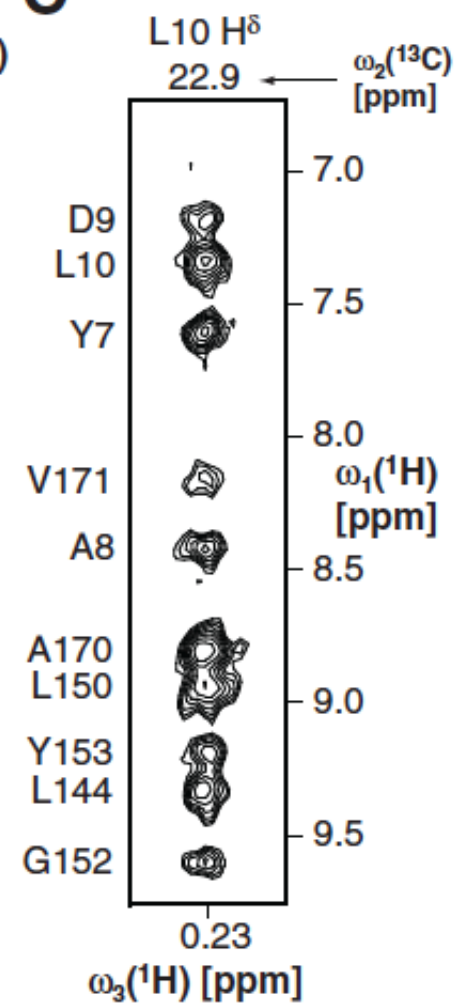
nOes between Protons Attached to 13C and Protons Attached to 13C

Examples of ^{15}N and ^{13}C dispersed NOESY

B



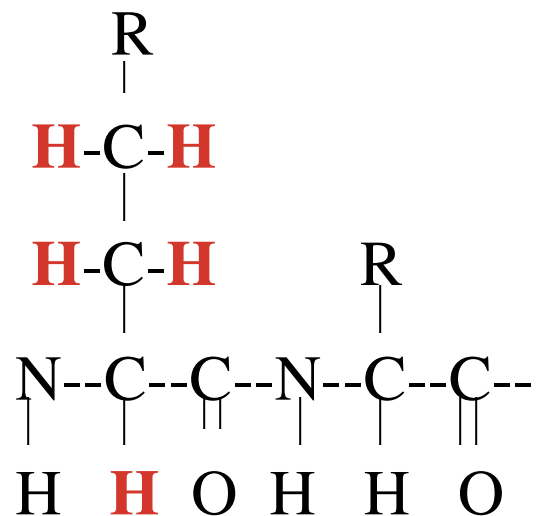
C



15N NOESY-HSQC

13C NOESY-HSQC

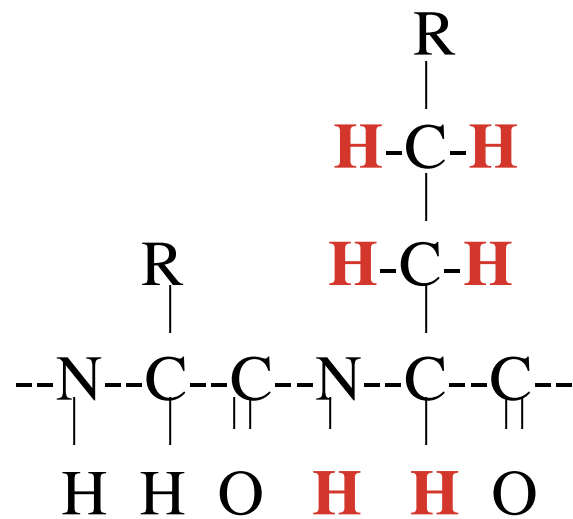
Side-chain protein assignments



H(CCO)NH-TOCSY

i - 1 res.

All Carbon's H's at i-1 to
N-H pair.

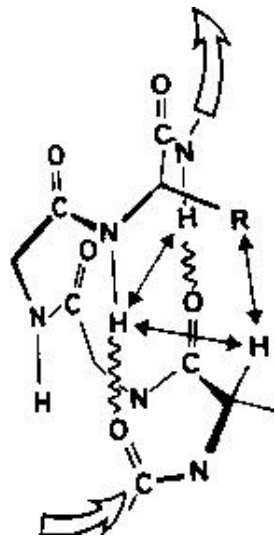


^{15}N -TOCSY i res.

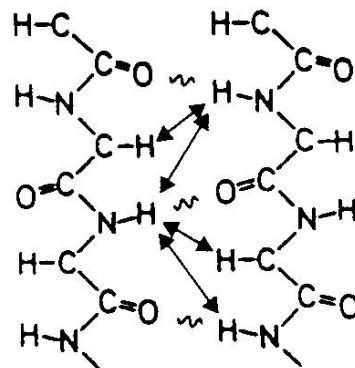
All H's at i to N-H pair.

TOCSY methods relies on
through-bond J Couplings

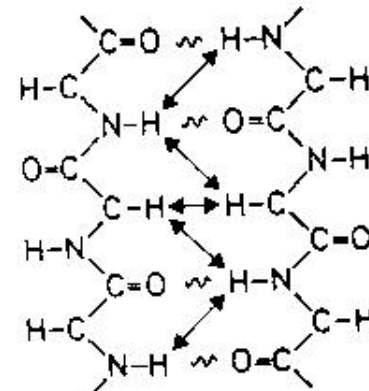
Close interatomic distances in secondary structures



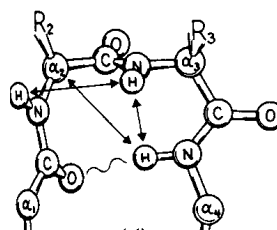
alpha-helix



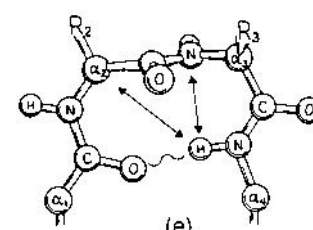
parallel beta-sheet



antiparallel
beta-sheet



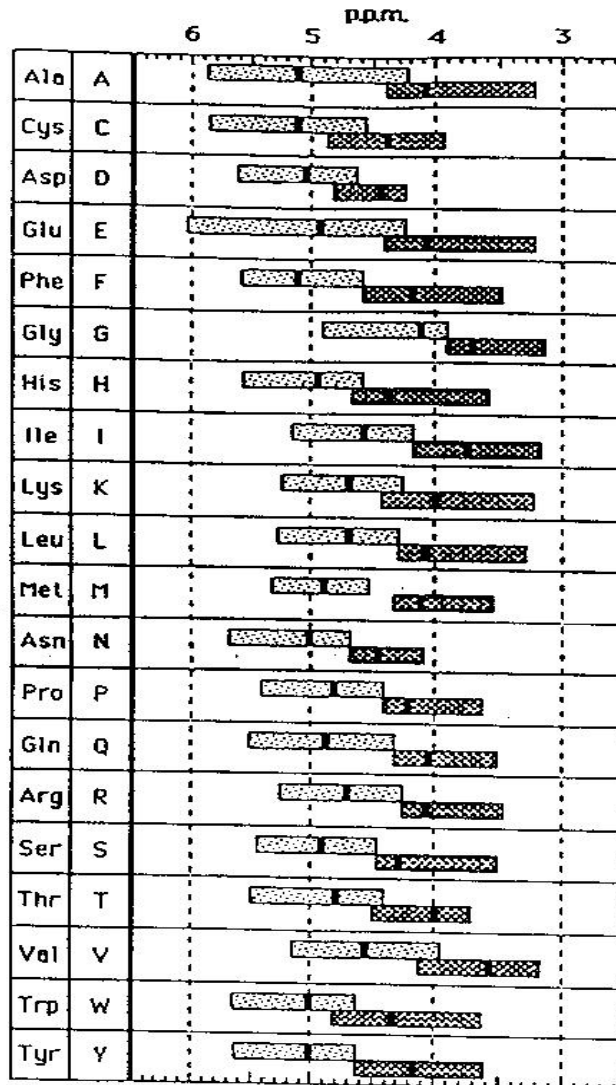
type I turn



type II turn

H^a chemical shifts and secondary structure

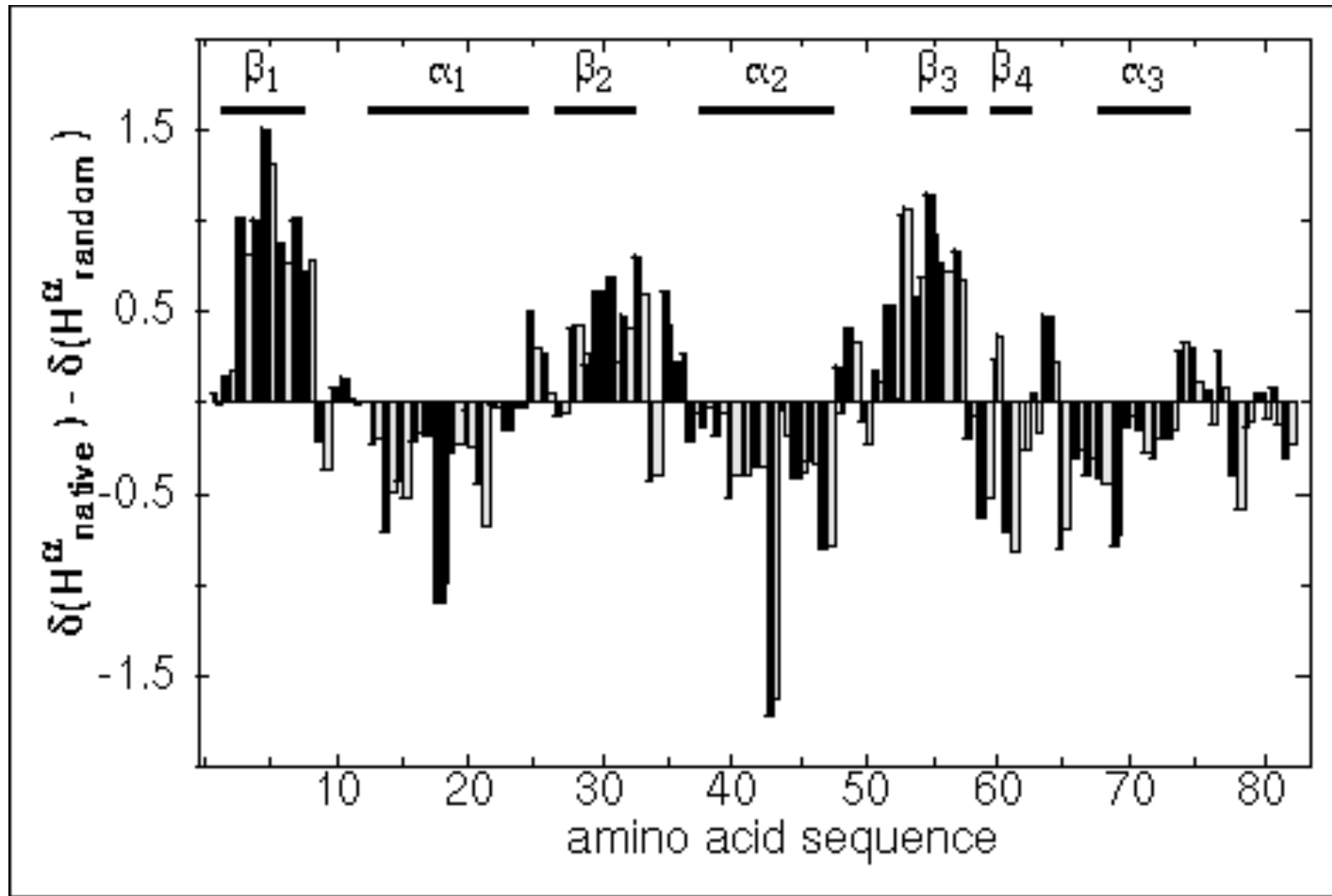
- the figure at right shows distributions of H^achemical shifts observed in sheets (lighter bars) and helices (darker bars).
- H^a chemical shifts in α -helices are on average **0.39 ppm below** “random coil” values, while β -sheet values are **0.37 ppm above** random coil values.



Wishart, Sykes & Richards

J Mol Biol (1991) **222**, 311 .

Secondary Shift vs Sequence



Reveals secondary structure !

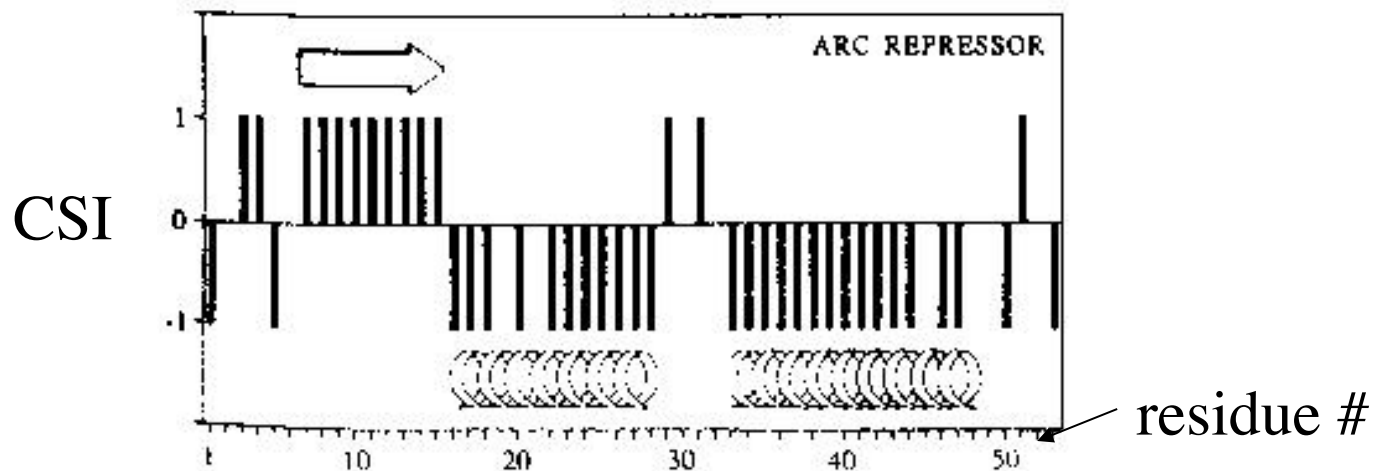
Chemical shift index (CSI)

- trends like these led to the development of the concept of the *chemical shift index** as a tool for assigning secondary structure using chemical shift values.
- one starts with a **table of reference values** for each amino-acid type, which is essentially a table of “random coil” H^a values
- CSI's are then assigned as follows:

<u>exp' tl H^a shift rel. to reference</u>	<u>assigned CSI</u>
within ± 0.1 ppm	0
>0.1 ppm lower	-1
>0.1 ppm higher	+1

*Wishart, Sykes & Richards *Biochemistry* (1992) **31**, 1647-51.

Chemical shift indices



- any “dense” grouping of four or more “-1’ s”, uninterrupted by “1’ s” is assigned as a helix, while any “dense” grouping of three or more “1’ s”, uninterrupted by “-1’ s”, is assigned as a sheet.
- a “dense” grouping means at least 70% nonzero CSI’ s.
- other one regions are assigned as “coil”
- **this simple technique assigns 2ndary structure w/90-95% accuracy**
- similar useful relationships exist for $^{13}\text{C}^{\alpha}$, $^{13}\text{C}^{\text{C=O}}$ shifts

3D structure calculation

- NMR provides information about structure
 - chemical shifts \Leftrightarrow local electronic environment
 - coupling constants \Leftrightarrow torsion angles
 - NOE, ROE \Leftrightarrow interproton distances
 - residual dipolar couplings \Leftrightarrow bond orientation
- and dynamics
 - relaxation times
 - NOE, ROE
- Most of the data describe
 - local environment of the protons
 - relative to each other
 - not the global conformation of the molecule

- **Distance**

NOE: The distance between i and j is a function of the NOE intensity $D_{ij} \sim C(\text{NOE}_{ij})^{-6}$

H-bonds: Identified by slowly exchanging amide H_N protons

- **Angles**

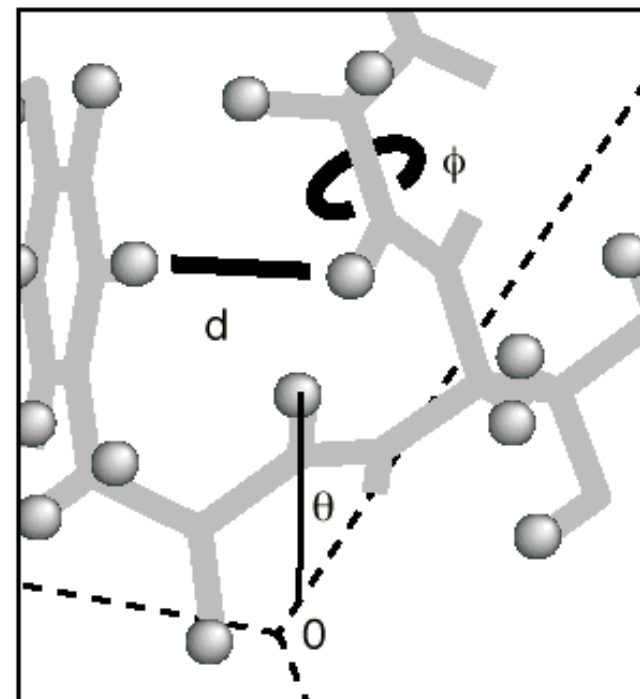
Side Chain ? and backbone torsion identified from J-coupling experiments

Chemical Shift also gives Angular Information

- **Residual Dipolar Couplings**

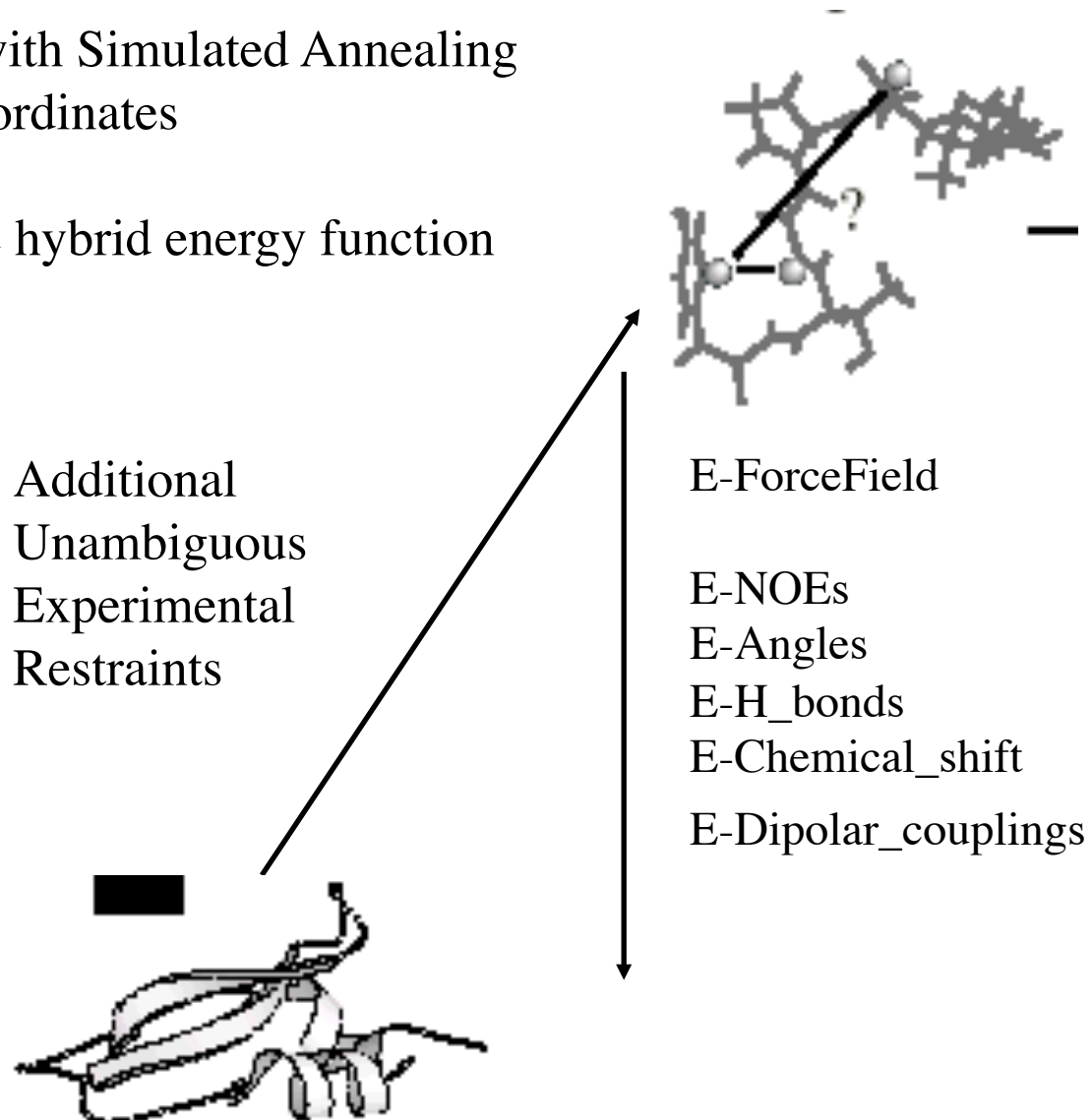
Bond Orientations Relative to an Alignment Tensor

Experimental data from NMR



3D structure calculation

- Molecular Dynamics with Simulated Annealing starting from random coordinates
- Goal is to minimize the hybrid energy function



The hybrid energy function

- Structure calculation = minimization of hybrid energy function (target function) which combines
 1. different experimental data
 2. *a priori* information (force field)

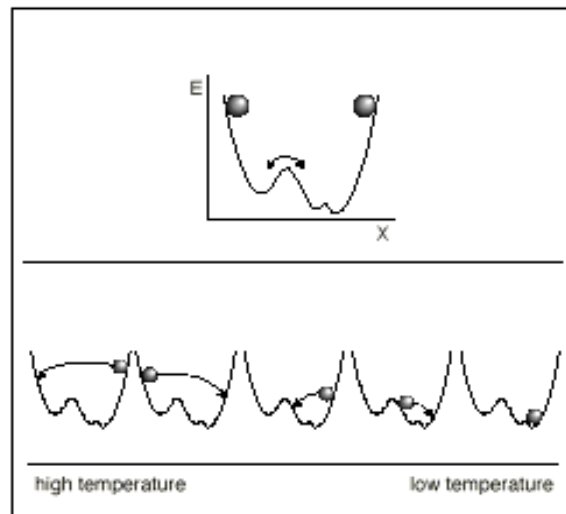
$$\begin{aligned}E_{hybrid} &= \sum_l w_l E_l = \\&\quad w_{bond} E_{bond} \\&+ w_{angle} E_{angle} \\&+ w_{improper} E_{improper} \\&+ w_{nonbonded} E_{nonbonded} \\&+ w_{unambig} E_{unambig} + w_{ambig} E_{ambig} + \dots \\&+ w_{torsion} E_{torsion} \\&+ w_{Jcoup} E_{Jcoup} \\&+ w_{RDC} E_{RDC} + \dots\end{aligned}$$

Minimization by molecular dynamics

- MD solves Newton's eqns. of motion:

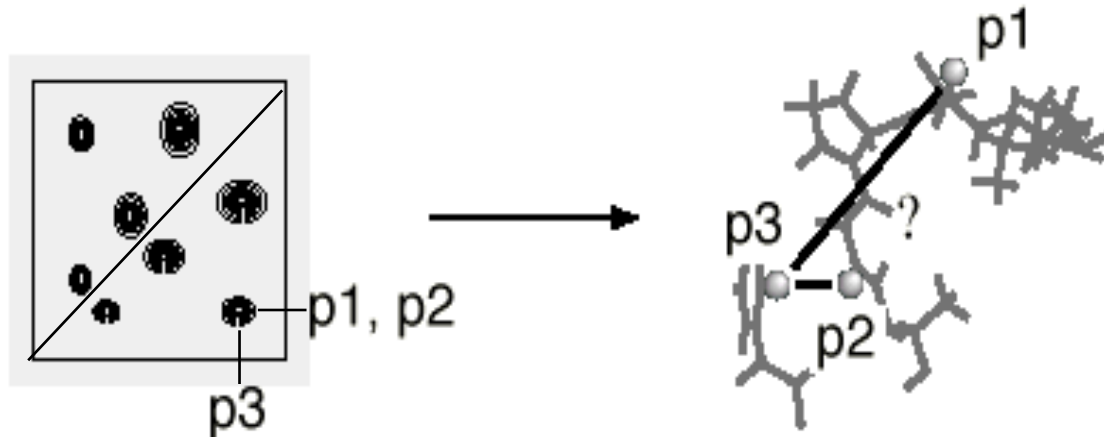
$$\frac{d^2\vec{r}_i}{dt^2} = -\frac{c}{m_i} \frac{\partial}{\partial \vec{r}_i} E_{hybrid}$$

- Molecular dynamics can overcome local energy barriers



- Temperature control and variation:
minimization by simulated annealing

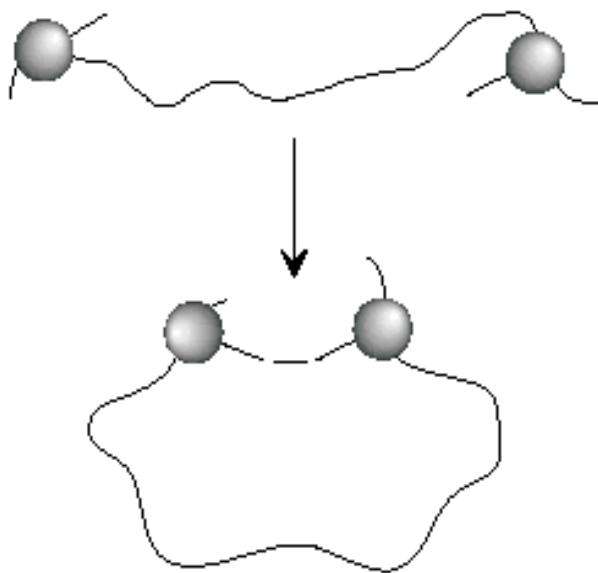
NOE ambiguities



- Key problem is ambiguity in NOE assignments
- Need for higher dimensional data: 3D & 4D
- Need for heteronuclear data
- Need for better calculational strategies that can deal with ambiguous data

Errors in data: error bounds

- Cumulative error in D_{ij} is treated by using loose error bounds $L \dots U$
- Precise value not (too) critical:
loose bounds restrict conformational space

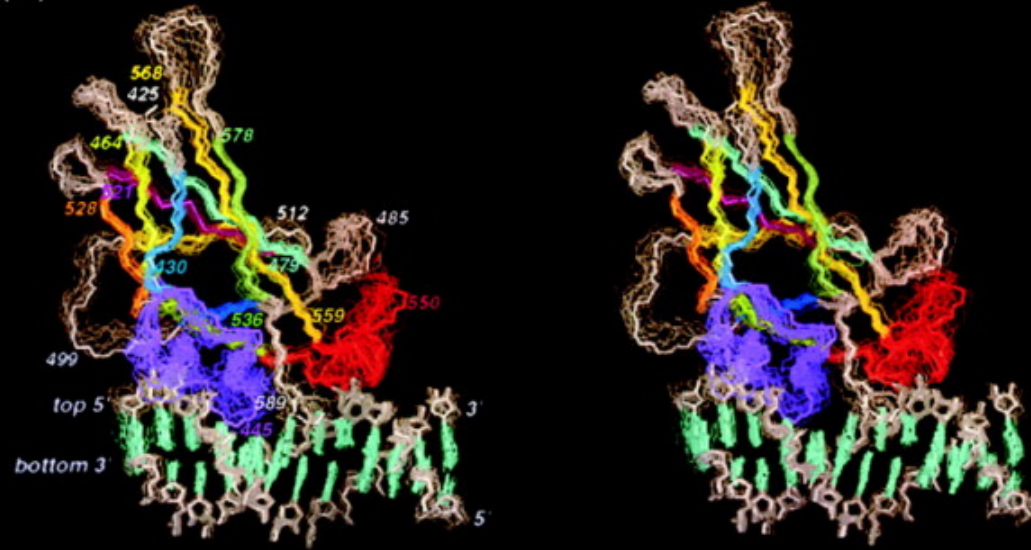


- However, consequences for:
 - precision of structure

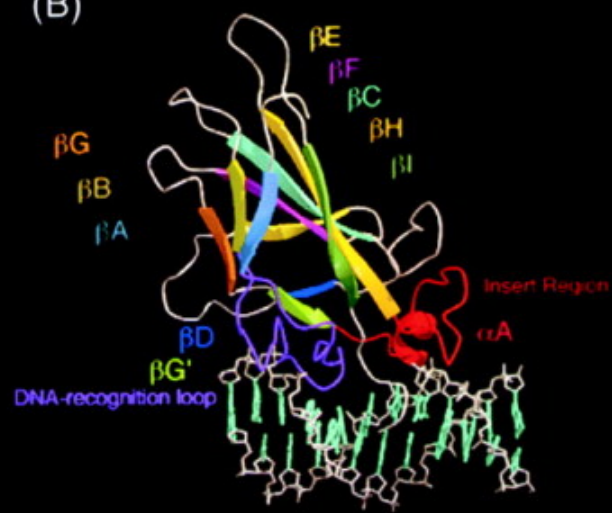
# residues	# restraints/residue
------------	----------------------

Solution Structure of the Core NFATC1/DNA Complex

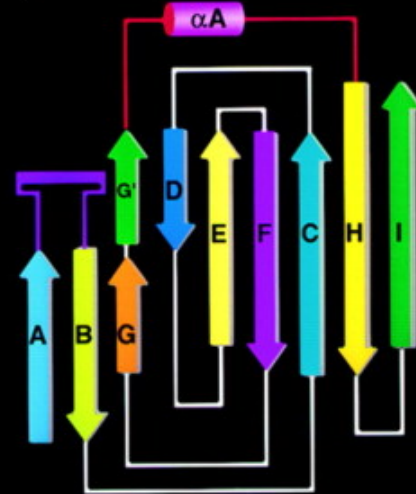
(A)



(B)



(C)



Zhou et al, Cell , 1998

Need to evaluate restraint numbers, violations and precision

Table 1. Structural Statistics for NFATC1-DBD*/DNA Complex

Protein		
Amino acids residues sequentially assigned (nonproline)	162 of 167	
Effective distance constraints	1050	
Intraresidue	236	
Sequential ($i_i - j_i = 1$)	374	
Medium-range ($i_i - j_i \leq 4$)	86	
Long-range ($i_i - j_i \geq 5$)	272	
H bonds	82	
Dihedral angle constraints	363	
DNA		
Effective distance constraints	276	
Intraresidue	146	
Sequential	131	
Interstrand	1	
H bond	58	
Protein-DNA interface		
Effective distance constraints	56	
Distance constraint violations > 0.2 Å (per structure)	1.81 ± 2.07	
Dihedral constraint violations > 3.0° (per structure)	1.44 ± 0.96	
X-PLOR potential energy (E_{LJ} , Kcal/mol, avg. per structure)	-501 ± 28.9	
R.m.s.d. to the mean for backbone heavy atoms of all β strands		
(residues 428–432, 460–464, 472–479, 493–495, 506–510, 515–521, 528–538, 559–568, 578–583)	0.62 ± 0.07	
R.m.s.d. to the mean for heavy atoms of all β strands		
(residues 428–432, 460–464, 472–479, 493–495, 506–510, 515–521, 528–538, 559–568, 578–583)	1.20 ± 0.14	
R.m.s.d. to the mean for backbone heavy atoms		
(residues 425–590)	1.14 ± 0.11	
R.m.s.d. to the mean for heavy atoms		
(residues 425–590)	1.58 ± 0.10	
R.m.s.d. to the mean for DNA heavy atoms		
(superposition of all DNA heavy atoms)	0.83 ± 0.21	
R.m.s.d. to the mean for protein + DNA heavy atoms		
(superposition of all β strand heavy atoms and DNA heavy atoms)	1.20 ± 0.16	
Ramachandran plot ^a		
	<u>Residues 425–590</u>	<u>Secondary Structures</u>
Most favorable region	60.4%	83.7%
Additionally allowed region	38.9%	14.0%
Generously allowed region	0.7%	2.3%
Disallowed region	0.0%	0.0%

How were restraints measured?

^a Laskowski et al., 1996.

Analysis of Table

Table 1. Structural Statistics for NFATC1-DBD*/DNA Complex

Protein		
Amino acids residues sequentially assigned (nonproline)	162 of 167	
Effective distance constraints	1050	(circled in red)
Intraresidue	236	
Sequential ($i_i - j_i = 1$)	374	
Medium-range ($i_i - j_i \leq 4$)	86	
Long-range ($i_i - j_i \geq 5$)	272	
H bonds	82	
Dihedral angle constraints	363	
DNA		
Effective distance constraints	276	
Intraresidue	146	
Sequential	131	
Interstrand	1	
H bond	58	
Protein-DNA interface		
Effective distance constraints	56	
Distance constraint violations $> 0.2 \text{ \AA}$ (per structure)	1.81 ± 2.07	
Dihedral constraint violations $> 3.0^\circ$ (per structure)	1.44 ± 0.96	
X-PLOR potential energy (E_{LJ} , Kcal/mol, avg. per structure)	-501 ± 28.9	
R.m.s.d. to the mean for backbone heavy atoms of all β strands		
(residues 428–432, 460–464, 472–479, 493–495, 506–510, 515–521, 528–538, 559–568, 578–583)	0.62 ± 0.07	
R.m.s.d. to the mean for heavy atoms of all β strands		
(residues 428–432, 460–464, 472–479, 493–495, 506–510, 515–521, 528–538, 559–568, 578–583)	1.20 ± 0.14	
R.m.s.d. to the mean for backbone heavy atoms		
(residues 425–590)	1.14 ± 0.11	
R.m.s.d. to the mean for heavy atoms		
(residues 425–590)	1.58 ± 0.10	
R.m.s.d. to the mean for DNA heavy atoms		
(superposition of all DNA heavy atoms)	0.83 ± 0.21	
R.m.s.d. to the mean for protein + DNA heavy atoms		
(superposition of all β strand heavy atoms and DNA heavy atoms)	1.20 ± 0.16	
Ramachandran plot ^a		
	<u>Residues 425–590</u>	<u>Secondary Structures</u>
Most favorable region	60.4%	83.7%
Additionally allowed region	38.9%	14.0%
Generously allowed region	0.7%	2.3%
Disalloweed region	0.0%	0.0%

^a Laskowski et al., 1996.

How many NOE restraints?

>6 per residue is acceptable

Analysis of Table

Table 1. Structural Statistics for NFATC1-DBD*/DNA Complex

Protein		
Amino acids residues sequentially assigned (nonproline)		162 of 167
Effective distance constraints		1050
Intraresidue		236
Sequential ($i_i - j_i = 1$)		374
Medium-range ($i_i - j_i \leq 4$)		86
Long-range ($i_i - j_i \geq 5$)		272
H bonds		82
Dihedral angle constraints		363
DNA		
Effective distance constraints		276
Intraresidue		146
Sequential		131
Interstrand		1
H bond		58
Protein-DNA interface		
Effective distance constraints		56
Distance constraint violations $> 0.2 \text{ \AA}$ (per structure)		1.81 ± 2.07
Dihedral constraint violations $> 3.0^\circ$ (per structure)		1.44 ± 0.96
X-PLOR potential energy (E_{LJ} , Kcal/mol, avg. per structure)		-501 ± 28.9
R.m.s.d. to the mean for backbone heavy atoms of all β strands		
(residues 428–432, 460–464, 472–479, 493–495, 506–510, 515–521, 528–538, 559–568, 578–583)		0.62 ± 0.07
R.m.s.d. to the mean for heavy atoms of all β strands		
(residues 428–432, 460–464, 472–479, 493–495, 506–510, 515–521, 528–538, 559–568, 578–583)		1.20 ± 0.14
R.m.s.d. to the mean for backbone heavy atoms		
(residues 425–590)		1.14 ± 0.11
R.m.s.d. to the mean for heavy atoms		
(residues 425–590)		1.58 ± 0.10
R.m.s.d. to the mean for DNA heavy atoms		
(superposition of all DNA heavy atoms)		0.83 ± 0.21
R.m.s.d. to the mean for protein + DNA heavy atoms		
(superposition of all β strand heavy atoms and DNA heavy atoms)		1.20 ± 0.16
Ramachandran plot^a		
	<u>Residues 425–590</u>	<u>Secondary Structures</u>
Most favorable region	60.4%	83.7%
Additionally allowed region	38.9%	14.0%
Generously allowed region	0.7%	2.3%
Disallowed region	0.0%	0.0%

^a Laskowski et al., 1996.

How are NOE restraints distributed?

Reading the NMR Statistics Structure Table

Table 1. Structural Statistics for NFATC1-DBD*/DNA Complex

Protein		
Amino acids residues sequentially assigned (nonproline)	162 of 167	
Effective distance constraints	1050	
Intraresidue	236	
Sequential ($i_i - j_i = 1$)	374	
Medium-range ($i_i - j_i \leq 4$)	86	
Long-range ($i_i - j_i \geq 5$)	272	
H bonds	82	
Dihedral angle constraints	363	
DNA		
Effective distance constraints	276	
Intraresidue	146	
Sequential	131	
Interstrand	1	
H bond	58	1
Protein-DNA interface		
Effective distance constraints	56	
Distance constraint violations $> 0.2 \text{ \AA}$ (per structure)	1.81 ± 2.07	
Dihedral constraint violations $> 3.0^\circ$ (per structure)	1.44 ± 0.96	
X-PLOR potential energy (E_{LJ} , Kcal/mol, avg. per structure)	-501 ± 28.9	
R.m.s.d. to the mean for backbone heavy atoms of all β strands (residues 428–432, 460–464, 472–479, 493–495, 506–510, 515–521, 528–538, 559–568, 578–583)	0.62 ± 0.07	
R.m.s.d. to the mean for heavy atoms of all β strands (residues 428–432, 460–464, 472–479, 493–495, 506–510, 515–521, 528–538, 559–568, 578–583)	1.20 ± 0.14	
R.m.s.d. to the mean for backbone heavy atoms (residues 425–590)	1.14 ± 0.11	
R.m.s.d. to the mean for heavy atoms (residues 425–590)	1.58 ± 0.10	
R.m.s.d. to the mean for DNA heavy atoms (superposition of all DNA heavy atoms)	0.83 ± 0.21	
R.m.s.d. to the mean for protein + DNA heavy atoms (superposition of all β strand heavy atoms and DNA heavy atoms)	1.20 ± 0.16	
Ramachandran plot^a		
	<u>Residues 425–590</u>	<u>Secondary Structures</u>
Most favorable region	60.4%	83.7%
Additionally allowed region	38.9%	14.0%
Generously allowed region	0.7%	2.3%
Disallowed region	0.0%	0.0%

How were H Bonds Determined?

^a Laskowski et al., 1996.

Reading the NMR Statistics Structure Table

Table 1. Structural Statistics for NFATC1-DBD*/DNA Complex

Protein		
Amino acids residues sequentially assigned (nonproline)		162 of 167
Effective distance constraints		1050
Intraresidue		236
Sequential ($ i - j = 1$)		374
Medium-range ($ i - j \leq 4$)		86
Long-range ($ i - j \geq 5$)		272
H bonds		82
Dihedral angle constraints		363
DNA		
Effective distance constraints		276
Intraresidue		146
Sequential		131
Interstrand		1
H bond		58
Protein-DNA interface		
Effective distance constraints		56
Distance constraint violations > 0.2 Å (per structure)		1.81 ± 2.07
Dihedral constraint violations > 3.0° (per structure)		1.44 ± 0.96
X-PLOR potential energy (E_{LJ} , Kcal/mol, avg. per structure)		-501 ± 28.9
R.m.s.d. to the mean for backbone heavy atoms of all β strands		
(residues 428–432, 460–464, 472–479, 493–495, 506–510, 515–521, 528–538, 559–568, 578–583)		0.62 ± 0.07
R.m.s.d. to the mean for heavy atoms of all β strands		
(residues 428–432, 460–464, 472–479, 493–495, 506–510, 515–521, 528–538, 559–568, 578–583)		1.20 ± 0.14
R.m.s.d. to the mean for backbone heavy atoms		
(residues 425–590)		1.14 ± 0.11
R.m.s.d. to the mean for heavy atoms		
(residues 425–590)		1.58 ± 0.10
R.m.s.d. to the mean for DNA heavy atoms		
(superposition of all DNA heavy atoms)		0.83 ± 0.21
R.m.s.d. to the mean for protein + DNA heavy atoms		
(superposition of all β strand heavy atoms and DNA heavy atoms)		1.20 ± 0.16
Ramachandran plot ^a		
	<u>Residues 425–590</u>	<u>Secondary Structures</u>
Most favorable region	60.4%	83.7%
Additionally allowed region	38.9%	14.0%
Generously allowed region	0.7%	2.3%
Disalloweed region	0.0%	0.0%

How many intermolecular NOEs?

^a Laskowski et al., 1996.

Reading the NMR Statistics Structure Table

Table 1. Structural Statistics for NFATC1-DBD*/DNA Complex

Protein		
Amino acids residues sequentially assigned (nonproline)		162 of 167
Effective distance constraints		1050
Intraresidue		236
Sequential ($ i - j = 1$)		374
Medium-range ($ i - j \leq 4$)		86
Long-range ($ i - j \geq 5$)		272
H bonds		82
Dihedral angle constraints		363
DNA		
Effective distance constraints		276
Intraresidue		146
Sequential		131
Interstrand		1
H bond		58
Protein-DNA interface		
Effective distance constraints		56
Distance constraint violations > 0.2 Å (per structure)		1.81 ± 2.07
Dihedral constraint violations > 3.0° (per structure)		1.44 ± 0.96
X-PLOR potential energy (E_{LJ} , Kcal/mol, avg. per structure)		-501 ± 28.9
R.m.s.d. to the mean for backbone heavy atoms of all β strands		
(residues 428–432, 460–464, 472–479, 493–495, 506–510, 515–521, 528–538, 559–568, 578–583)		0.62 ± 0.07
R.m.s.d. to the mean for heavy atoms of all β strands		
(residues 428–432, 460–464, 472–479, 493–495, 506–510, 515–521, 528–538, 559–568, 578–583)		1.20 ± 0.14
R.m.s.d. to the mean for backbone heavy atoms		
(residues 425–590)		1.14 ± 0.11
R.m.s.d. to the mean for heavy atoms		
(residues 425–590)		1.58 ± 0.10
R.m.s.d. to the mean for DNA heavy atoms		
(superposition of all DNA heavy atoms)		0.83 ± 0.21
R.m.s.d. to the mean for protein + DNA heavy atoms		
(superposition of all β strand heavy atoms and DNA heavy atoms)		1.20 ± 0.16
Ramachandran plot ^a		
	<u>Residues 425–590</u>	<u>Secondary Structures</u>
Most favorable region	60.4%	83.7%
Additionally allowed region	38.9%	14.0%
Generously allowed region	0.7%	2.3%
Disalloweed region	0.0%	0.0%

^a Laskowski et al., 1996.

Criteria for publication:
 No distance violations >0.5 Å
 No dihedral angle violations >5°

How many
 violations ?

1.81 ± 2.07
 1.44 ± 0.96
 -501 ± 28.9

Read methods section to evaluate table

Resonance Assignments

1-HNCA/HN(CO)CA
2-Amino-acid specific labeling
3-NOESY experiments:
Homonuclear and heteronuclear

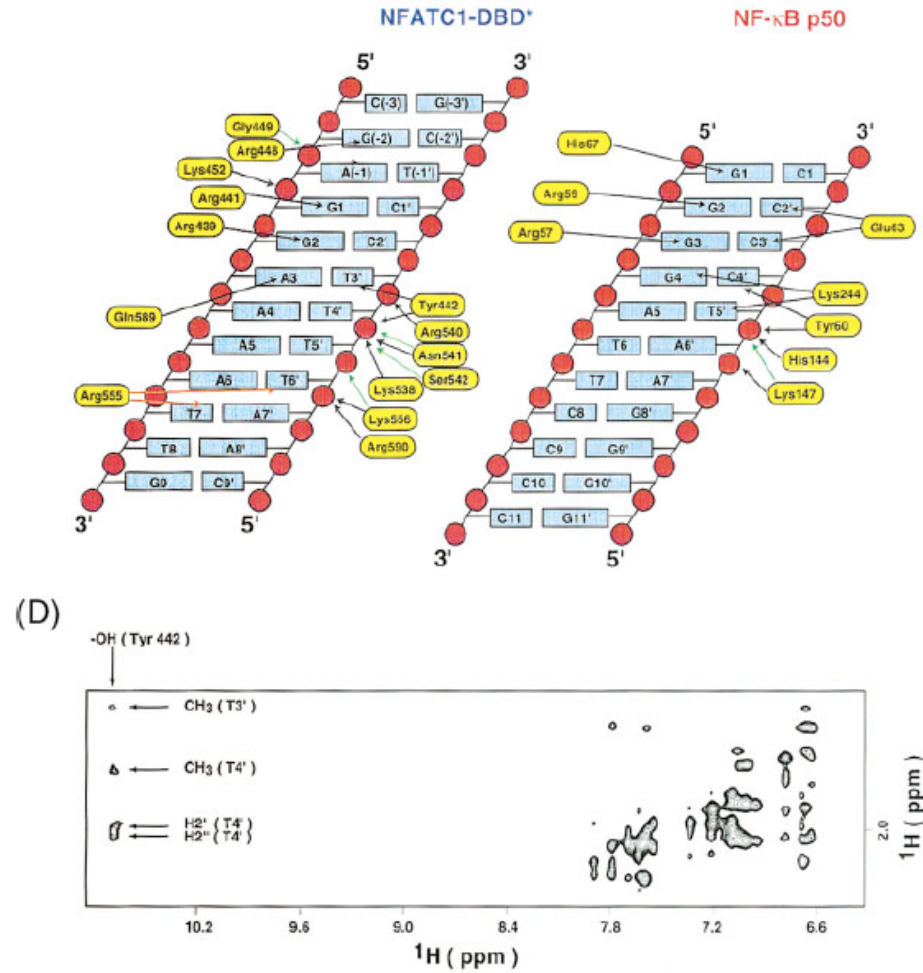
Distance Restraints

1-2D and 3D NOESY at longer mixing times to get weak NOEs
2-HD exchange to get hydrogen bonds

Many of these experiments performed with a specific labeling scheme to facilitate NOEs assignment

Side chain assignments from NOESY, caveats?

Assymmetric isotope labelling to get intermolecular NOEs



Protein is deuterated, DNA protonated experiment done in D₂O solvent
Caveats?

Structures of larger proteins and complexes

Sample Deuteration Increases Sensitivity and Resolution

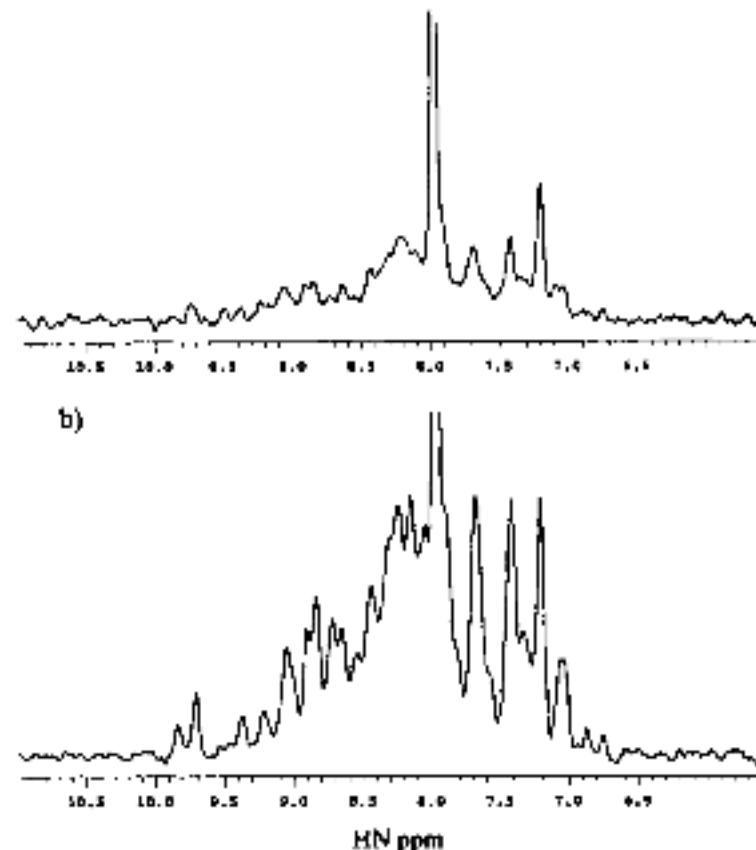
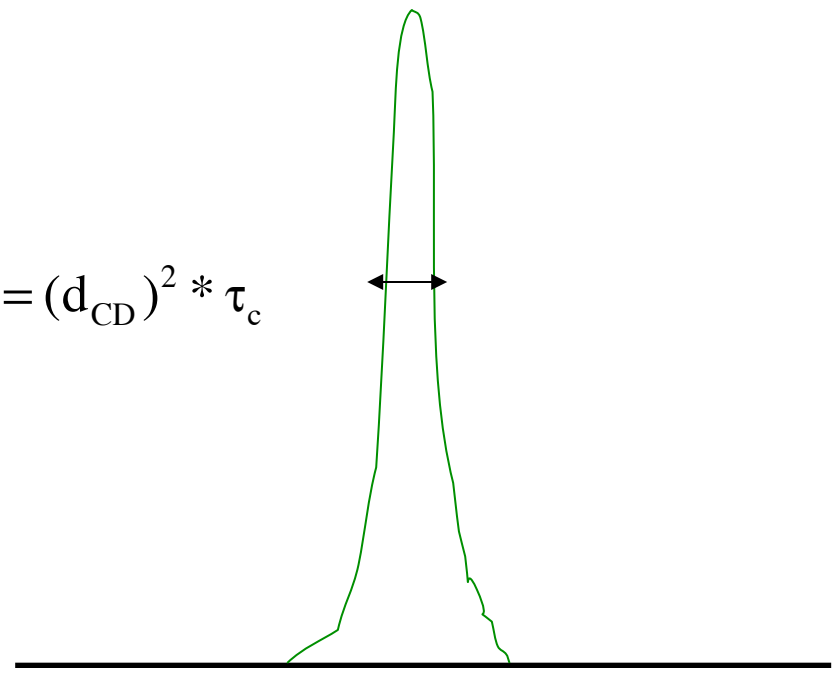
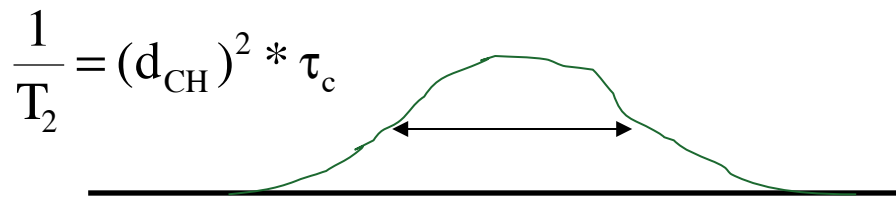


Figure 14. Comparative 1D spectra of fully protonated (a) and $\sim 70\%$ deuterated (b) $^{15}\text{N}, ^{13}\text{C}$ trpR using the HN(CA)CB scheme (Figure 2c). A total of 1024 transients were recorded for the ^2H sample and 6928 transients (1024×2.6^2) for the ^1H sample which is a factor of 2.6 more dilute. The rms noise levels are normalized in the plots.

Why does deuteration help?

$$d_{CH} = \frac{\gamma_C \gamma_H}{r^3} \frac{3\cos^2(\theta) - 1}{2}$$

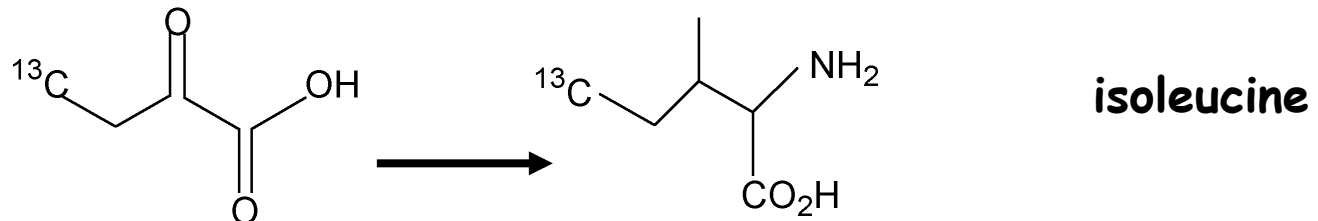
$$\frac{1}{T_2} = (d_{CD})^2 * \tau_c$$



Dipolar coupling for CH spin pair 6.5 times stronger than for CD--->roughly 50 fold reduction in linewidth with increase in S:N.

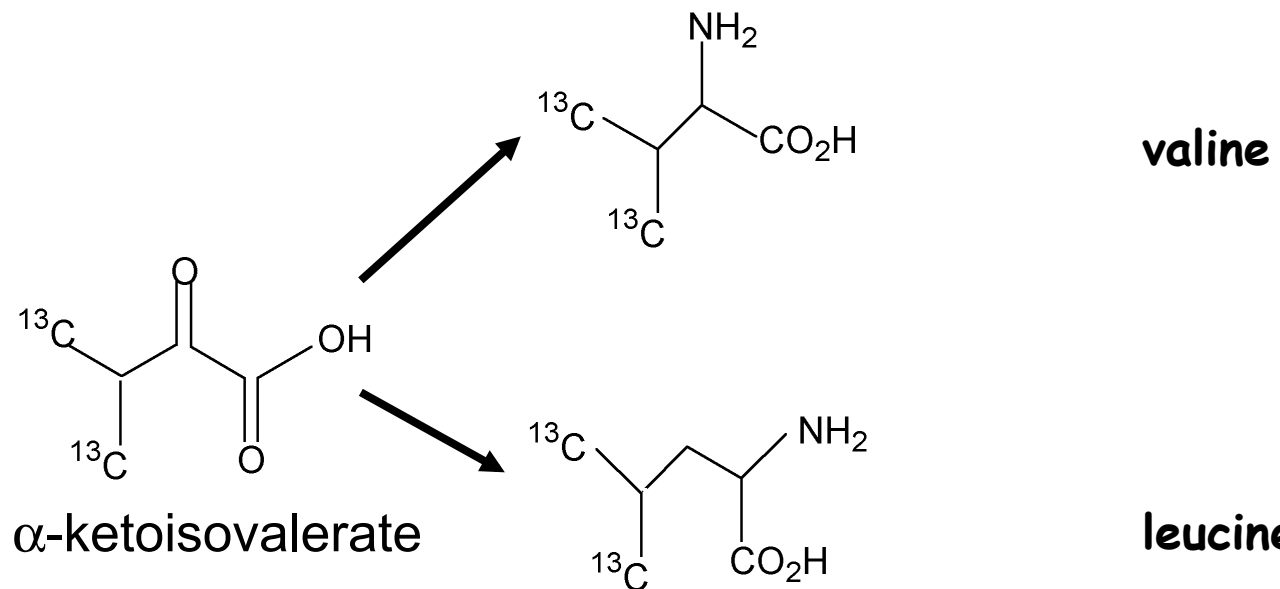
Need methods for measuring distance restraints in sparse ¹H environment

Selective Re-introduction of Protons for NOE experiments



α -ketobutyrate

isoleucine

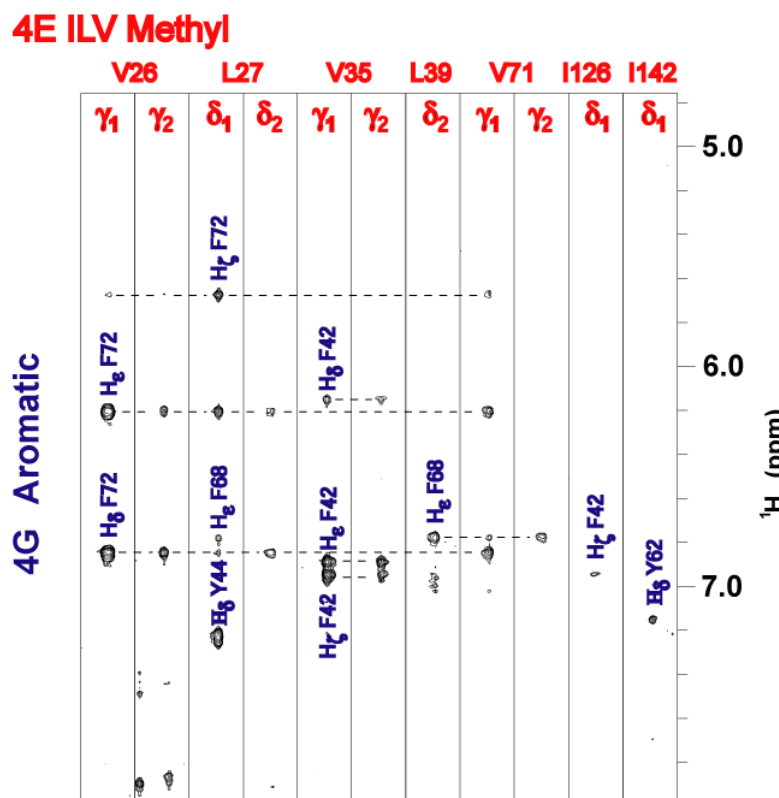
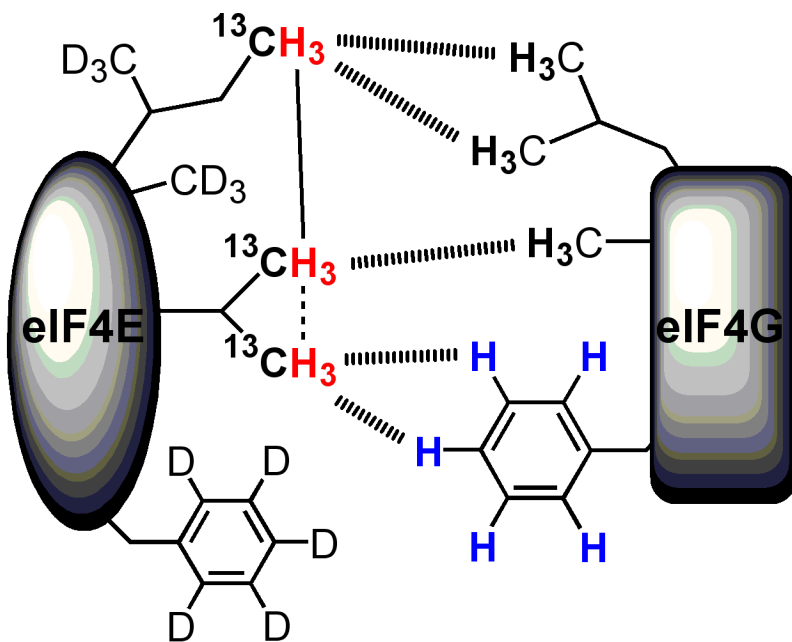


α -ketoisovalerate

leucine

Grow E. coli in D₂O and deuterated glucose, add precursors to introduce 1H/¹³C methyl labels

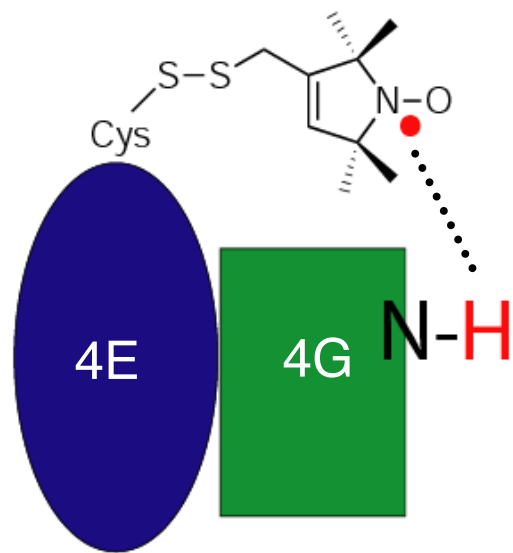
Measurement of Intermolecular NOEs using Asymmetric Deuteration with ILV Labeling



Aromatic/methyl NOEs are unambiguously identified

Gross , Gelev and Wagner, J Biomol NMR 2003

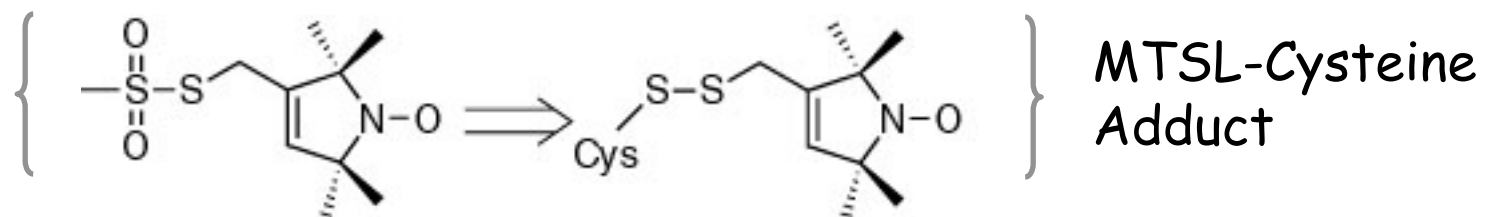
Determining Long Range Distances through Paramagnetic Relaxation Enhancements



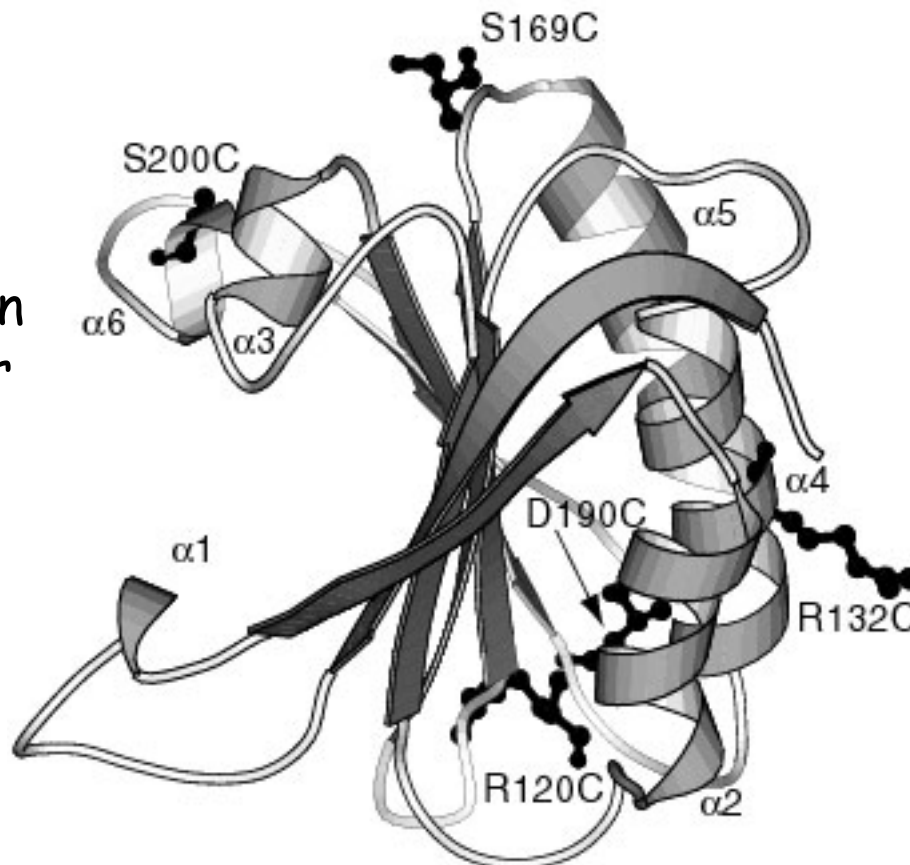
Dipolar broadening between unpaired electron and ^1H :
 $1/r^6$ dependence.

Provides long range distance information (15-20 angstroms)

Site-Directed Spin Labeling for PRE

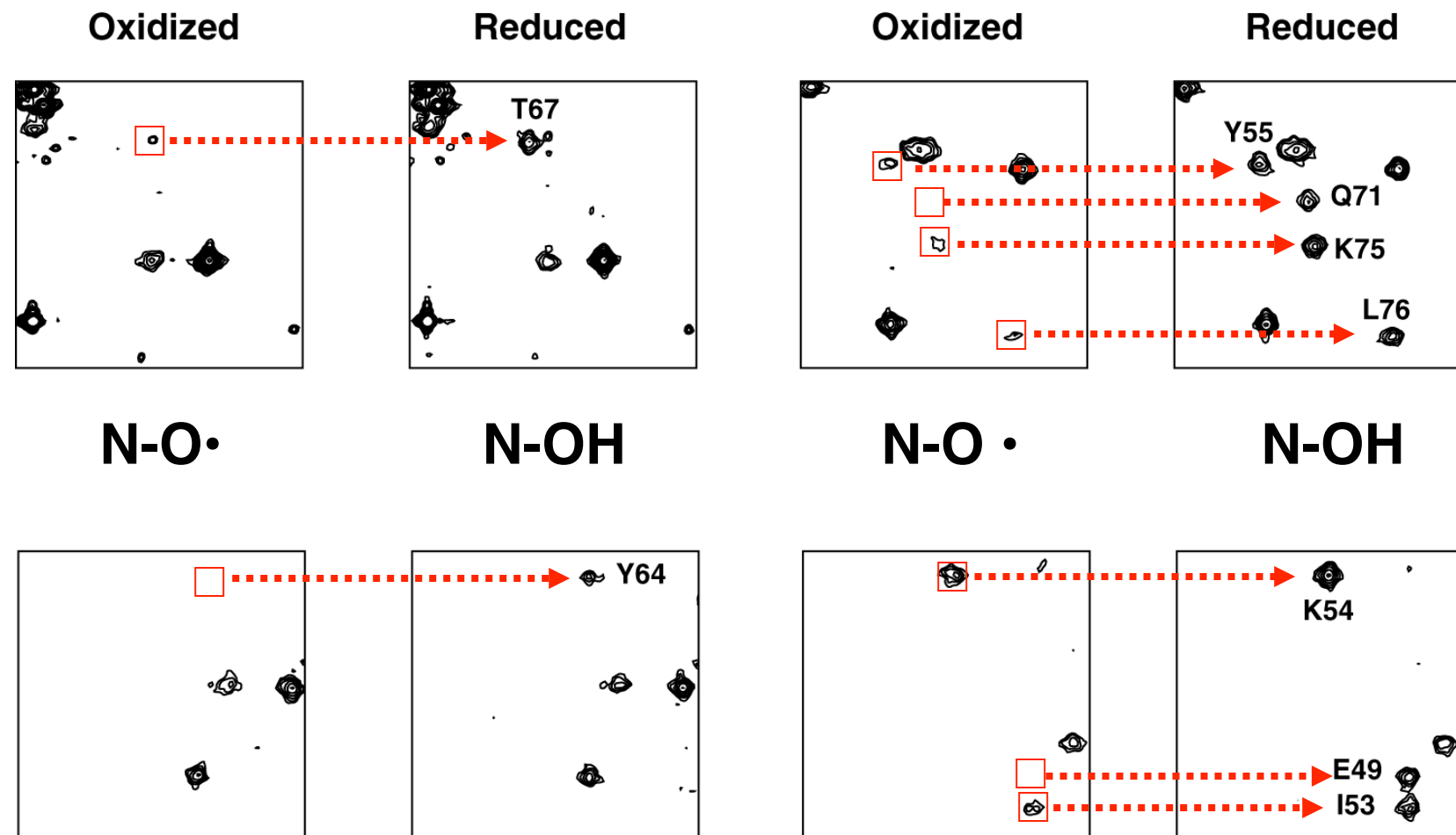


Cysteine mutation
in surface loop or
helix



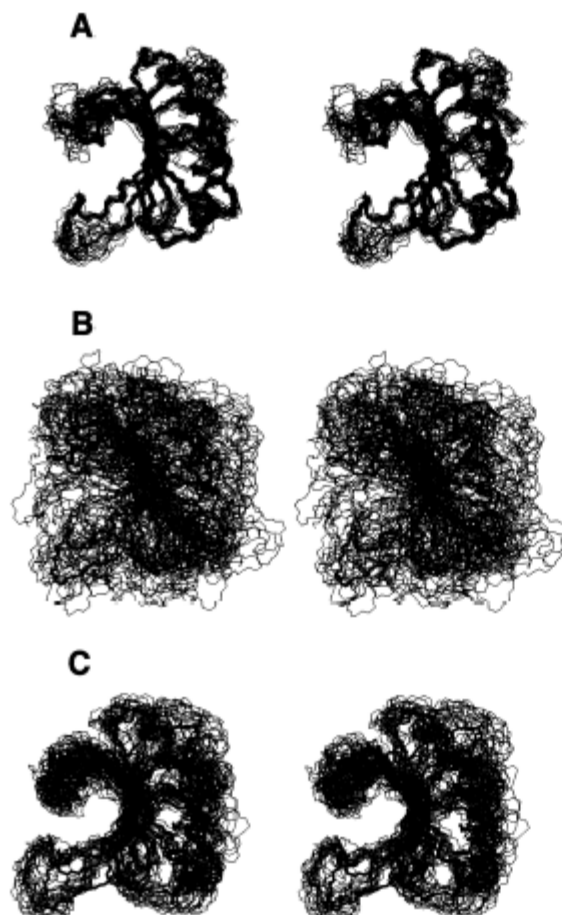
Record HSQC
In absence and
presence of
reductant

Paramagnet Relaxation Enhancement from Site-Directed Spin Labelling



Intensity reduction from dipolar coupling ($1/r^6$), so distances can be extracted

Impact of PRE restraints for structure determination

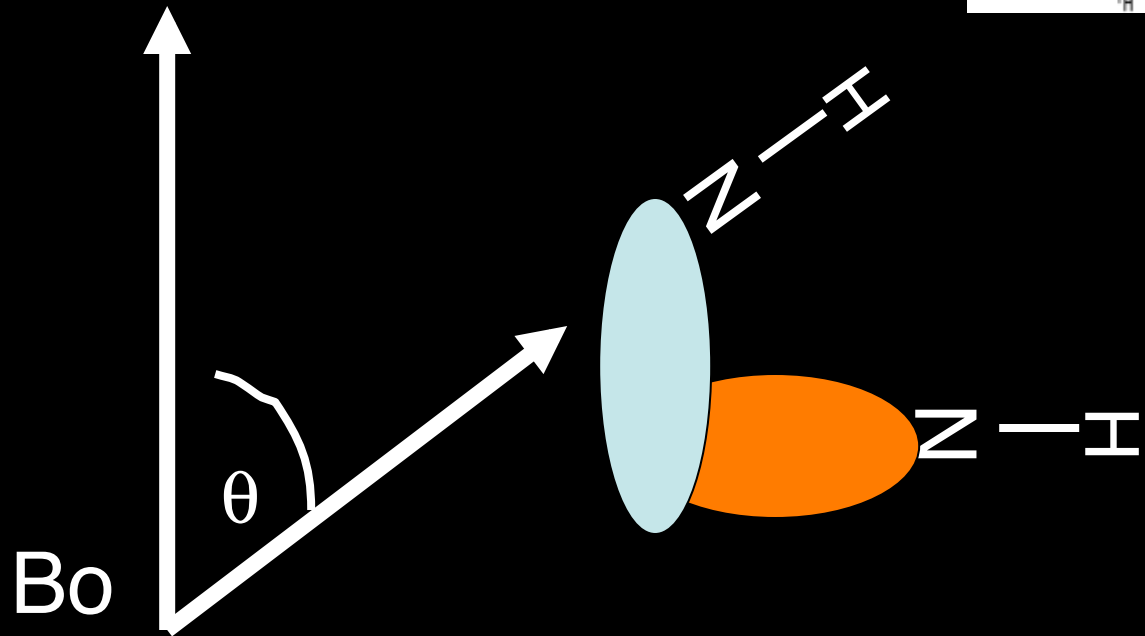
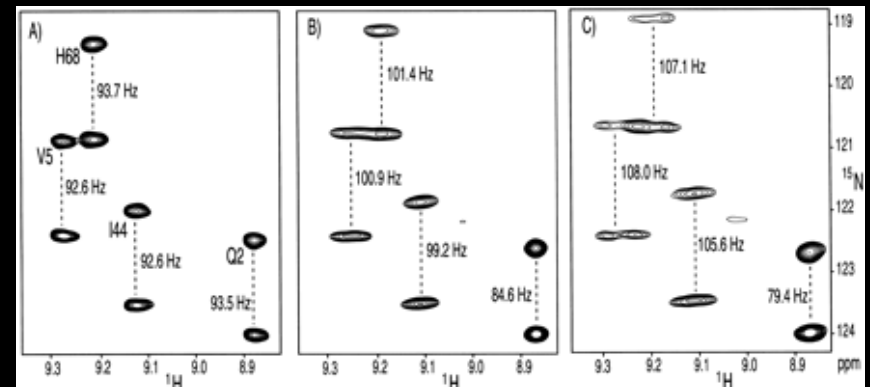
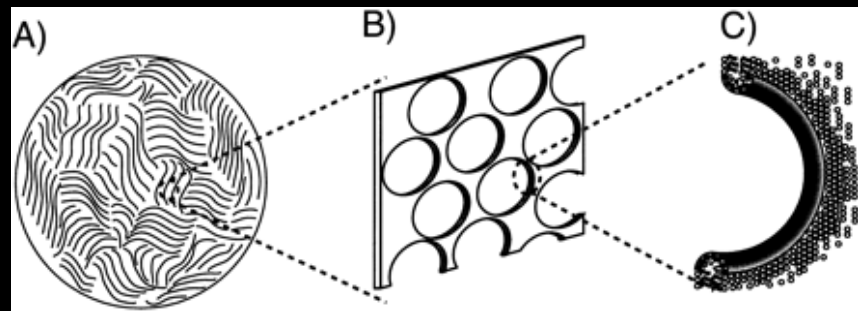


ALL NOEsm (2014)

ONLY HN-HN NOEs (403)

HN-HN NOEs + PRE (515)

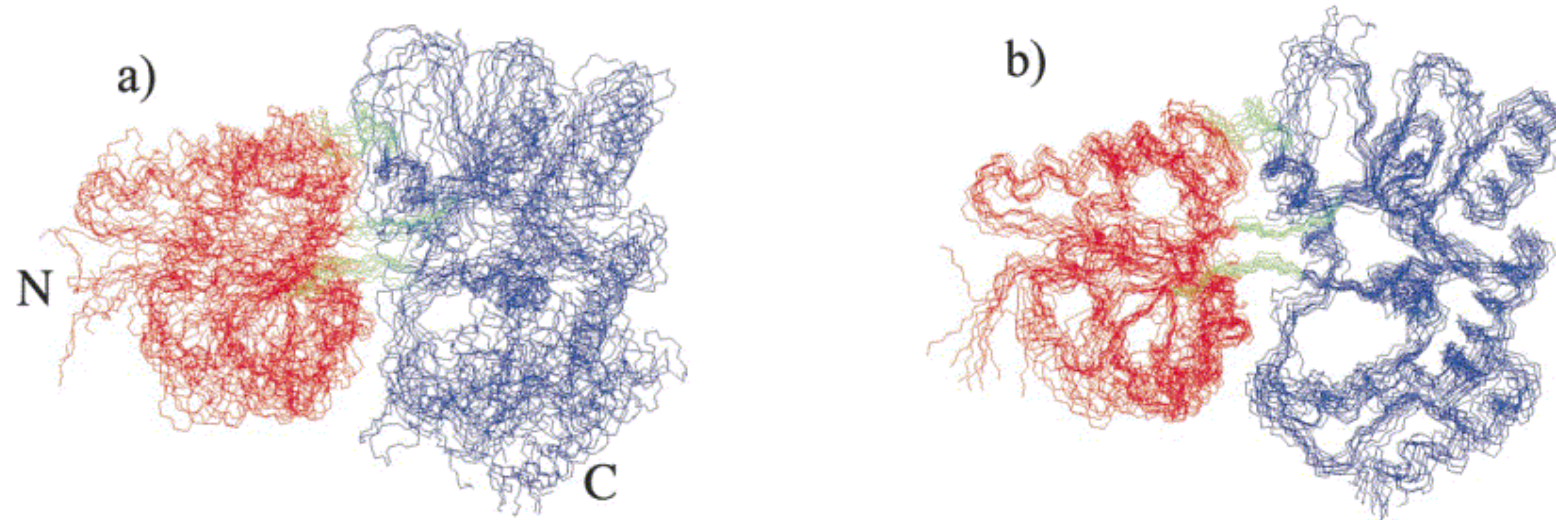
Residual Dipolar Couplings



$$d_{\text{NH}} [3\cos^2\theta - 1]/2$$

$$d_{\text{NH}} \sim \frac{\gamma_c \gamma_h}{r^3}$$

Impact of RDCs on Precision and Accuracy: MBP, a 42 kDa test Case



RMSD

Precision:	5.5 Å	2.2 Å
Accuracy:	5.1 Å	3.3 Å

From Mueller et. Al. JMB 300(1) 197-212 2000

Prospects for even Larger Proteins

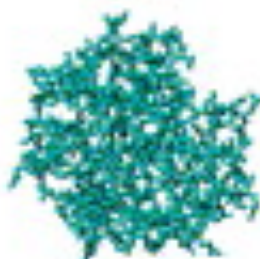
Ubiquitin
76 residues



Lysozyme
156 residues



Adenylate Kinase
214 residues



Maltose binding
protein (MBP)
370 residues



Malate synthase G
723 residues



- i. NMR assignments
- ii. Structure determination
- iii. Dynamics

requires ^{15}N , ^{13}C labeling

- i. NMR assignments
- ii. Global fold/structure determination
- iii. Domain orientation
- iv. Dynamics

requires ^{15}N , ^{13}C , ^2H labeling



X-ray

vs

NMR

- crystal
- single structure-best fit to electron density

- solution
- ensemble of 20-50 structures that equally fit experimental data

Limitations of NMR

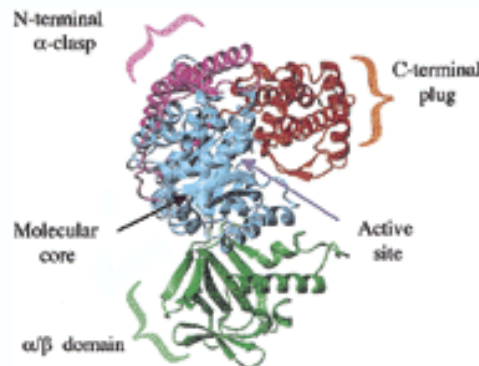
- small proteins (20-30 kD max, although this is changing)
- must be soluble and nonaggregating at 1-3 mM conc
- lots of protein needed

Advantages of NMR

- don't need crystal
- observe protein in solution
- more than a method for determining structure dynamics
 - ligand binding (drug/protein/DNA/etc)
 - protein folding
 - conformational change
 - chemistry, chemical reactions, protonation states.....

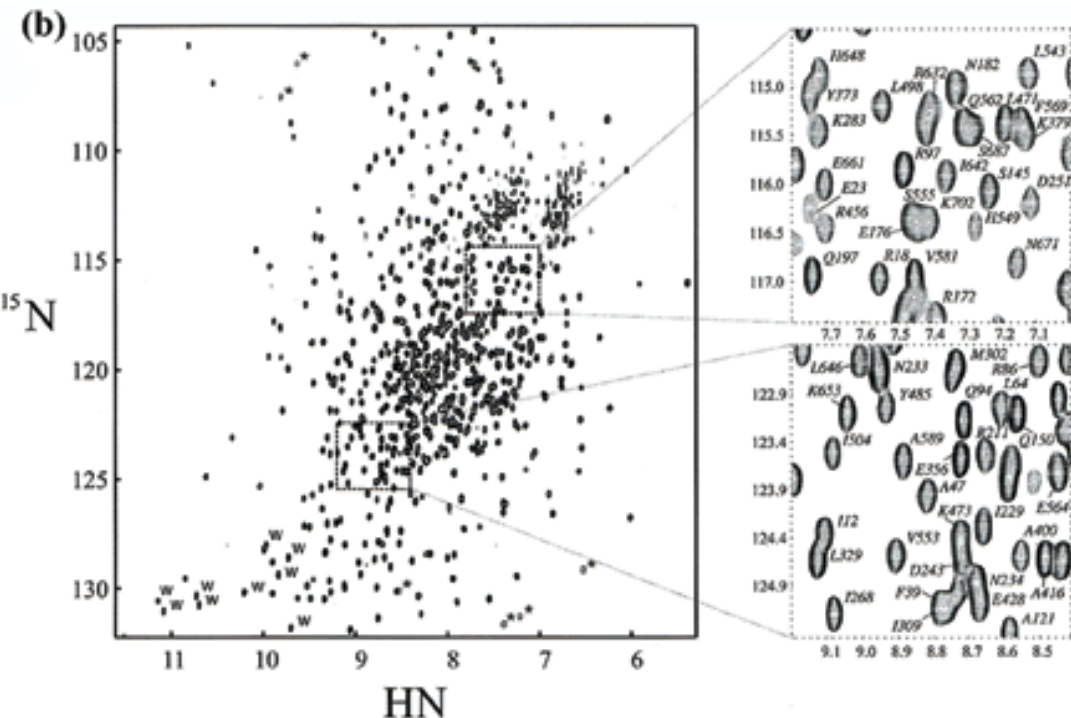
TROSY

(a)



Malate Synthase G

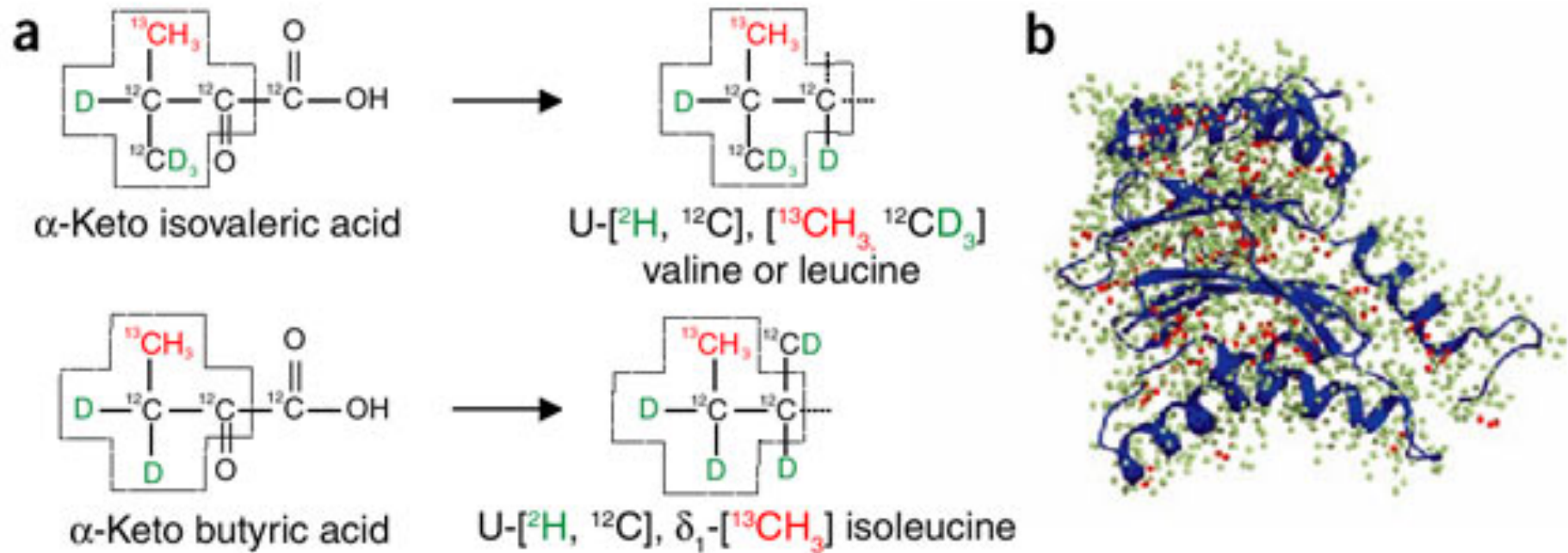
80 kDa



Turgarinov et al, JACS 2002

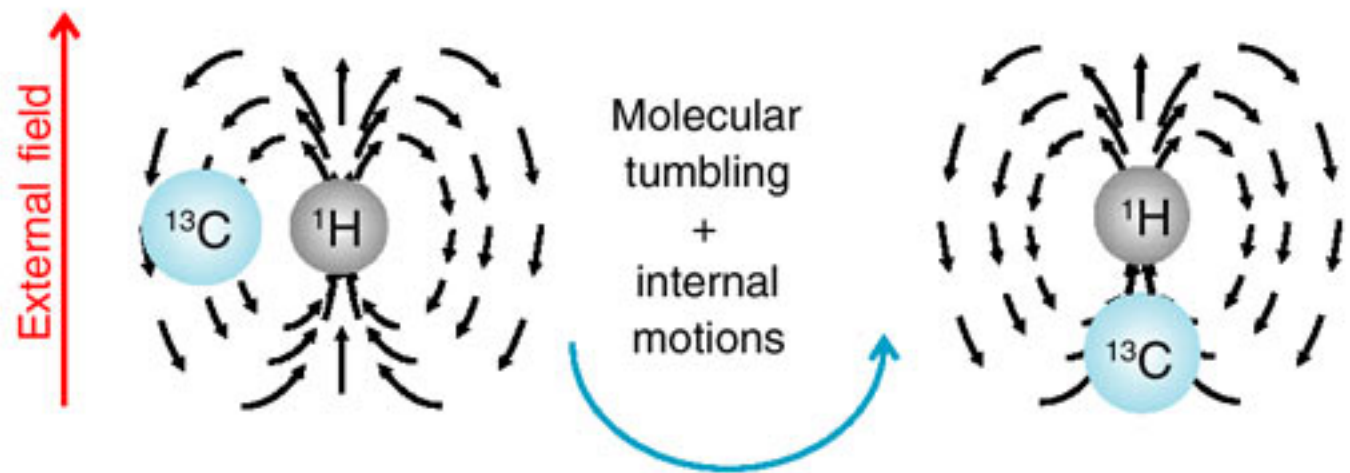
Same info as ^{15}N HSQC

Methyl-group labeling

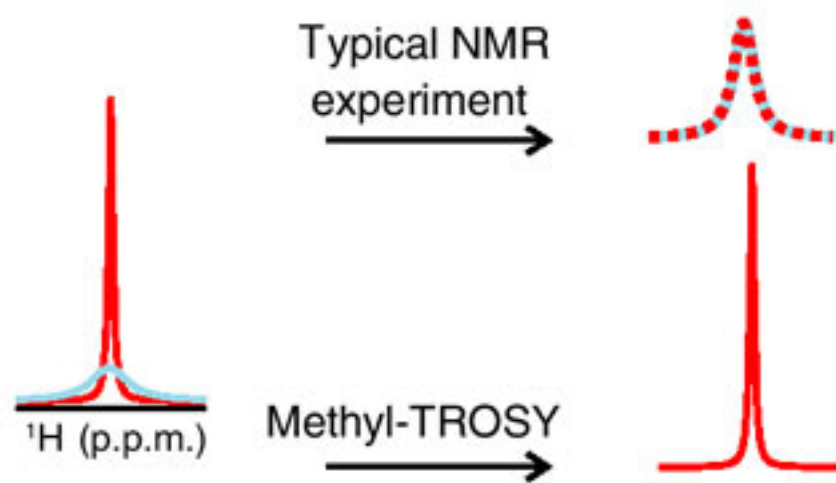


Methyl-TROSY

a



b

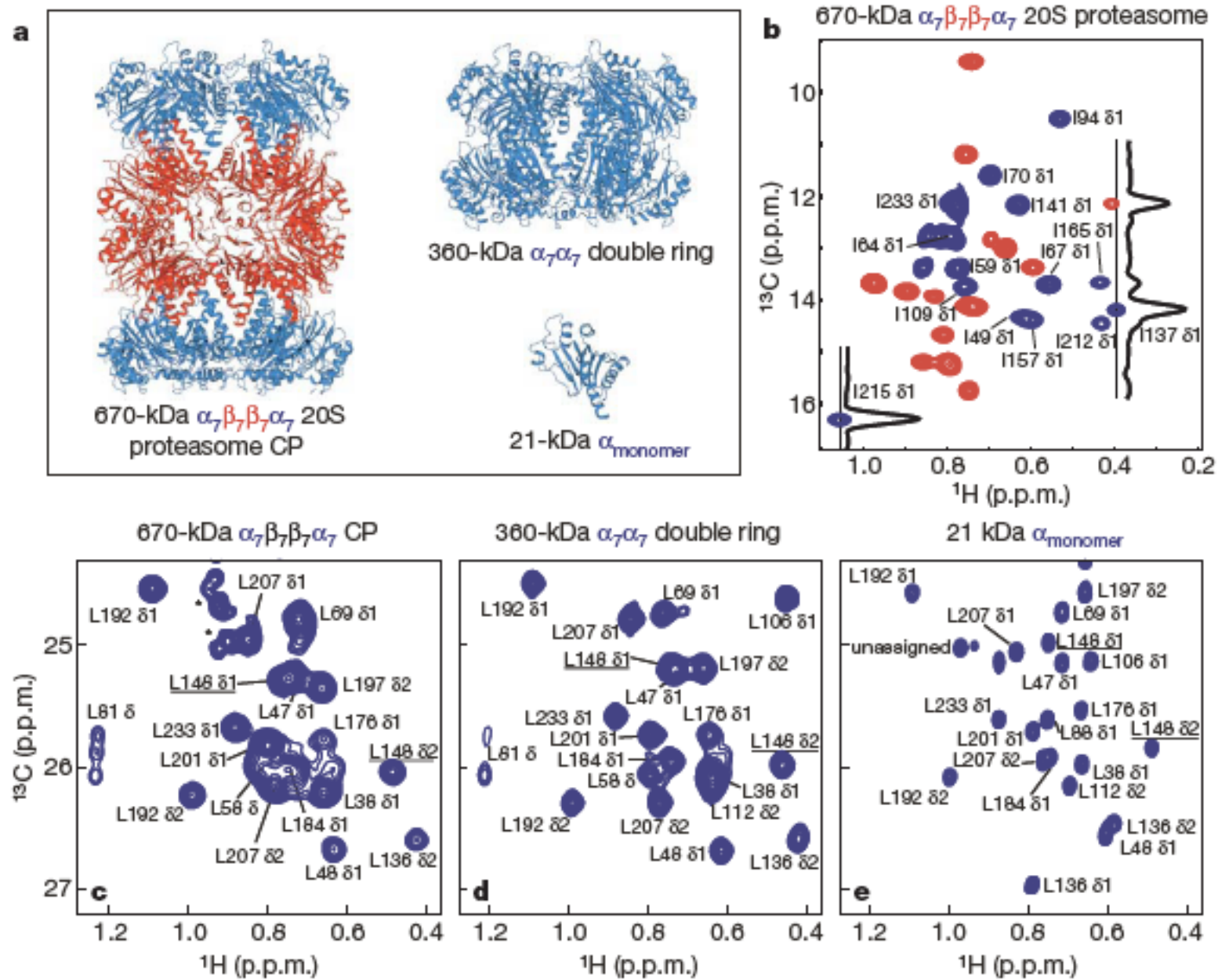


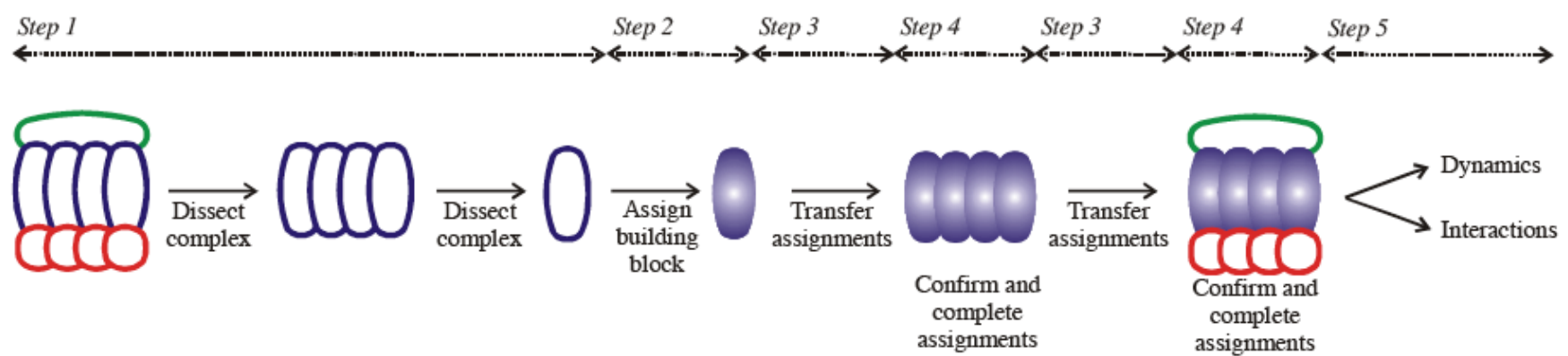
ARTICLES

Quantitative dynamics and binding studies of the 20S proteasome by NMR

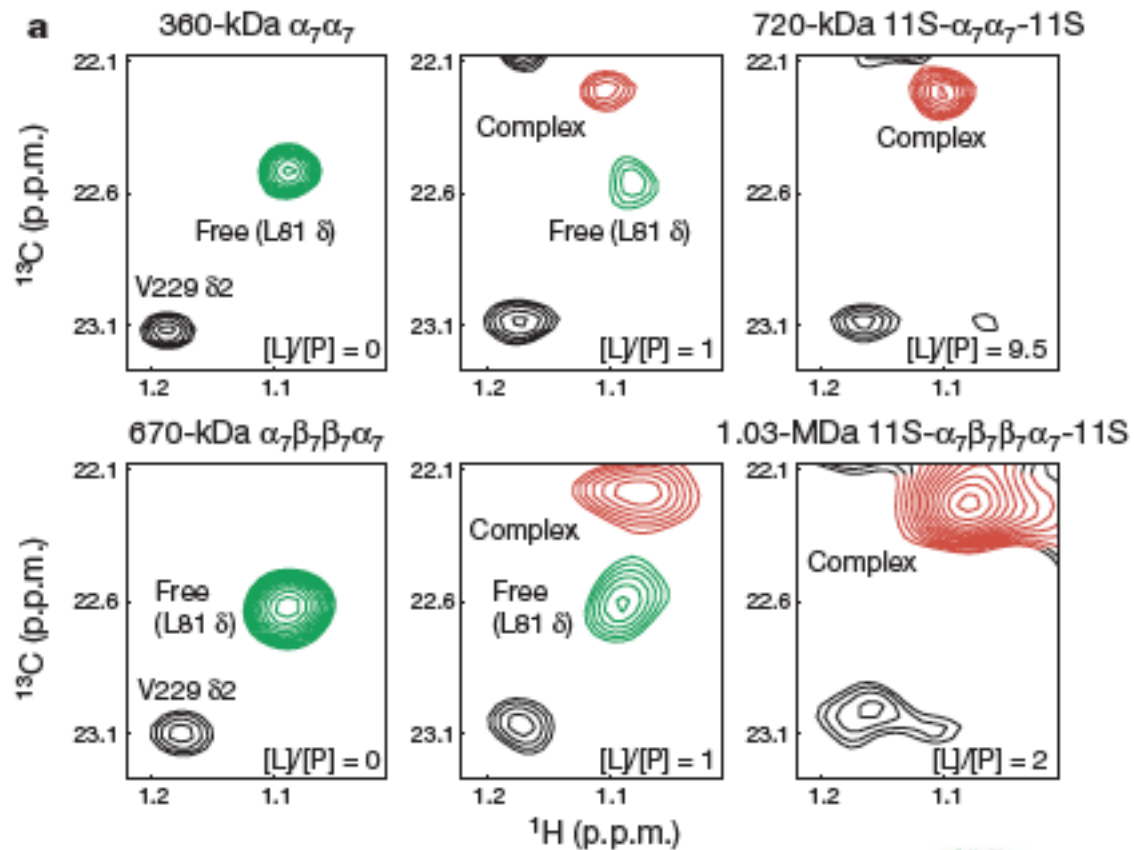
Remco Sprangers¹ & Lewis E. Kay¹

ILV METHYL ASSIGNMENTS OF 670 KDa COMPLEX

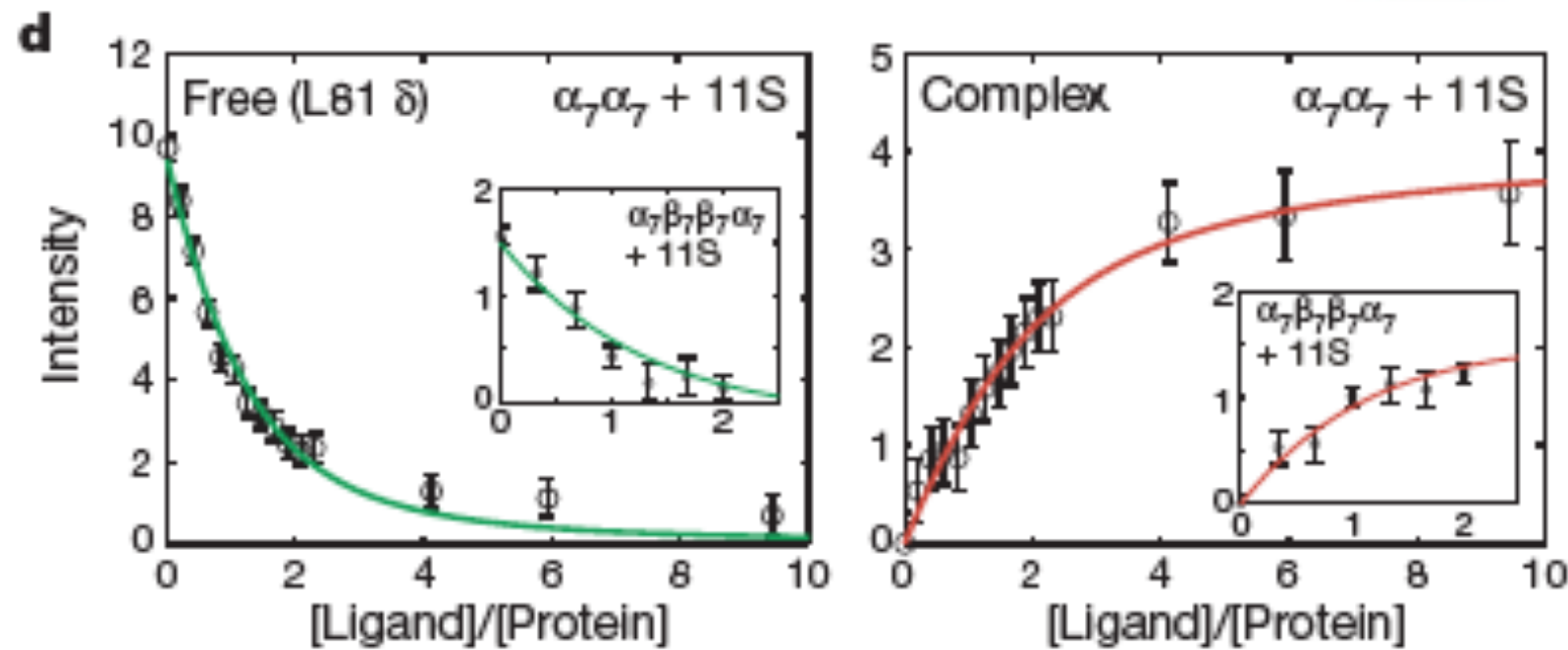




11S ACTIVATOR BINDING



11S BINDING CURVES



Applications for NMR

- Mapping protein interactions
- Fragment based drug discovery, SAR-by-NMR
- Structure of macromolecules ($\leq 40\text{KDa}$ is practical limit)
- TROSY , deuteration and ILV labeling for large systems
- Protein folding
- Protein dynamics